

NASA Contractor Report 188242

**National Aeronautics and Space Administration  
(NASA)/American Society for Engineering Education  
(ASEE) Summer Faculty Fellowship Program—1992**

**Volume 1**

**Richard B. Bannerot and Stanley H. Goldstein, Editors**

**Grant NGT 44-005-803**

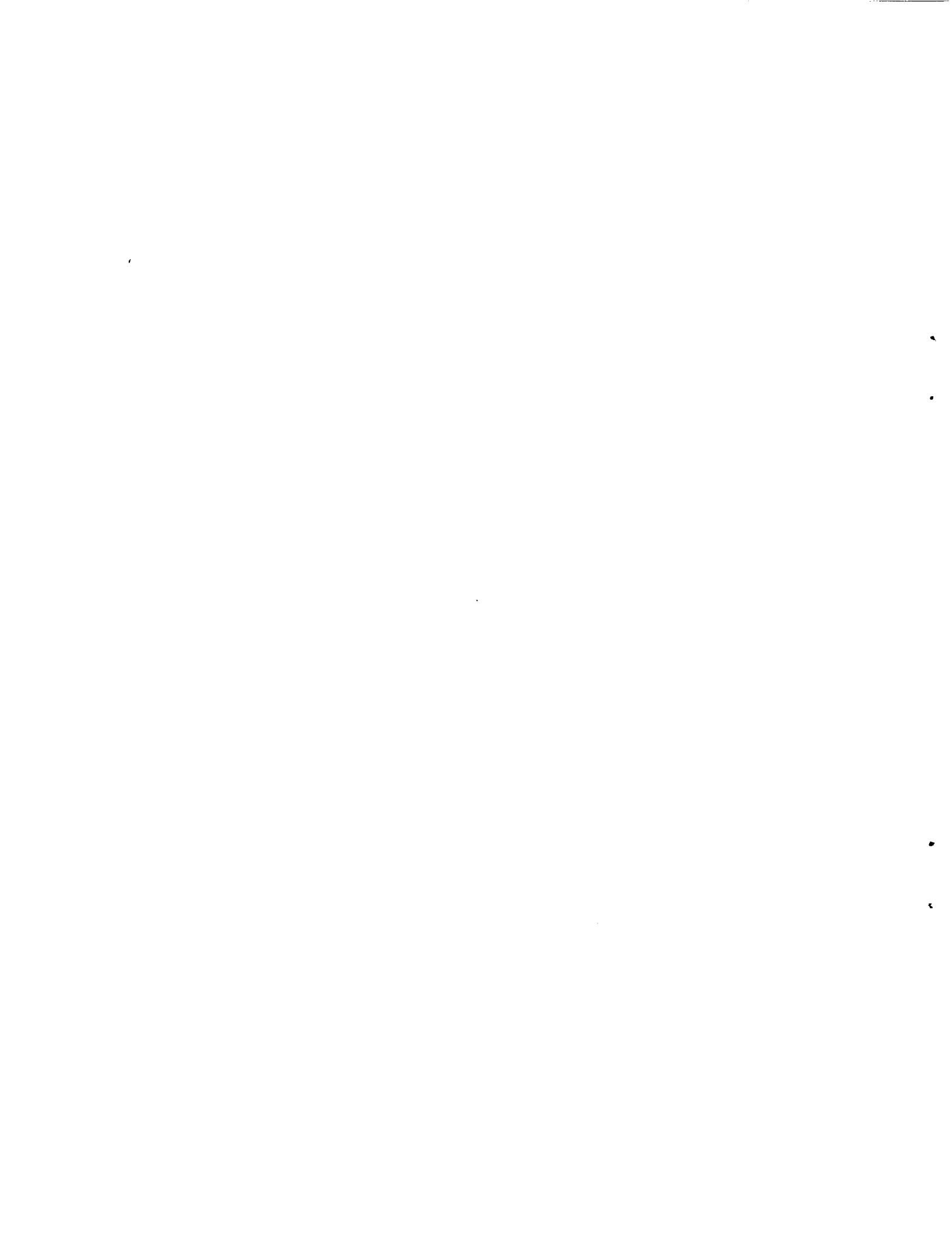
**December 1992**



(NASA-CR-188242-Vol-1) NATIONAL  
AERONAUTICS AND SPACE  
ADMINISTRATION (NASA)/AMERICAN  
SOCIETY FOR ENGINEERING EDUCATION  
(ASEE) SUMMER FACULTY FELLOWSHIP  
PROGRAM, 1992, VOLUME 1 (NASA)  
142 p

N93-26058  
--THRU--  
N93-26069  
Unclass

G3/99 0157389



NASA Contractor Report 188242

**National Aeronautics and Space Administration  
(NASA)/American Society for Engineering Education  
(ASEE) Summer Faculty Fellowship Program—1992**

**Volume 1**

Richard B. Bannerot, Editor  
*Mechanical Engineering Department  
University of Houston--University Park  
Houston, Texas*

Stanley H. Goldstein, Editor  
*University Programs Office  
Lyndon B. Johnson Space Center  
Houston, Texas*

Grant NGT 44-005-803

December 1992

National Aeronautics and Space Administration  
Lyndon B. Johnson Space Center  
Houston, Texas



## **Preface**

The 1992 Johnson Space Center (JSC) National Aeronautics and Space Administration (NASA)/American Society for Engineering Education (ASEE) Summer Faculty Fellowship Program was conducted by the University of Houston and JSC. The program at JSC, as well as the programs at other NASA Centers, was funded by the Office of University Affairs, NASA Headquarters, Washington, D.C. The objectives of the program, which began nationally in 1964 and at JSC in 1965, are

1. To further the professional knowledge of qualified engineering and science faculty members
2. To stimulate an exchange of ideas between participants and NASA
3. To enrich and refresh the research and teaching activities of participants' institutions
4. To contribute to the research objectives of the NASA Centers

Each faculty fellow spent at least 10 weeks at JSC engaged in a research project in collaboration with a NASA/JSC colleague. This document is a compilation of the final reports on the research projects done by the faculty fellows during the summer of 1992. Volume 1 contains reports 1 through 12, and Volume 2 contains reports 13 through 24.



# CONTENTS

## Volume 1

1. Andrews, George A. Jr.: "Data Analysis and Interpretation of Lunar Dust Exosphere".....	1-1
2. Barrera, Enrique V.: "Composite Materials for the Extravehicular Mobility Unit" .....	2-1
3. Bishu, Ram R.: "Investigation of the Effects of Extra Vehicular Activity (EVA) and Launch and Entry (LES) Gloves on Performance" .....	3-1
4. Bustin, Roberta: "Volatiles in Interplanetary Dust Particles: A Comparison with CI and CM Chondrites" .....	4-1
5. Carrasco, Hector R.: "Use of Taguchi Design of Experiments to Optimize and Increase Robustness of Preliminary Designs" .....	5-1
6. Chyu, Ming-C: "Study of Plate-Fin Heat Exchanger and Cold Plate for the Active Thermal Control System of Space Station".....	6-1
7. DeAcetis, Louis A.: "A Prototype for Simulation of the Space-to-Ground Assembly/Contingency System of Space Station Freedom" .....	7-1
8. Ferebee, Robert N.: "Metabolic Response of Environmentally Isolated Microorganisms to Industrial Effluents: Use of a Newly Described Cell Culture Assay" .....	8-1
9. Field, Stephen W.: "Geochemistry and Petrology of Primitive Achondrite Meteorites LEW 88280, MAC 88177, ALHA 81187, EET 84302, and LEW 88663" .....	9-1
10. Gilbert, Joyce A.: "The Role of Pyridoxine as a Countermeasure for In-Flight Loss of Lean Body Mass" .....	10-1
11. Lee, Tze-San: "Analysis of the Lettuce Data From the Variable Pressure Growth Chamber at NASA-Johnson Space Center: A Three-Stage Nested Design Model" .....	11-1

## Volume 2

12. Magee, Michael: "A Vision Architecture for the Extravehicular Activity Retriever".....	12-1
13. Mayfield, Blayne E.: "A Study of Mapping Exogenous Knowledge Representations Into Config".....	13-1



14. O'Brien, Edward M.: "Investigation into the Common Mode Rejection Ratio of the Physiological Signal Conditioner Circuit" .....	14-1
15. Raiman, Laura B.: "Implementation of Quality Improvement Techniques for Management & Technical Processes in the ACRV Project" .....	15-1
16. Richards, Stephen F.: "Distributed Project Scheduling at NASA: Requirements for Manual Protocols and Computer-Based Support" .....	16-1
17. Roberson, Bobby J.: "Development of a Pyrolysis Waste Recovery Model with Designs, Test Plans, and Applications for Space-Based Habitats" .....	17-1
18. Rodgers, Sandra L.: "Utilization of the Graded Universal Testing System to Increase the Efficiency for Assessing Aerobic and Anaerobic Capacity" .....	18-1
19. Sanders, Richard: "A Hybrid Multigrid Technique for Computing Steady-State Solutions to Supersonic Flows" .....	19-1
20. Skowlund, Christopher T.: "Modeling of the WSTF Frictional Heating Apparatus in High Pressure Systems" .....	20-1
21. Smith, Dean Lance: "Spacelab, Spacehab, and Space Station Freedom Payload Interface Projects" .....	21-1
22. Williams, Trevor: "Model Reduction for Space Station Freedom" .....	22-1
23. Yaden, David B. Jr.: "The Adult Literacy Evaluator: An Intelligent Computer-Aided Training System for Diagnosing Adult Illiterates" .....	23-1
24. Vargas, Carolina: "The Reuse of Logistics Carriers for the First Lunar Outpost Alternative Habitat Study" .....	24-1



**N 9 3 - 2 6 0 5 9**

**DATA ANALYSIS AND INTERPRETATION OF LUNAR DUST  
EXOSPHERE**

**Final Report**

**NASA/ASEE Summer Faculty Fellowship Program--1992**

**Johnson Space Center**

<b>Prepared By:</b>	<b>George A. Andrews Jr.</b>
<b>Academic Rank:</b>	<b>Assistant Professor of Physics</b>
<b>University &amp; Department:</b>	<b>LeTourneau University Division of Natural Sciences Longview, Texas 75607</b>
<b>NASA/JSC</b>	
<b>Directorate:</b>	<b>Space and Life Sciences</b>
<b>Division:</b>	<b>Solar System Exploration</b>
<b>Branch:</b>	<b>Space Science</b>
<b>JSC Colleague:</b>	<b>Andrew Potter, Ph.D.</b>
<b>Date Submitted:</b>	<b>August 21, 1992</b>
<b>Contract Number:</b>	<b>NGT-44-005-803</b>

## **ABSTRACT**

The lunar horizon glow observed by Apollo astronauts and captured on film during the Surveyor mission is believed to result from the scattering of sunlight off lunar fines suspended in a dust layer over the lunar surface. For scale heights on the order of tens of kilometers, it is anticipated that the size of the dust particles will be small enough to admit Rayleigh scattering. Such events would result in scattered light which is polarized to a degree which is a function of observation angle and produce spectra containing large high frequency components ("bluing"). Believing these signatures to be observable from ground based telescopes, observational data has been collected from McDonald Observatory and the task of reduction and analysis of this data is the focus of the present report.

## INTRODUCTION

Evidence for electrically charged lunar fines existing and migrating above the moon's surface was recorded by the LEAM experiments conducted on the Moon [Berg et al., 1976]. In these experiments, charged particles were detected by three detectors with peak activity occurring with the passage of the terminator. In addition, the Surveyor photographs taken at sunset [Rennilson and Criswell, 1974] and the Lunokhod-2 detection of "lunar twilight" brightness [Severny et al., 1974], as well as observations sketched and reported by astronauts just before sunrise, provide powerful evidence for the existence of light-scattering dust particles in the vicinity of the terminator.

For particles possessing a greater size than the wavelength of the incident light (tenths of a micron), the scattering is independent of wavelength and is classified as Mie or Tyndall scattering. However, if the scattering particle has a size that is smaller than the incident wavelength, the intensity of the scattered light has a functional dependence on wavelength and is classified as Rayleigh scattering. For Rayleigh scattering, the intensity of the scattered light is inversely proportional to the fourth power of the wavelength; hence, shorter wavelength (blue) light will be preferentially scattered. Such a "bluing" of light collected across the moon's terminator would reveal itself in the light's spectra and thus provide evidence for dust in the vicinity of the terminator. In this report, we summarize the results and analysis of observations taken at four different lunar latitudes using the 82 inch reflecting telescope at the McDonald observatory. These spectra were obtained when the moon was at first quarter on the thirteenth and fourteenth of December 1991.

## REDUCTION & ANALYSIS

### The Signal

Light arriving at the telescope from the moon's surface consists of three components: 1) sunlight scattered directly off the surface, 2) "earthshine" back-scattered off the moon's surface and 3) luminescence from the lunar soil. While the magnitude of the luminescent light can be substantial [Kopal 1966], its occurrence is transient in nature and tends to be confined both in locality and to emission of photons possessing longer wavelengths; hence, in our hunt for dust, we can reasonably ignore this source.

The spectrum of the back-scattered earthshine was obtained by analyzing an approximate 200km region of the slit that was positioned within the dark side of the terminator. This spectrum was then subtracted from the signal across the entire 370km slit leaving only the scattered sun light as a source of illumination.

From the before-mentioned probes and observations, as well as possible solar wind effects, the dust particles causing lunar horizon glow (LHG) would be expected to have a maximum density between 50km to 100km from the terminator in the anti-sun (dark side) direction. Thus, within this region, any relative increase in the intensity and in the degree of polarization of light possessing wavelengths below 4000Å compared to longer wavelengths can be taken as indicative of the probable existence of submicron dust. However, due to the extremely small signal-to-noise ratio, conclusive evidence based on present data can not be expected. Estimates of the brightness of the "bluing" were produced by Herbert Zook and were found to be compatible with the brightness of the LHG reported by the astronauts (Zook and McCoy, 1991, and private communication).

## **The Data**

All representative plots in this report were referenced to a fiducial spectrum. This reference spectrum was obtained from a position on the bright moon found at 41 degrees latitude. Also, all plots reveal the averaged spectral lines of a 64km region just past the apparent terminator. That is, each plot was created by averaging over 20 pixels beginning approximately 12km from the terminator with each pixel equal to 3.2km on the moon.

Finally, a conspicuous intensity "spike" centered around 4300A appears in all spectral plots (see for example figure 2-b.) It has been determined to be an artifact of the data acquisition procedure; therefore, it can be ignored. The fact that it did not cancel out in the "flat-fielding" procedure may indicate a need for further analysis.

## **Data Analysis**

The IRAF software package (developed by NOAO for analysis of astronomical CCD image data) was used to analyze the image data. The CCD images were analyzed by the following steps:

- (1) Subtraction of CCD chip bias.
- (2) "Flat-fielding" the image by dividing the image by an image of blue sky. This step corrected the data for varying pixel responses.
- (3) Registration of blue and red ends of the spectra. This step was necessary to correct for geometrical misalignment of the chip and for atmospheric refraction effects.
- (4) Ratioing of the registered image to "fiducial" spectrum of the lunar surface. This step removed the filter transmission and spectral response curves from the data.
- (5) Subtraction of the earthshine and scattered moonlight from the image data.

The data after this last step represented the spectra of any residual light in the region just beyond the terminator. This is where we expected to find evidence for a suspended dust layer.

## **Discussion**

It is hypothesized that the higher latitude sites should produce greater scattering due to an optical depth increase. To this end, data was collected at four different northern latitudes along the terminator which bisected the moon at 2 degrees west longitude. Of course, lunar terrain differences must be kept in mind; for as is well known, different chemical composites of lunar soil, topographical changes and albedo differences result in variance of spectra.

### *Site 1*

Figure 1 reveals the data obtained for two different transmission axis angles of the polarization analyzer for the lunar site having coordinates 78 degrees north latitude. These angles are measured with respect to the scattering plane so a perpendicular setting allows maximum transmission of the scattered light. For our purposes, only relative measures of polarization are necessary; hence the ordinate reflectance intensities are in arbitrary units. Wavelengths, in units of Angstroms, are plotted as abscissae.

In this figure, 1-a reveals the spectrum of light having its polarization plane perpendicular to the scattering plane and 1-b depicts the spectrum of light produced after the analyzer has been rotated by 45 degrees. In 1-b, the intensities of all wavelengths suffer a decrease but careful examination of wavelengths below 5000A (ignoring the range of wavelengths  $4100\text{A} < x < 4500\text{A}$  as previously warned) does in fact reveal a greater degree of polarization than at longer wavelengths.

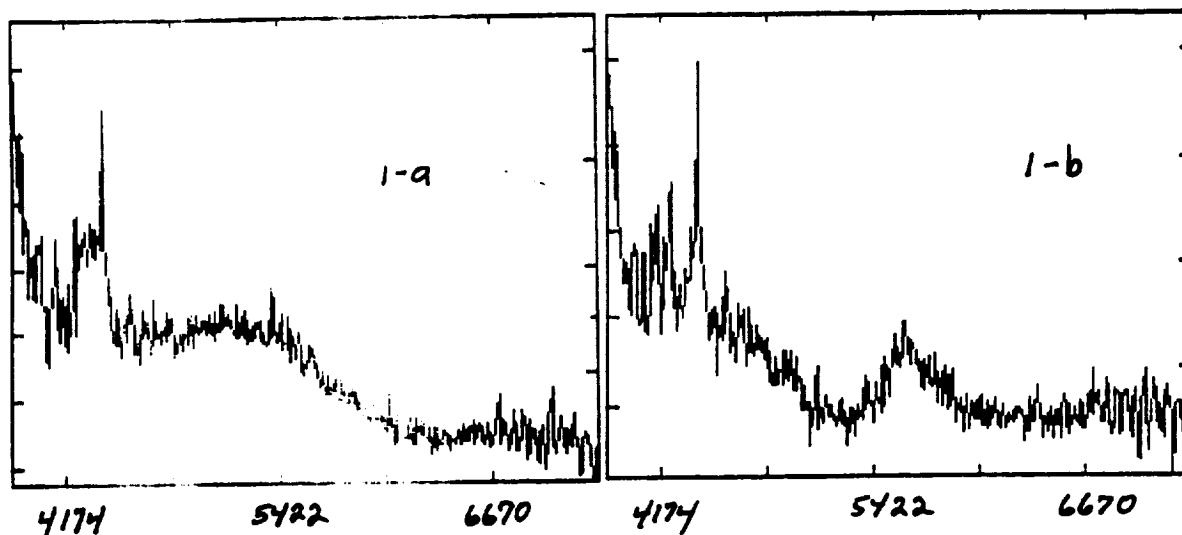


FIGURE 1. - Averaged spectrum of a 60km region of the moon just past the terminator for the 78 degree north latitude site.

When the analyzer is again rotated an additional 45 degrees (not shown), the intensities of all wavelengths actually increase to levels even greater than the intensities associated with the perpendicularly oriented analyzer. This negative polarization occurs in all cases and has been well documented by others in their lunar observations (Kopal, 1966.)

A note of caution must be sounded for this site. While compensating for terrestrial atmospheric effects, it was discovered that this site did not exhibit the expected dispersion and hence, did not need the required numerical correction as did the other sites studied. This is a curiosity that is still in need of an explanation.

*Site 2*

Figure 2 reveals the spectra of light captured from the region on the moon having coordinates of 60 degrees north latitude and 2 degrees west longitude. In figure 2-a, the perpendicular angle, the intensity is maximum for wavelengths below 4100A. In figure 1-b, the analyzer has been rotated 45 degrees with the evident consequence of a sharp decrease in the relative intensity of wavelengths of light below 5000A with the maximum decrease occurring for wavelengths less than 4100A! As mention in the introduction, such an increase of relative polarization of "blue" over "red" can be interpreted as a signature of Rayleigh scattered light. The forewarned artificial spike around 4300A is most evident in this plot.

The analyzer was rotated an additional 45 degrees so as to be parallel to the scattering plane but no further relative decrease for lower wavelengths was observed. However, as before, there is an actual increase in intensity of all wavelengths as well as the appearance off additional albedo structure not shown in this report and may serve to conceal the expected small signal that is indicative of dust.

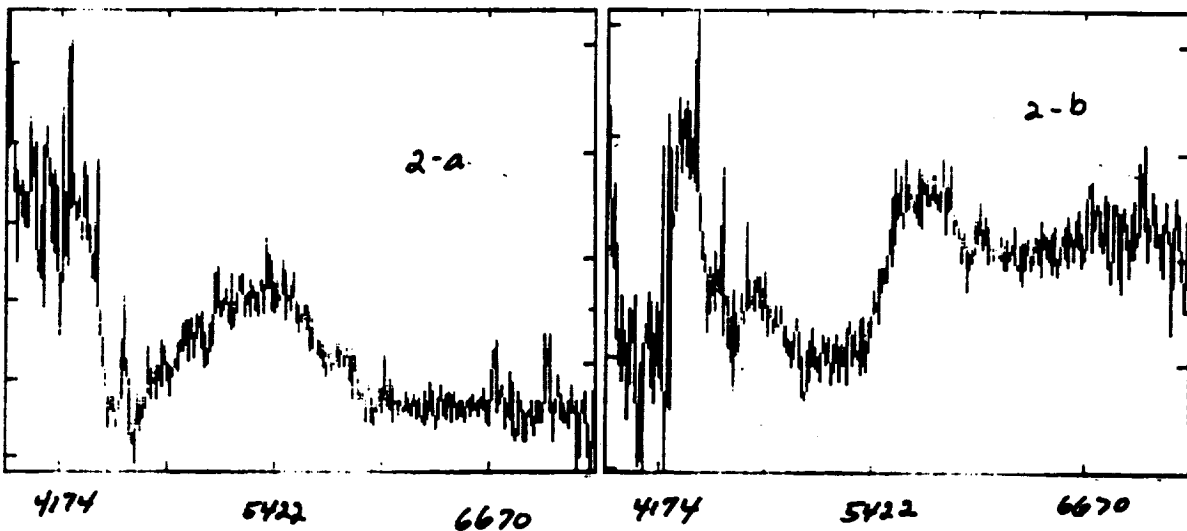


**FIGURE 2. - Averaged spectrum of a 60km region of the moon just past the terminator for the 60 degree north latitude site.**

*Site 3*

The next observational data came from a lunar region located 41 degrees north latitude. The resulting spectral plots are shown in figure 3. As in Figure 2, Figure 3-b is the spectrum for the analyzer angle at 45 degrees and 3-a is for the perpendicular case; again polarization effects for wavelengths less than 5000A are evident. However, close examination of the wavelengths less than 4100A reveal less of a relative change than the 60 degree case. One possible interpretation is a decrease in scatterers do to a decrease on optical depth.

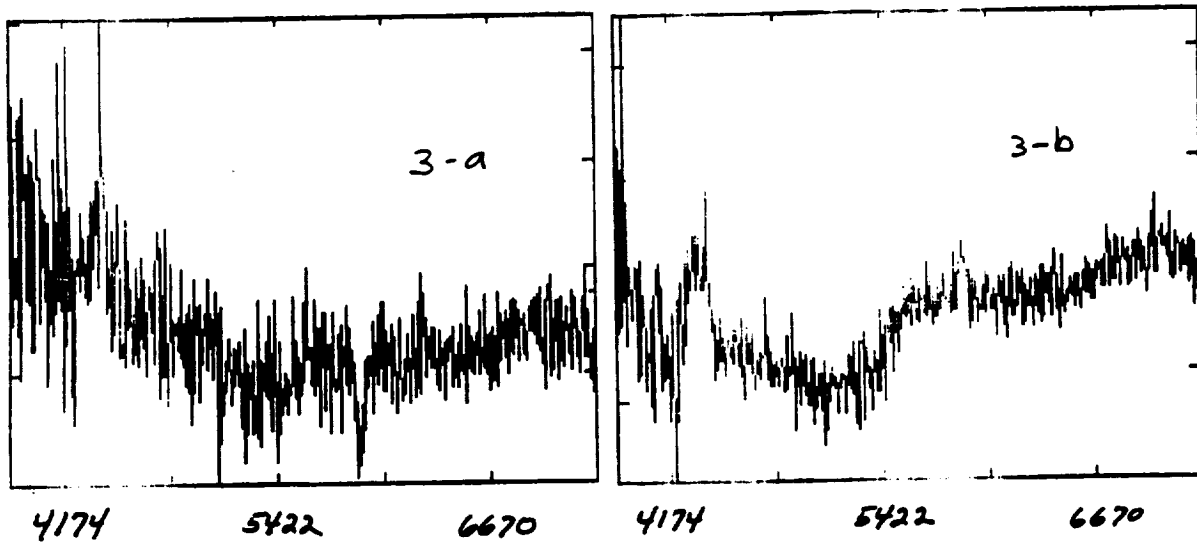


FIGURE 3. - Averaged spectrum of a 60km region of the moon just past the terminator for the 41 degree north latitude site.

*Site 4*

Our final data set comes from a location on the lunar surface close to the equator. The coordinates of this site are 2 degrees north latitude and 2 degrees west longitude. This region is in Sinus Medii and possesses the lowest albedo of all previous sites. Figure 4 displays the spectral data for this site and analysis reveals that there is a very slight *increase* in lower wavelengths as the polarizer is rotated. This increase is anomalous in that it is the only site in which it occurs and is counter-intuitive if dust is the cause. It must be recalled however, that the signal to noise ratio is expected to be lowest here at small latitudes due to optical depth. This fact then precludes any conclusive interpretation at this point.

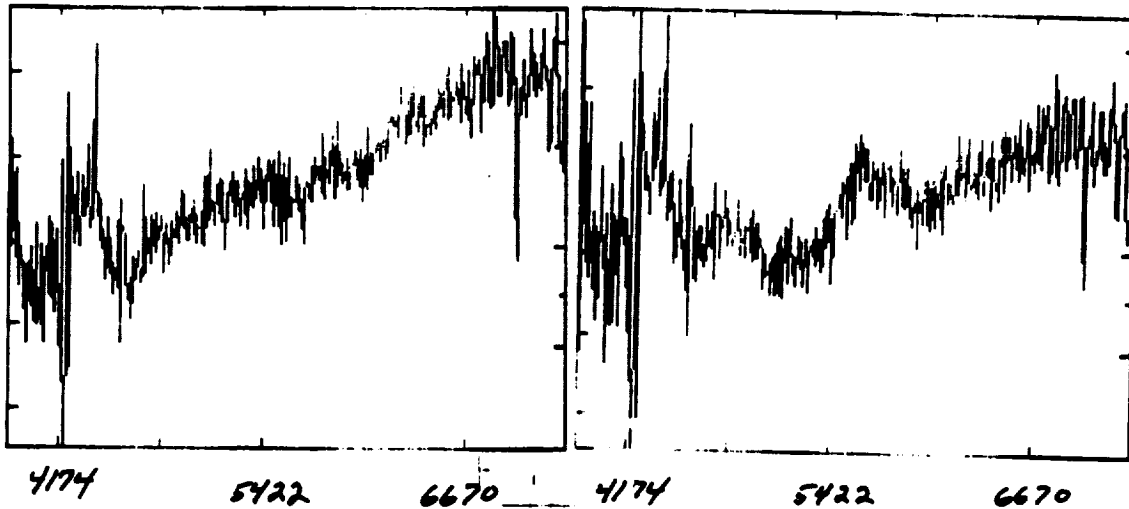


FIGURE 4. - Averaged spectrum of a 60km region of the moon just past the terminator for the 2 degree north latitude site.

When the perpendicular spectra for each site are compared against each other, an increase in intensity of lower wavelengths from site to site is observed with increasing latitude, i.e. the spectra shift to the blue. Such a comparison is shown in figure 5. Ignoring other parameters concerning geography, the case for lunar dust particles is substantiated by such a comparison.

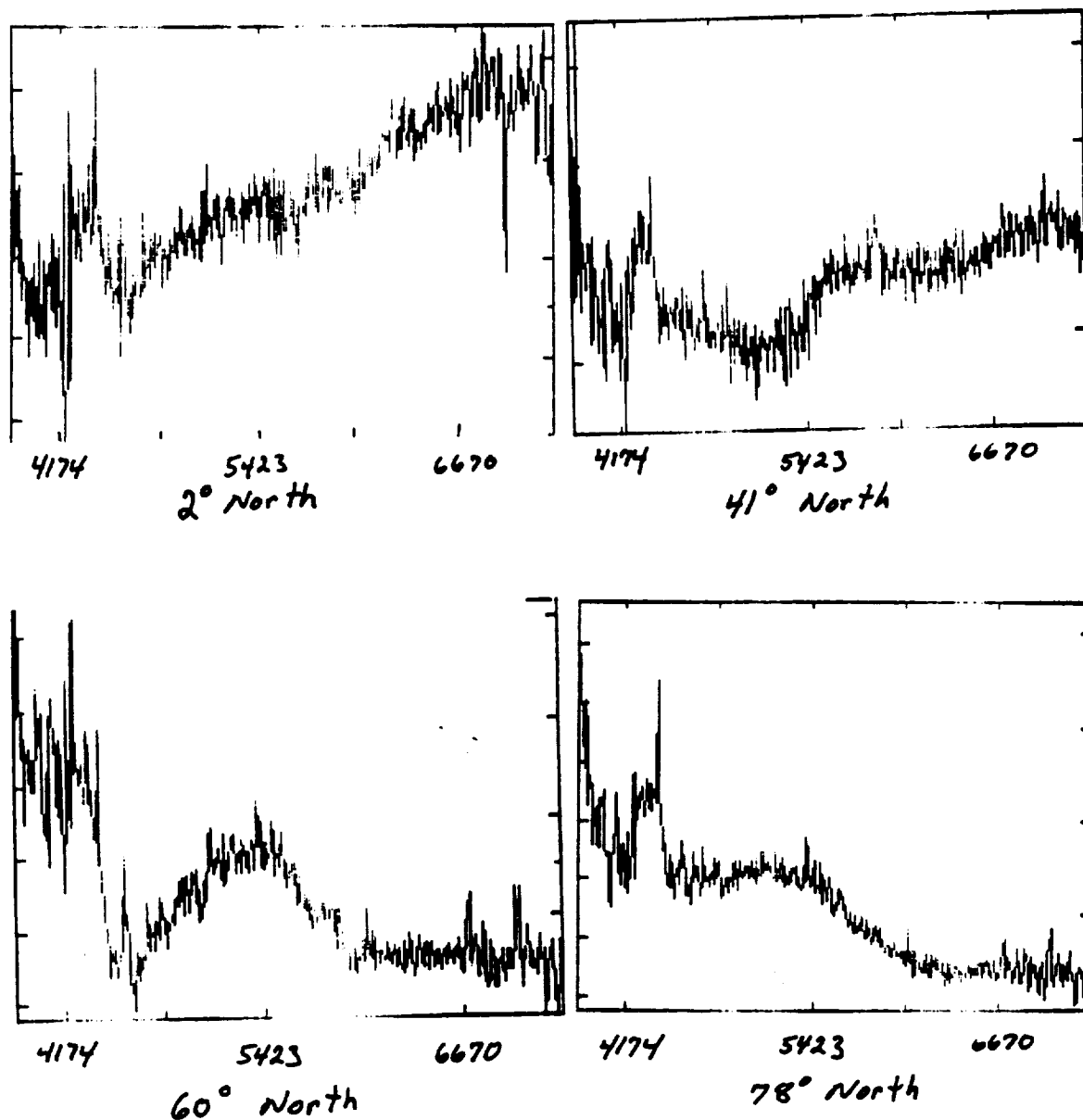


FIGURE 5 Comparison of spectra from all latitudes studied.

### *Summary and Conclusion*

In this report, it has been shown that the degree of polarization of reflected light scattered off of the surface of the moon is greater for wavelengths residing at the blue end of the visible spectrum than for the longer wavelength red. In addition, the functional dependence of the intensity change with analyzer angle is in accord with that expected from Rayleigh scattering of light. This dependence is observed to have the expected direction (i.e., intensity increases with analyzer angle) in all cases except the one closest to the equator. It has also been demonstrated that the color of the spectra shifts toward the blue with increasing latitude; a fact which is also in agreement with The Rayleigh hypothesis in that with increased latitude there is an accompanying increase of scatterers.

## REFERENCES

Berg,O.E.,H.Wolf, and J.Rhee, Lunar soil movement registered by the Apollo 17 cosmic dust experiment., *Interplanetary Dust and Zodiacal Light* (H.Elsasser and H.Fechtig, eds.), Springer-Verlag, New York, 233-237, 1976.

Kopal,Z , Astrophysics and Space Sciences Library, *An Introduction to The Study of The Moon 4*, D.Reidel, New York, 1966.

Rennilosn,J.J. and D.R.Criswell, Surveyor observations of lunar horizon glow, *The Moon 10*, 121-142, 1974.

Severny,A.B., E.I.Terez, and A.M.Zvereva, The measurements of sky brightness of Lunokhod-2, *The Moon 14*, 123-128, 1975

Zook,H.A. and McCoy,J.E., Large Scale Horizon Glow and a High Altitude Lunar Dust Exosphere, *J. Geophys. Res.* **18**, 2117-2120, 1991



**COMPOSITE MATERIALS FOR THE EXTRAVEHICULAR  
MOBILITY UNIT**

**Final Report  
NASA/ASEE Summer Faculty Fellowship Program--1992  
Johnson Space Center**

**Prepared By: Enrique V. Barrera  
Academic Rank: Assistant Professor of Materials Science**

**Hector M. Tello  
Graduate Student and NASA-ASEE  
Summer Student Participant**

**University & Department: Rice University  
Department of Mechanical Engineering  
and Materials Science  
Houston, TX 77251-1892**

**NASA/JSC**

**Directorate: Engineering  
Division: Crew and Thermal Systems  
Branch: Systems Engineering Analysis Office  
JSC Colleague: Dr. Frederic S. Dawn  
Date Submitted: August 7, 1992  
Contract Number: NGT-44-005-803**

## ABSTRACT

The extravehicular mobility unit (EMU), commonly known as the astronaut space suit assembly (SSA) and primary life support system (PLSS), has evolved through the years to incorporate new and innovative materials in order to meet the demands of the space environment. The space shuttle program which is seeing an increasing level of extravehicular activity (EVA), also called space walks, along with interest in an EMU for Lunar-Mars missions means even more demanding conditions are being placed on the suit and PLSS. The project for this NASA-ASEE Summer Program was to investigate new materials for these applications. The focus was to emphasize the use of composite materials for every component of the EMU to enhance the properties while reducing the total weight of the EMU. To accomplish this, development of new materials called fullerene reinforced materials (FRM's) was initiated. Fullerenes are carbon molecules which when added to a material significantly reduce the weight of that material. The Faculty Fellow worked directly on the development of the fullerene reinforced materials. A chamber for fullerene production was designed and assembled and first generation samples were processed. He also supervised with the JSC Colleague, a study of composite materials for the EMU conducted by the student participant in the NASA-ASEE Program, Hector Tello a Rice University graduate student, and by a NASA Aerospace Technologist (Materials Engineer) Evelyne Orndoff, in the Systems Engineering Analysis Office (EC7), also a Rice University graduate student. Hector Tello conducted a study on beryllium and Be alloys and initiated a study of carbon and glass reinforced composites for space applications. Evelyne Orndoff compiled an inventory of the materials on the SSA. Ms. Orndoff also reviewed SSA material requirements and cited aspects of the SSA design where composite materials might be further considered. Hector Tello spend part of his time investigating the solar radiation sensitivity of anodic coatings. This project was directed toward the effects of ultra-violet radiation on high emissivity anodic coatings. The work of both Evelyne Orndoff and Hector Tello is of interest to the Engineering Directorate at NASA/JSC and is also directed toward their research as Rice University graduate students.

## INTRODUCTION

For the most part, the extravehicular mobility unit is already a composite in itself, the separation of the EMU into major components such as the arm assembly, lower torso assembly, glove, and etc; combination of flexible to non-flexible materials; the arrangement of numerous layers where each plays a different but important roll; and even the layers themselves like the outer layer of the Thermal Micrometeoroid Garment (TMG) which is a composite of Gore-tex fiber, Nomex fiber, and Kevlar fiber. The total design is well engineered and the long time work of Dr. Frederic S. Dawn, NASA/JSC, and the numerous contractors of which Hamilton Standard, and ILC are the current contractors, deserve our recognition in this report.

In this research, a study was initiated to further extend the use of composite materials on the EMU. To accomplish this a new material was proposed by Rice University and accepted by NASA/JSC for development, an inventory of the existing materials on the EMU was completed, studies of the EMU requirements and of new composite materials were initiated, and design synthesis was accomplished. In this report the details of the various tasks will be elaborated. Task I, the development of the new materials of fullerene reinforced aluminum and stainless steel, is a multi-year project. The premise of the design will be given, as will the status of the project and the future plans for the material development. Task II is the inventory of the materials used on the space suit assembly (SSA), the SSA properties requirements and the design synthesis is also a multi-year project and this will be discussed. And Task III is the study of the new and available composite materials, this too will be the subject of a continuing study, which will be discussed in this report.

The significant accomplishments which will be discussed in this report include: the attainment of fullerene reinforced material samples, the inventory of the materials used on the EMU, the findings of a study of beryllium and Be alloys, the findings from a study on composite materials which are carbon and glass reinforced polymer matrix materials, the findings from the design synthesis, and a plan by which the work initiated here will be continued. Other findings obtained during this study, such as the preliminary findings of a study of anodized coatings, which is a side

effort, will also be contained in this report for completeness. The detailed findings of that discussed in this report can be obtained from the authors.

## **COMPOSITE MATERIALS: DEVELOPMENT, SELECTION, DESIGN, AND EVALUATION**

### **Composite development**

In the early Spring of 1992 Dr. E. V. Barrera and D. L. Callahan started development of a material which would have as a second phase or reinforcing phase the recently discovered fullerenes, the most famous of which, the Buckminsterfullerene C<sub>60</sub> called "Bucky balls" [1,2]. The premise of the design was that the fullerenes, which are nanometer size molecules, would serve as a strengthening and toughening agent in structural matrices such as aluminum and stainless steel. Use of the fullerenes would lead to substantial weight savings. Aluminum has a density of 2.7 gm/cm<sup>3</sup> (0.1 lb/in<sup>3</sup>) and iron in the stainless steel has a density of 7.87 gm/cm<sup>3</sup> (0.285 lb/in<sup>3</sup>) while carbon has a density as high as 2.22 gm/cm<sup>3</sup> (0.08 lb/in<sup>3</sup>) compared to the C<sub>60</sub> with a density of 1.2 gm/cm<sup>3</sup> (0.043 lb/in<sup>3</sup>). Strengthening would come from fullerene properties including, the soccer ball shape of the C<sub>60</sub> (see Figure 1), their capability of being deformed, and their proven chemical stability as reported in numerous papers including that by R. E. Smalley of Rice University who was a principal discoverer of fullerenes [3].

The project is at a stage where composite samples have been made and a fullerene production chamber has been assembled. The processing of composite samples was conducted by Hector M. Tello and E. V. Barrera. The first generation sample of fullerene reinforced aluminum was produced with a concentration of fullerenes not exceeding 1%, yet enough to show that mechanical deformation processing would lead to a final sample. NASA's interest in this material sparked by Dr. F. S. Dawn, E. S. Orndoff, and Dr. C. Lin, occurred early in this development process and soon the sample development was directed toward materials to be used on the astronaut primary life support subsystem (PLSS). The material now had a well defined and highly visible application whereby further fullerene composite research by other researchers was sure to follow.

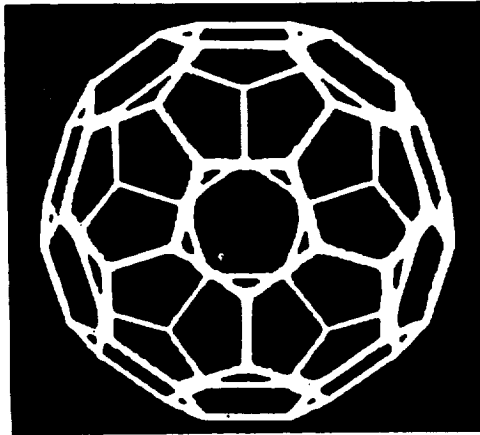


Figure 1. The truncated icosahedron soccer ball structure of the fullerene  $C_{60}$ .

Fullerene reinforced material (FRM) development was set and has followed a well defined plan. Dr. Barrera conducted the material processing while at the Johnson Space Center as a NASA/ASEE Summer Faculty Fellow. The Rice University student participant in the NASA/ASEE Summer Program, H. M. Tello would be partly involved in this work. During this time, fullerenes and fullerene containing soot [4] were purchased from Polygon Enterprises in Waco, TX, matrix materials were obtained without cost and processing was continued with appropriate experimental analysis. Early samples were processed with a pure aluminum matrix, processing was conducted during the NASA/ASEE summer term using a 7075-O matrix where the final properties of the composite were expected to surpass that of a 7075-T6 material. This material was obtained at no cost to the project. 2219-T851 aluminum will be used as the project continues because this is the material used by Hamilton Standard for fabrication of the current PLSS. The results to be discussed here will be directed toward that of the pure Al and 7075 matrix fullerene reinforced materials.

During the summer term Dr. Barrera also started work on the assembly of a fullerene production chamber based on carbon arc generation of fullerenes [4]. The chamber was assembled yet fullerene production was not started until after the summer program was over. The purpose of the production chamber or "bucky ball factory" was to allow for production of the fullerenes rather than continuing to buy the

fullerenes at a price of \$20/gm (\$9000/lb). A site visit is planned for August 24, 1992 to observe the Bucky Ball Factory in use.

Sample processing by a mechanical deformation method involved rolling of sheets and foils with fullerenes sandwiched in between. The foil surfaces were roughened to insure mechanical bonding. The fullerenes were suspended in toluene and applied to the surface using an eye dropper. The toluene would evaporate leaving the fullerenes on the surface of the foils. The foils with the fullerenes on the inner surfaces were laid up between steel patents and rolled to a reduction where the limit was the formation of edge cracks. Careful hardness measurements and annealing treatments were used to minimize edge cracking. Additional materials analysis was in the form of x-ray diffraction (XRD) conducted by D. L. Callahan and E. V. Barrera. XRD of the fullerenes and the soot show distinct differences in the x-ray powder patterns. The soot had peaks for that of graphite while the fullerenes showed peaks for a crystalline carbon structure. Even though the soot contained fullerenes of a percentage of 2-5% the powder pattern did not show this, indicating that the fullerenes were well dispersed in the soot and not in a crystalline form.

The following abstract has been submitted to the Fall 1982 TMS Conference in Chicago: E. V. Barrera, H. M. Tello, D. L. Callahan, E. S. Orndoff, and F. S. Dawn, "Emerging Composites with Fullerene Reinforcements" and was well received. The work is in progress and Dr. Barrera will present this paper at the conference.

## **Selection and design**

In this section the inventory of the non-metallic materials, which includes the nonflexible materials, will be discussed. This study by E. S. Orndoff was to be the first stage of her Rice University graduate research. It also has served to better familiarize herself with the EMU of which her NASA responsibilities are focused. The inventory discussed here will focus on the SSA only and not on the PLSS [5]. In this study each component of the suit including the arm, lower torso assembly, glove, Hard Upper Torso (HUT), liquid cooling ventilation garment, helmet, extravehicular visor assembly, and urine collect device were reviewed. The review was directed toward investigating the current materials used, to

determine the requirements (project conditions) and potential areas where composite materials could be used or designed to reduce weight [6].

### Thermoplastic and thermoset materials

The major groups of non-metallic materials used in the Space Shuttle EMU (this was the subject EMU of the inventory) which are on the SSA are thermoplastic polymers, elastomers, fluorocarbons, fiberglass, adhesives, and lubricants [5]. Some general requirements are imposed on the entire SSA. The suit must be lightweight, resistant to wear, abrasion, and tear. They must resist fungi and bacteria growth, and be nontoxic. They must resist extreme temperatures, be nonflammable, and protect against impact of orbital debris and micrometeoroids. However, these requirements vary from one component of the suit to another.

Among the thermoplastic polymers, two groups are prominently represented in the SSA: polyamides and polyesters. The polyamides are nylon and two aramids: Nomex and Kevlar. The polyesters are woven Dacron fiber and mylar film. The properties of nylon and Dacron are similar, differences occur in that where both melt and drip at around 250°C (482°F), they can be distinguished from one another by the odor and the smoke. They have excellent fatigue properties, the same modulus and strength, with the exception of the high tenacity polyester. They differ in elongation properties, moisture regain and overall chemical resistance. Nylon can elongate twice as much as a polyester and regains ten times more moisture than the polyesters. The aramids used in the space suit are in the form of flexible fibrous woven structures to cover and protect the astronaut's body and accommodate body mobility (another requirement). Nomex and Kevlar have similar molecular structures, they both contain aromatic rings which contribute to their increased thermal stability. Both polyamides and polyesters satisfy the general requirements previously mentioned. However, for the components of the suit where flammability resistance is an essential criterion, only the aramids can be used.

In general woven polyamides and polyesters have been used successfully in the different areas of the space suit. Some consideration has been given to making changes where a single layer will be used to replace two or more layers. This would only be of interest if a weight loss occurs and if the astronaut's mobility is increased. One problem was cited in that

the aluminized mylar used for its thermal radiative properties can tear easily even with the nylon scrim reinforcement. The nylon scrim has also been shown to separate from the aluminized mylar. It is also prone to blocking of the adjacent layers. Research has shown that these conditions have not effected the thermal radiative properties of the material. As EVA time is increased and suits become non retrievable, it may be necessary to further consider these physical properties.

## **Elastomers**

The different elastomers used in the space suit are spandex, polyurethane, neoprene, and silicone rubber. The critical properties for these materials are strength and moderate elongation. The applications are diverse and include using polyurethane and neoprene for coatings on woven nylon, flocked polyurethane film used as the pressure bladder on the glove, and patterned silicone rubber RTV 157 used on the palms and fingers to provide non-skid surfaces. The gloves are designed with excess material which forms folds when pressurized and this aggravates the bulkiness of the glove. Research indicates that the astronaut's hands become too cold when at rest and easily overheat when at work. Increased mobility and improved thermal management are on going research topics for the glove.

In addition to the glove and pressure bladder, elastomers are also used for micrometeoroid protection. A neoprene-coated nylon woven fabric provides some protection against small particle impact but this protection is minimal and does not substantially reduce the risk of injury. As EVA time is increased as will occur with the building of the space station and lunar bases, etc., the potential of micrometeoroid collisions increases therefore better protection becomes more important.

## **Fluorocarbons**

Teflon fluorocarbon fibrous structures are used on the TMG as the outermost material exposed to the environment. It was chosen for its unique combination of properties which are relatively independent of fabrication conditions; stability at high temperatures, low coefficient of friction, and flexibility at low temperatures. Chemically it is also resistant

to corrosive reagents, nonflammable, nonsoluble, and nonabrasive. Teflon has proved to be a good outer layer of the suit for occasional and short duration EVA's. However, since Teflon is not resistant to atomic oxygen, it is a less likely candidate for long duration EVA's. Therefore, more research is needed to develop a suit protection with atomic oxygen exposures in mind.

## **Fiberglass**

Fiberglass molded with epoxy resin is currently used as the Hard Upper Torso (HUT). In combination with the metal bearings on the suit, the HUT contributes to most of the weight on the EMU with exception of the PLSS. Presently materials are being developed (see the section on fullerene reinforced materials being designed for the PLSS but also useful on the HUT), and other are considered (Be and Be alloys and carbon or glass reinforced composites, see the next section on Evaluation) to replace the fiberglass/epoxy currently used.

## **Summary**

In summary, with the exception of the adhesives and the lubricants, eight components of the suit were researched where the following five points are suggested for further consideration.

- 1. Materials development for thermal protection of the suit in general could be considered.**
- 2. Improvement of micrometeoroid protection of the suit especially as the number and duration of EVA's increase.**
- 3. Reduction of the bulkiness and improved mobility of the glove by considering different or developing new elastomeric materials.**
- 4. Development of a material for protection against atomic oxygen bombardment.**
- 5. Reduction of the total weight of the suit by considering FRM's, beryllium and Be alloys and carbon and glass reinforced composites.**

## **Evaluation**

### **Rigid materials for possible EMU use**

In this section an evaluation of rigid materials for possible EMU use, which include beryllium and Be alloys and polymer matrix composites, will be discussed. This review was the subject of the NASA/ASEE project set aside for the Student Participant, Hector M. Hello. Included in this section will be brief comments on anodized coatings ultra-violet (UV) radiation sensitivity.

### **Beryllium and Be alloys**

Perhaps the reason a study of Be and Be alloys for space applications comes up every so often is attributed for the most part to their high specific mechanical properties. Beryllium has a density of  $1.85 \text{ gm/cm}^3$  ( $0.067 \text{ lb/in}^3$ ) compared to Al with a density of  $2.7 \text{ gm/cm}^3$  ( $0.1 \text{ lb/in}^3$ ) and Ti with a density of  $4.5 \text{ gm/cm}^3$  ( $0.160 \text{ lb/in}^3$ ). The low density attributes to a specific modulus approximately 4.5 times that of Al, Ti, and Fe. The fact that the Be materials can be rolled into sheets or extruded into bar, rod or tubing is also attractive. Beryllium can also be machined to close tolerances and can be joined by brazing and adhesive bonding. The disadvantages are anisotropic properties, forming constraints and of course the toxicity hazard. While Be materials have high specific strengths they are still inherently brittle and have a low fracture toughness [7,8]. This is important from the standpoint of impact loading where even small defects in the material will lead to crack advancement. Still they exhibit good fatigue properties and a coefficient of thermal expansion well matched to that of stainless steel, nickel and cobalt. It is also clear that these materials can withstand continuous operation at temperatures up to  $260^\circ\text{C}$  ( $500^\circ\text{F}$ ) depending on the strength requirements.

As for manufacturing, Be is available in pressed billets, sheet, plate, rod, bar, and tubing. Billet sizes are from  $0.8 \times 0.75 \text{ m}$  ( $32" \times 30"$ ) up to  $1.8 \text{ m}$  ( $72"$ ) diameters by  $1.7 \text{ m}$  ( $66"$ ) lengths [9]. Forming requires temperatures in the range of  $700\text{-}732^\circ\text{C}$  ( $1300\text{-}1350^\circ\text{F}$ ) where sheet bends up to  $90^\circ$  are possible. Chemical milling is typically required before forming to prevent microcracking. Machining is possible but damage is

usually caused and must be removed. Beryllium can be anodized as well as plated with nickel, silver, gold or aluminum.

Where improved manufacturing is needed, Be alloys (Be-Al) are being developed. Alloys such as Lockalloy (Be 38 Al) have been around for at least twenty years [10] and similar alloys are being considered in the National Aerospace Plane (NASP). The Be alloys exhibit an elastic modulus much closer to that of aluminum and increased density but also offer superior forming and deformation characteristics compared to pure beryllium.

#### **Be design considerations and remarks**

The properties of beryllium and Be alloys are directly related to its microstructure therefore precise controls must be used in all forming and machining operations. Fastening of Be to other materials is preferred compared to bolting. Match fit holes are usually required to minimize stress concentrations and because the anisotropic behavior of the Be does not redistribute applied stresses as well as aluminum or steel. NSTS 14046, Payload Verification Requirements, details specific requirements for use of Be such as:

1. machined/mechanically disturbed surfaces must be chemically milled to ensure removal of surface damage,
2. all Be components must be penetrant inspected for crack-like flaws,
3. provisions must be made for containment of unconstrained pieces of a failed part.

Evaluation of Be materials has been that even though they periodically are considered for aerospace applications, they are frequently not selected because of their low fracture toughness, their special manufacturing requirements and toxicity issues. The data base for beryllium within NASA dates back to pre-Apollo days. The typical cost of manufacturing a Be part is about 3 times that of the same aluminum component although the additional safety and verification requirements may increase the final cost substantially.

## Polymer matrix composites

### Reinforcements

Polymer matrix composites were considered in this study for replacement materials for metallic materials on the PLSS and HUT on the EMU, MKIII, and other prototype suits. The criteria were weight savings, impact resistance, good strength and modulus, meeting the requirements of flammability, toxicity, thermal vacuum stability, and manufacturing ease and flexibility. Reinforcement materials that were considered were carbon fibers, Kevlar, E-glass and S-glass. Coefficients of thermal expansion (CTE) are important when reinforcements are incorporated into a matrix. The CTE's of glass reinforcements are better matched to the matrices than that of carbon and Kevlar. The reinforcements have comparable strength levels as compared to their matrix counterparts. In comparison, glass and aramid reinforced composites exhibit 2 to 3 times the impact strength of the carbon reinforced composites [11] however, the compression after impact strength of the carbon reinforced materials is substantially greater for moderate impact levels. The density of the glasses are greater than that of carbon therefore weight savings is compromised. Aramids offer the most weight savings but also have the lowest compression strength. From an impact and CTE matching standpoint, S-glass appears to be the best candidate. For maximum weight savings carbon fibers are typically used yet hybrid materials such as mixtures of graphite and glass layered with Kevlar or graphite are seeing increasing usage. Stitching with aramid yarn has also shown to increase the impact resistance of polymer matrix/carbon reinforced composites.

### Matrix materials

Three types of matrix materials were considered in this study: toughened epoxies, cyanate esters, and thermoplastics. Toughened epoxies are the most widely used, they offer good impact resistance, good hot/wet properties, and low moisture absorption. Maximum service temperature for these materials is typically in the 90-150°C (200-300°F) range. The material that was used in the prototypical hardware exhibits good impact resistance and was a good selection.

Cyanate esters (CE's) generally exhibit the same mechanical properties as the toughened epoxies but are superior in toughness. Some of the newer materials are 2-7 times tougher than the epoxies. CE's have a higher service temperature where the glass transition temperature is higher than that of epoxies [12]. They are also capable of being used at much lower temperatures. They exhibit less outgassing and better dimensional stability.

Polyetheretherketone (PEEK) has become the thermoplastic matrix of choice in the aerospace industry. The density and mechanical properties of PEEK are approximately that of epoxies and its toughness is several times that of epoxies. The material ratings for PEEK are "A" for flammability in the cabin environment, "K" for toxicity (over 100 lbs usage is acceptable), and "A" for TVS after vacuum cured a few hours. Thermoplastics are favored to thermoset materials for repair and post forming operations. In fact, thermoplastics can be repaired by re-melting or by local heating (welding or ultrasonic welding).

#### **Polymer composite considerations and remarks**

Where the PEEK has pronounced superior properties to the other polymeric matrices mentioned, it has a lower glass transition temperature than the epoxies which limits its operating temperature. Furthermore, the percent crystallinity of the thermoplastics must be taken into consideration as well when it comes to long term operations. The data base for thermoplastics is large with extensive work having been done at Wright R&D Labs and by NASA-LaRC.

#### **Further remarks on polymer matrix composites**

1. The use of S-glass/epoxy may offer weight savings of 25% or more over aluminum.
2. Kevlar reinforced composites offer the best weight savings and good impact resistance. However, consideration must be given to the negative CTE (poor coefficient of thermal expansion matching with the matrix) and UV sensitivity in their design.

3. Thermoplastics matrices have superior impact resistance although their service temperatures may limit their use.
4. When designing hardware for a manned mission to the moon or Mars, consider the ability to repair damaged component.
5. This study is a continuous process since new materials are continually being developed for FAA and DoD applications.

#### **Anodized coatings**

Hector Tello and E. V. Barrera also worked with Steve Jacobs in the Structures and Mechanics Division (SMD) on anodized coatings, their UV radiative properties. Samples were obtained from McDonnell Douglas, Huntington Beach, optical properties were measured, x-ray photoelectron spectroscopy was conducted, and transmission electron microscopic samples are being made. An extensive literature search is underway.

### **CONCLUSIONS AND FUTURE WORK**

The significant accomplishments include the attainment of fullerene reinforced material samples, the assembly of the "Bucky Ball Factory", the inventory of the materials used on the EMU, the findings from the design synthesis, the findings from the study of beryllium and Be alloys and that from the study of composite materials which are carbon and glass reinforced.

The plan by which the work initiated here will be continued includes a Rice graduate student, John Sims to continue the research on the fullerene reinforced materials with Drs. Barrera and Callahan. Dr. Barrera will continue to work with the Systems Engineering Analysis Office in the continuing study of composite materials to be used on the EMU. It is likely that this may be on a consulting basis. Hector Hello will continue to be a part of the fullerene reinforced materials project but will direct a majority of his time toward the study of anodized coatings for space station radiator applications.

## REFERENCES

1. Kroto, H. W., et al., "C<sub>60</sub>: Buckminsterfullerene", *Nature*, 318 (1985) 162-163.
2. Kratschmer, K., et al., "Solid C<sub>60</sub>: a new form of carbon", *Nature*, 347 (1990) 354-357.
3. Smalley, R. E., "Great Balls of Carbon", *The Sciences*, Mar./Apr. (1990) 22-28.
4. Haufler, R. E., et al., "Carbon Arc Generation of C<sub>60</sub>". *Mat. Res. Symp.*, 206 (1991) 627-637.
5. Hamilton Standard internal publication, Space Shuttle Extravehicular Mobility Unit, Space Suit Assembly (SSA)-Mini Data Book.
6. *Textile World*, 138 (8) (1982).
7. Lemon, D. D. and Brown, W. F., Jr., "Fracture Toughness of Hot-Pressed Beryllium", *J. Testing and Evaluation*, 113 (2), Mar. (1985) 152-161.
8. MIL-HNBK-5.
9. Brush Wellman Catalog, (1989).
10. Final Report for Evaluation of Beryllium for Space Shuttle Components, LMSC-D159319, Sept., (1972).
11. *Eng. Mat. Handbook*, v. 1-Composites, ASM Intern., (1987).
12. *Adv. Composites*, 7 (3), (1992) 28-37.



**INVESTIGATION OF THE EFFECTS OF EXTRA VEHICULAR ACTIVITY (EVA) AND  
LAUNCH AND ENTRY (LES) GLOVES ON PERFORMANCE**

**Final Report  
NASA/ASEE Summer Faculty Fellowship Program-1992  
Johnson Space Center**

<b>Prepared by:</b>	<b>Ram R. Bishu, Ph.D.</b>
<b>Academic Rank:</b>	<b>Associate Professor</b>
<b>University and Department</b>	<b>Industrial and Management Systems Engineering Department, University of Nebraska-Lincoln, Nebraska 68588-0518</b>
<b>NASA/JSC Directorate:</b>	<b>Space and Life Sciences</b>
<b>Division:</b>	<b>Man Systems</b>
<b>Branch:</b>	<b>Crew Interface Analysis</b>
<b>Laboratory:</b>	<b>Anthropometry and Biomechanics</b>
<b>JSC Colleague:</b>	<b>Glenn Klute</b>
<b>Date Submitted:</b>	<b>August 5, 1992</b>
<b>Contract Number:</b>	<b>NGT-44-005-803</b>

## ABSTRACT

Human capabilities such as dexterity, manipulability, and tactile perception are unique and render the hand as a very versatile, effective and a multipurpose tool. This is especially true for unknown environments such as the EVA environment. In the microgravity environment interfaces, procedures, and activities are too complex, diverse, and defy advance definition. Under these conditions hand becomes the primary means of locomotion, restraint and material handling. Facilitation of these activities, with simultaneous protection from the cruel EVA environment are the two, often conflicting, objectives of glove design. The objectives of this study was a) to assess the effects of EVA gloves at different pressures on human hand capabilities, b) to devise a protocol for evaluating EVA gloves, c) to develop force time relations for a number of EVA glove-pressure combinations, and d) to evaluate two types of launch and entry suit gloves. The objectives were achieved through three experiments. The experiments for achieving objectives a, b, and c were performed in the glove box in building 34. In experiment 1 three types of EVA gloves were tested at five pressure differentials. A number of performance measures were recorded. In experiment 2 the same gloves as in experiment 1 were evaluated in a reduced number of pressure conditions. The performance measure was endurance time. Six subjects participated in both the experiments. In experiment 3 two types of launch and entry suit gloves were evaluated using a paradigm similar to experiment 1. Currently the data is being analyzed. However for this report some summary analyses have been performed. The results indicate that a) With EVA gloves strength is reduced by nearly 50%, b) performance decrements increase with increasing pressure differential, c) TMG effects are not consistent across the three gloves tested, d) some interesting gender glove interactions were observed, some of which may have been due to the extent (or lack of) fit of the glove to the hand, and e) differences in performance exist between partial pressure suit glove and full pressure suit glove, especially in the unpressurized condition.

## INTRODUCTION

Human capabilities such as dexterity, manipulability, and tactile perception are unique and render the hand as a very versatile, effective and a multipurpose tool. This is especially true for unknown environments such as the EVA environment. In the microgravity environment interfaces, procedures, and activities are too complex, diverse, and defy advance definition. Under these conditions hand becomes the primary means of locomotion, restraint and material handling. Facilitation of these activities, with simultaneous protection from the cruel EVA environment are the two, often conflicting, objectives of glove design. The conflict associated with providing hand protection while permitting adequate hand functioning has been widely recognized. Hand gloves are the primary protection device for the hands.

Numerous articles have been published in the area of the effect of gloves on task performance. Lyman and Groth (1958) reported that when gloves were worn, subjects exerted more force than when bare handed while inserting pins into a pegbox. Bradley (1969) studied the operation time of five types of control tasks with bare hand, wool gloves, and leather over wool gloves. The results of his research showed that the operation time depends on the type of gloves, the type of control operations, and the physical characteristics of the controls. Cochran et al (1986) studied grasp force degradation of some commercially available gloves. Five types of gloves and bare hand conditions were compared and the results showed that all the gloves tested reduced the maximum grasp force significantly when compared to bare hand condition. Wang et al (1987) also found similar results. The most common finding from all the published studies on gloves is that hand performance is compromised with gloves.

While most of the studies have addressed performance compromises with commercial gloves, very few studies have attempted to assess the effects of EVA gloves on basic hand capabilities (see O'Hara et., al., (1988) have provided a detailed list of the studies that have assessed the impact of EVA gloves on hand capabilities. The authors have also listed some of the non EVA pressure glove studies. The overall findings of these studies are a) gloves reduce strength capabilities, and b) gloves reduce dexterity and manipulability. The studies listed in Table 1 have each assessed certain aspects of glove effect on performance. Perhaps the most comprehensive study performed on the assessment of performance decrements with EVA gloves is the one done by O'Hara et. al. (1988). The authors had studies two levels of hand conditions (gloved and bare handed), two levels of pressure differential (0 psid, and 4.3 psid), and three levels of hand size (small, medium, and large). 11 subjects participated in an experiment where six categories of performance measures were recorded. The performance categories were 1) range of motion, 2) strength, 3) tactile perception, 4) dexterity, 5) fatigue, and 6) comfort. The salient findings were:

- 1) On the range of motion the glove and pressure effects were diverse and motion dependent. Effects for flexion were different from that for extension.
- 2) Glove reduced grip strength and pressure reduced it further. However, neither the glove nor the pressure had any effect on pinch strength.
- 3) The degradation in tactile perception was more with glove than with pressure.
- 4) Dexterity was reduced by both glove and pressure. Unpressurized glove reduced dexterity by 50%, while pressurizing reduced it further by 30%.
- 5) The fatigue effects were most uninterpretable due to complex EMG signatures at different test conditions.
- 6) Perceived comfort reduced by 100% with unpressurized gloved conditions. Pressurizing reduced it further by 600%.

The rationale for this investigation evolved out of the above study. The O'Hara (1988) investigation used one type of glove and one pressure level. It is recognized that in EVA tasks the prebreath time before donning the suit is a function of the pressure. Greater the pressure, shorter the prebreathing time. However, the performance decrement is also a function of pressure, with larger decrements at greater pressure. An important information that is needed, and which is currently unavailable, is the pressure performance profile for the various EVA gloves. Therefore one of the objective was to develop functional relations between performance decrements and pressure differential for EVA gloves.

O'hara et. al., (1988) measured fatigue through shifts in the median frequency of the EMG power spectrum. The results were uninterpretable for a number of reasons. A number of researchers have used the functional relationship between force exerted by a muscle group and the time of endurance as a predictor of muscle fatigue (Rohmert, 1960; Monod and Scherrer, 1965). In general endurance time increases with decreasing force. Bishu et. al. (1989) have used endurance time for evaluating container handles. The second objective was to develop force time relationships for a variety of EVA glove - pressure combinations.

A third objective for this study evolved out of the reasoning that while some research existed on the effects of EVA gloves on performance, none existed for the effects of launch and entry suit (LES) gloves.

#### OBJECTIVES

1. To assess the effects of EVA gloves at different pressures on human hand capabilities.

2. To devise a protocol for evaluating EVA gloves.
3. To develop force time relations for a number of EVA glove-pressure combinations.
4. To evaluate two types of launch and entry suit gloves.

The objectives were achieved through three experiments described below.

#### EXPERIMENT 1

**Objective:**

To assess the effects of eva gloves at different pressures on human hand capabilities.

**Subjects:**

Six subjects (three males and three females) participated in this experiment. Their participation was voluntary.

**Independent variables:**

The independent variables tested in this experiment were gender, glove type, pressure differential, and glove make. The six subjects were equally split between two genders to provide the gender differences. Two types of glove assembly were used namely, with and without thermal meteorite garment (TMG). An EVA glove is an assemblage of two major units-an inner pressurizing glove, and an outer TMG glove. One of the objective was to assess the exact effect of TMG on performance. Current shuttle gloves operate at 4.3 psid. Certain developmental gloves are being designed to operate at 8.3 psid. The rationale being at higher pressure differentials the prebreathing time is reduced considerably. Five levels of pressure differentials were used in this experiment ie., 0 psid, 3.2 psid, 4.3 psid, 6.3 psid, and 8.3 psid. The intent was to develop a pressure-performance decrement profile. Three different gloves were tested here, namely current shuttle gloves (referred to hereafter as GLOVE C), and two developmental gloves (referred to hereafter as GLOVES A and B). To summarize the independent variables with their respective levels were:

- |               |                       |
|---------------|-----------------------|
| 1. Gender     | male and female.      |
| 2. Glove type | with and without TMG  |
| 3. Pressure   | 0, 3.2, 4.3, 6.3, 8.3 |
| 4. Glove make | A, B, and C.          |

**Performance measures:**

The performance measures were selected based on the O'Hara (1988) study, and comprised two strength measures (grip and pulp pinch strength), two dexterity measures (nuts-bolts test, and rope tying test), and a tactility measure (two point discrimination test). The criteria for selection of performance measures were a) they should be generic, and hence repeatable, and b) they should be reasonably representative of the EVA

activities. Grip and pinch strengths measure a person's force capabilities, while the two point discrimination test provides a valid measure for tactility. Dexterity and manipulability were measured by the the rope tying test, and the nuts-bolts test.

**Glove box:**

The testing was done in Advanced Suit Laboratory in Building 34. The actual tests were conducted inside a glove box. The glove box is cylindrical in shape, approximately 2 ft in diameter and 4 ft in length with an internal volume of 13 ft<sup>3</sup>. On either sides of the glove box were two end caps, made of plexiglass and bolted through 8 bolts. About midway along the axis of the glove box were 2 six in. circular openings in the cylinder wall, placed shoulder width apart, which provided access and attachment points for the EVA glove and arm assemblies. The glove box was connected to a vacuum pump and could be evacuated to any desired pressure level. There was a gauge on the outer cylinder wall calibrated to read the pressure differential inside.

**Procedure:**

The levels of independent variables were factorially combined to yield 26 experimental conditions. There were 26 experimental conditions in this experiment (see table 1). The order of presentation of these was randomized for each subjects.

Table 1: Experimental design

GLOVE CONDITIONS						
PRESSUR	A	A with TMG	B	B with TMG	C	C with TMG
0 psi						
3.2 psi						
4.3 psi						
6.3 psi					na	na
8.3 psi					na	na

In addition all the subjects performed a 'Bare handed' condition on the last day. Within a condition the order of presentation of the five tasks (grip, pinch, nuts-bolts, rope tying, and 2PD test) was also randomized for each subject. As stated earlier six subjects participated in this study. Gender was a between subject factor. Each subject performed one condition per day, resulting in 26 days of experimentation in all. A trial consisted of the following steps.

1. The glove box was pressurized to the required level.
2. The subject donned a pair of comfort gloves and the gloves for that day's trial.

3. Grip strength was recorded through a Jamar Hand Dynamometer connected to a digital read out, and to a Teac Recorder.
4. Pulp pinch strength was measured following a 2 minute rest period using a pinch gauge.
5. For the nuts-bolts test, three pairs of nuts and bolts (large medium and small size) were mounted on a wooden panel. The task involved removing the nut from its respective bolt, and mounting the nut back again. The time for this activity was recorded with a stop watch.
6. The rope tying test consisted of tying a simple shoe lace knot on the same wooden panel that had the nuts and bolts. Three sizes of ropes (small, medium, and large) were used and the time to tie was recorded with a stop watch.
7. 2 PD test consisted of the subjects sliding their right index finger along the edges of the 'V block'. The distance of the point at which they felt two edges from their starting point was recorded as their tactility score. In order to keep the force at the point of contact constant the 'V block' had a balancing weight on the other side (see Figure 1).

Figure 1 shows the sketch of the experimental set up with nuts-bolts panel, and the 2PD test. Figure 2 shows the sketch of the three gloves tested. A trial lasted for about 20 minutes. Figure 3 shows a sample data collection sheet.

#### Results:

As of writing this report the data is in a raw form and will be analyzed in the academic year 1992-1993. The complete results are expected to be written up as a NASA Technical Paper in that period.

## EXPERIMENT 2

#### Objective:

To develop force time relations for a number of EVA glove-pressure combinations.

#### Subjects:

Six subjects (three males and three females) participated in this experiment. Their participation was voluntary.

#### Independent variables:

The independent variables tested in this experiment were gender, glove make, pressure differential, and level of exertion. The six subjects were equally split between two genders to provide the gender differences. Three levels of pressure differentials were used in this experiment i.e., 0 psid, 4.3 psid, and 8.3 psid. The intent was to develop a pressure-performance decrement profile. Three different gloves were tested here, namely current shuttle gloves (referred to hereafter as GLOVE C), and two developmental gloves (referred to hereafter as GLOVES A

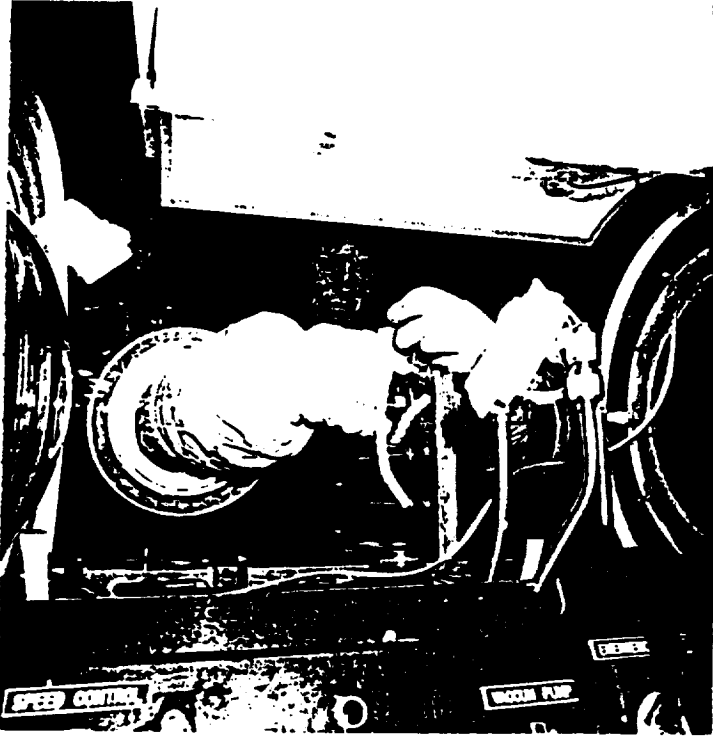


Figure 1: Nuts & Bolts Test: Experiment 1

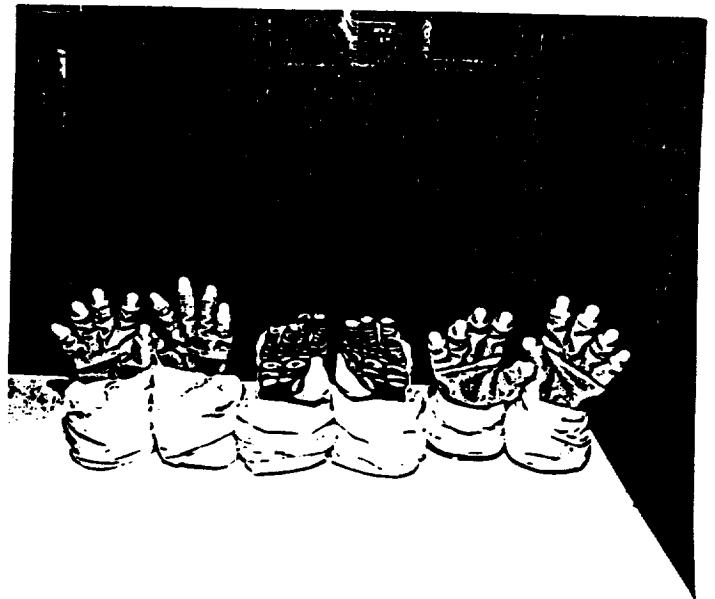


Figure 2: EVA Gloves: Experiments 1 & 2



Figure 3: Launch and Entry Suit Gloves

and B). Four levels of exertion, i.e., 100%, 75%, 50%, and 25% of maximal voluntary contraction were used here. The performance measure was the time to quit. To summarize the independent variables with their respective levels were:

1. Gender male and female.
2. Pressure 0, 4.3, 8.3
3. Glove condition A, B, C, and Bare hand
4. Level of exertion 100%, 75%, 50%, and 25%.

**Procedure:**

There were 36 different treatment conditions in this experiment. The order of presentation of the 36 conditions was randomized for each subject. Table 2 shows experimental design for this study.

**Table 2: Experimental design for Experiment 2:**

PRS	A 100%	A 75%	A 50%	A 25%	B 100%	B 75%	B 50%	B 25%	C 100%	C 75%	C 50%	C 25%
0 PSI												
4.3 PSI												
8.3 PSI									*	*	*	*

\* Bare handed condition at 100, 75, 50, and 25% MVC.

Initially the maximum voluntary contraction (MVC) for each glove-pressure combination was measured using a Jamar hand dynamometer. The dynamometer was wired to a TEAC recorder. The four levels of exertion at any glove-pressure combination was computed with respect to the MVC at that glove-pressure. A trial consisted of the following steps.

1. The exertion level for the 'condition of the day' was first calculated.
2. The subject then exerted to the computed level on the Jamar hand dynamometer.
3. The subject maintained the level of exertion for as long as he/she could, before quitting voluntarily.
4. The endurance time was recorded through the TEAC recorder and a stop watch.

A 24 hour rest period was followed between trials. As a result the subjects performed one trial per day for 36 consecutive days.

**Results:**

As of writing this report the data is in a raw form and will be analyzed in the academic year 1992-1993. The complete results

are expected to be written up as a NASA Technical Paper in that period.

### EXPERIMENT 3

#### Objective:

To evaluate two types of launch and entry suit gloves.

#### Subjects:

Ten subjects (five males and five females) participated in this experiment. Their participation was voluntary.

#### Independent variables:

The independent variables tested in this experiment were gender, and glove type. There were four glove conditions, namely unpressurized partial pressure glove (LES unpressurized), pressurized partial pressure glove (LES pressurized), unpressurized full pressure glove (ACES), and bare handed condition. Figure 3 shows the sketch of the gloves used in this experiment.

#### Performance measures:

The performance measures were selected based on the O'Hara (1988) study, and were similar to the ones used in Experiment 1 above. The measures comprised two strength measures (grip and pulp pinch strength), two dexterity measures (panel test, and rope tying test), and a tactility measure (two point discrimination test).

#### Procedure:

There were four treatment conditions in this experiment. The order of presentation of these was randomized across each subject. Within a treatment condition the order of presentation of the tasks (grip strength, pinch strength, panel test, rope tying, and 2PD test) was also randomized. A trial consisted of the following steps.

1. Grip strength was recorded through a Jamar Hand Dynamometer connected to a digital read out, and to a Teac Recorder.
2. Pulp pinch strength was measured following a 2 minute rest period using a pinch gauge.
3. The panel test consisted of flipping a number of toggle switches, and unscrewing/screwing a number of bulbs mounted on a panel. A panel with a large number of toggle switches, screwed bulbs was used in the test. The time for this activity was recorded with a stop watch.
4. The rope tying test consisted of tying a simple shoe lace knot on the same wooden panel that had the nuts and bolts. Three sizes of ropes (small, medium, and large) were used and the time to tie was recorded with a stop watch.

5. 2 PD test consisted of the subjects sliding their right index finger along the edges of the 'V block'. The distance of the point at which they felt two edges from their starting point was recorded as their tactility score. In order to keep the force at the point of contact constant the 'V block' had a balancing weight on the other side (see Figure 1).

#### Results:

As of writing this report the data is in a raw form and will be analyzed in the academic year 1992-1993. The complete results are expected to be written up as a NASA Technical Paper in that period.

### OVERALL DISCUSSION

The data for all the experiments described above are, currently, in a raw unanalyzed form. It is expected that they will be analyzed in the following months, and will be output as distinct NASA Technical Papers. However, in order to make this report complete, some rough summary analyses have been performed, and are described in this section. Figure 4 shows the plot of Glove effect on grip strength. It is seen that a) a significant gender effect exists, and b) Glove B, and C exhibit greater grip strength. The most glaring finding is that donning gloves reduces strength by nearly 50%. Figure 5 shows a plot of the pressure differential effect. As expected performance reduces with increasing pressure differential. It appears that there are two levels of performance decrements with pressure. Performance at 3.2 and 4.3 psi look similar while performance at 6.3 and 8.3 psi appear similar, and worse than other pressure differentials. Figure 6 shows the plot of TMG effect on grip strength. A Gender Tmg interaction appears to exist, with the female strength reducing with TMG, while the male strength increasing with TMG. Size and extent of fit may be causing this result. Figure 7 shows the plot of the TMG \* Glove interaction. Glove C seems to stand out from the other two. TMG seems to reduce strength on Glove C, while opposite effect is observed on gloves A, and B.

Figures 8 through to 12 deal with dexterity as measured by the total time taken on the Nuts and Bolts test. Figure 8 shows Glove effect. Two findings are interesting: a) there is a five fold decrease in dexterity when gloves are donned (60 seconds to 300 seconds), and b) male subjects' performance improves in the order A, B, and C; while female subjects' performance improves in the opposite order C, B, and A. Figure 9 shows the Pressure effect on dexterity, and as expected, performance is seen to decrease with increasing pressure. Figure 10 shows the TMG effect on dexterity. Again performance with TMG is superior to that without TMG. This was expected. However, what was not expected is shown in Figure 11. TMG \* Glove interaction on dexterity is shown in Figure 11. The TMG of glove B appears to be the best, while that of glove C is the worst. The results suggest that in case of glove C TMG does not change the performance level, while it does offer the needed protection.

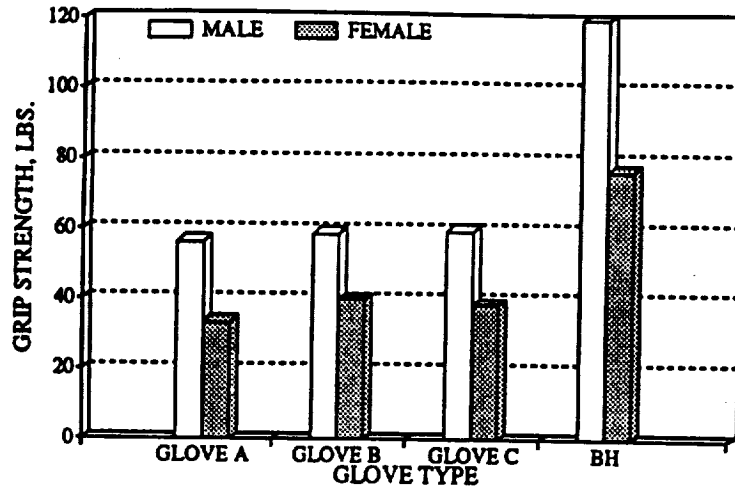


Figure 4: Glove Effect

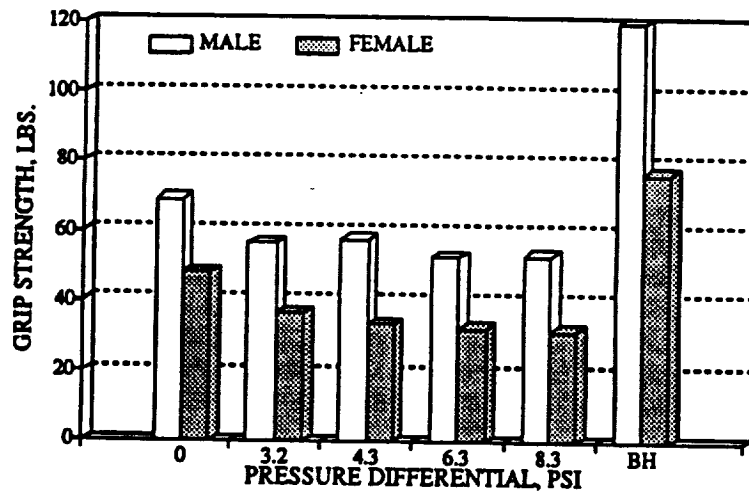


Figure 5: Pressure Effect

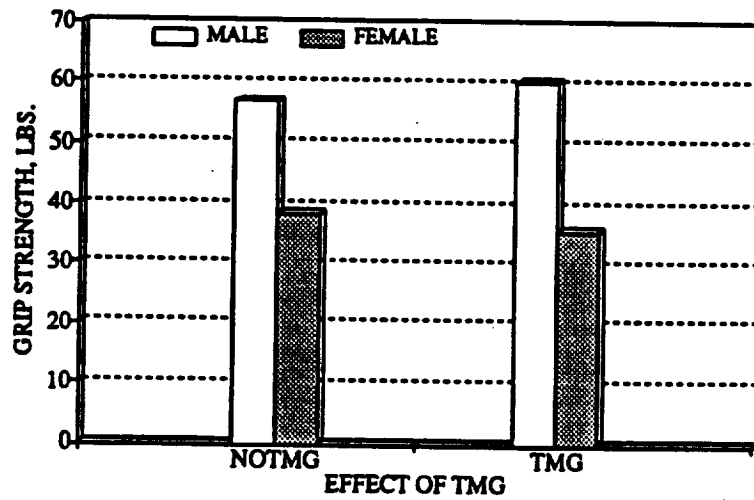


Figure 6: TMG Effect

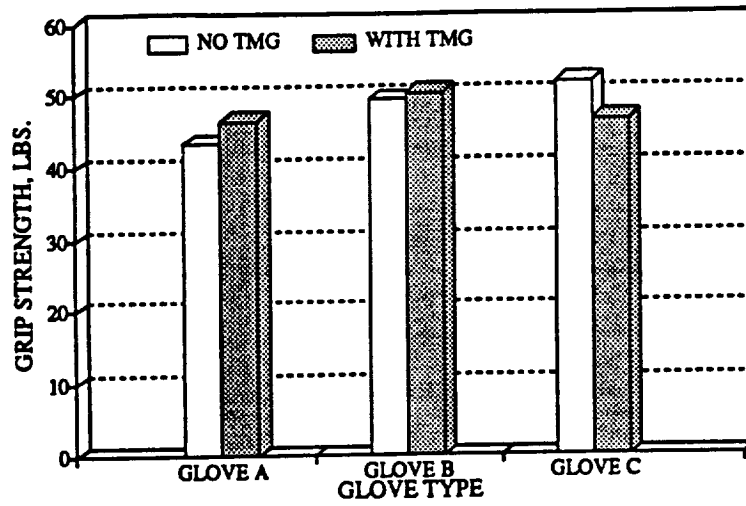


Figure 7: Glove x TMG Interaction

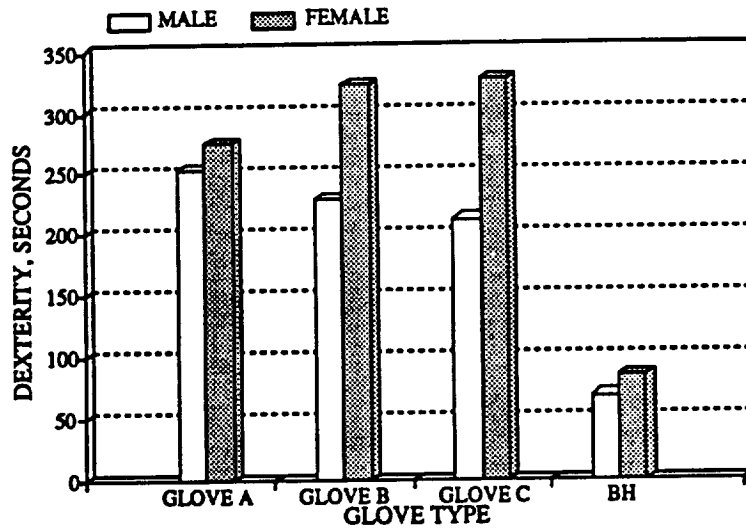


Figure 8: Glove Effect

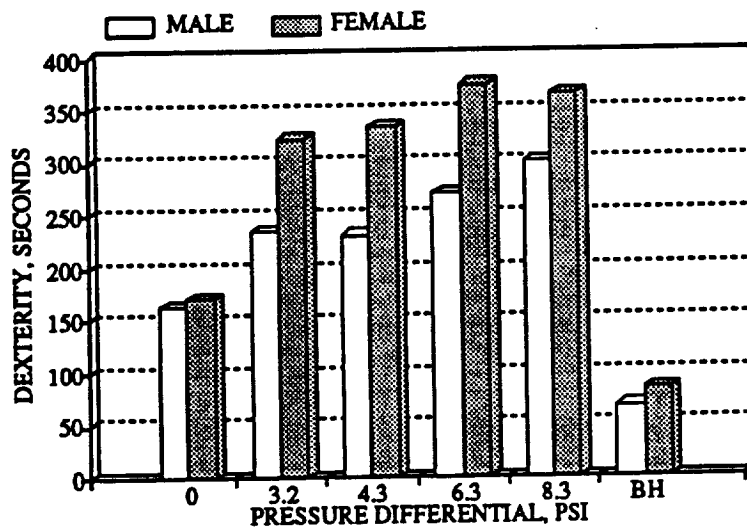


Figure 9: Pressure Effect

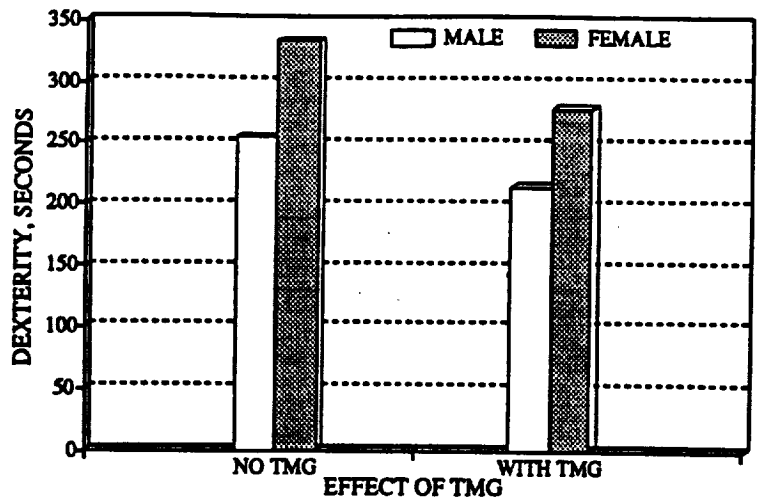


Figure 10: TMG Effect

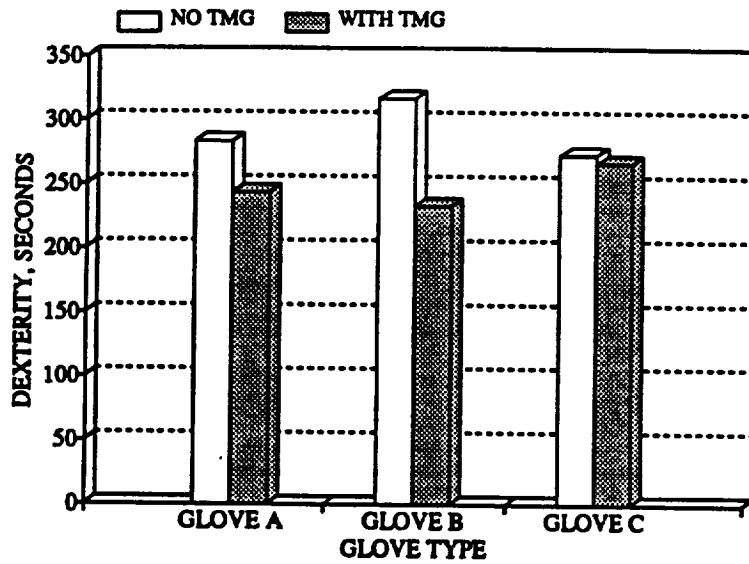


Figure 11: TMG Glove Interaction

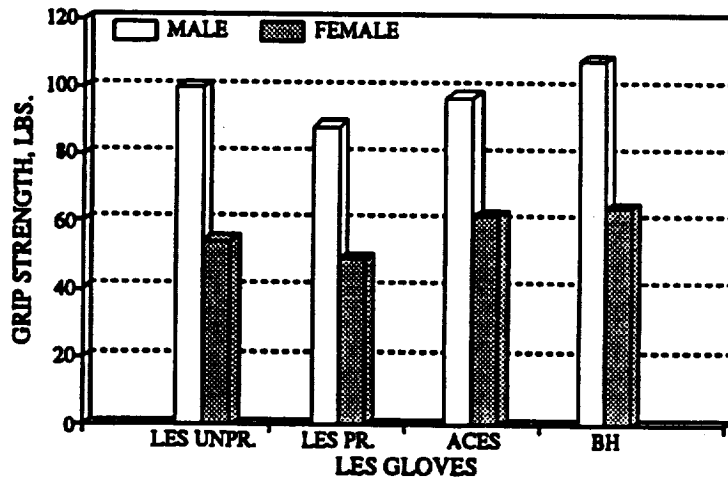


Figure 12: Glove Effect: Experiment 3

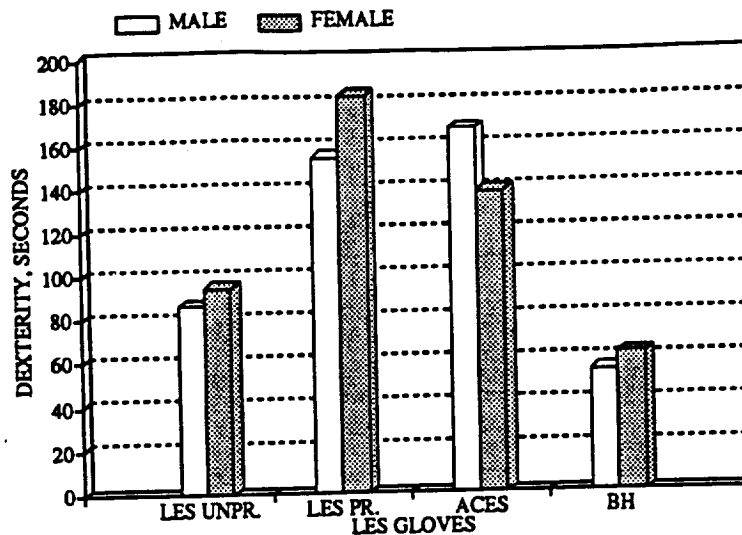


Figure 13: Glove Effect: Experiment 3

The TMG of glove B, and A in addition to the providing protection against environment seem to improve performance as well.

Figures 12 and 13 deal with the summary analysis of experiment 3 described above. Figure 12 shows the plot of Glove effect. The strength decrement is largest in case of LES glove pressurized to 2.8 psi (approximately 80% of the bare handed strength). The full pressure gloves (ACES) and partial pressure gloves seem to have similar performance in the unpressurized condition. Figure 13 shows the plot of Glove effect on dexterity, as measured by the total time taken on the panel test. The full pressure suit glove appears to be worse in performance than the partial pressure suit glove in the unpressurized condition.

### CONCLUSIONS

Although the detailed analyses is still to be done, the summary analysis described above reiterates the fact that gloves do reduce hand capabilities. The findings can be summarized as follows:

1. Strength is reduced by nearly 50%.
2. Performance decrements increase with increasing pressure differential.
3. TMG effects are not consistent across the three gloves tested. More research is needed.
4. Some interesting gender glove interactions were observed. Some of these may have been due to the extent (or lack of) fit of the glove to the hand.
5. Differences in performance exist between partial pressure suit glove and full pressure suit glove, especially in the unpressurized condition.

### REFERENCES

A complete list of references on this report will be published along with the detailed analysis through the NASA Technical Papers to be published at a future date. Meanwhile interested persons can contact the author for a detailed reference list.



VOLATILES IN INTERPLANETARY DUST PARTICLES -  
A COMPARISON WITH CI AND CM CHONDRITES

Final Report  
NASA/ASEE Summer Faculty Fellowship Program--1992

Johnson Space Center

Prepared By:	Roberta Bustin
Academic Rank:	Professor
University & Department:	Natural Science and Mathematics Division Arkansas College Batesville, AR 72501
NASA/JSC	
Directorate:	Space and Life Sciences
Division:	Solar System Exploration
Branch:	Planetary Science
JSC Colleague:	Everett K. Gibson, Jr.
Date Submitted:	August 21, 1992
Contract Number:	NGT-44-005-803

## ABSTRACT

In an effort to classify and determine the origin of interplanetary dust particles (IDPs), 14 of these particles were studied using a laser microprobe/mass spectrometer. The mass spectra for these particles varied dramatically. Some particles released hydroxide or water which probably originated in hydroxide-bearing minerals or hydrates. Others produced spectra which included a number of hydrocarbons and resembled meteorite spectra. However, none of the individual IDPs gave spectra which could be matched identically with a particular meteorite type such as a CI or CM carbonaceous chondrite. We believe this was due to the fact that 10-20  $\mu\text{m}$  size IDPs are too small to be representative of the parent body. To verify that the diversity was due primarily to the small particle sizes, small grains of approximately the same size range as the IDPs were obtained from two primitive meteorites, Murchison and Orgueil, and these small meteorite particles were treated exactly like the IDPs. Considerable diversity was observed among individual grains, but a composite spectrum of all the grains from one meteorite closely resembled the spectrum obtained from a much larger sample of that meteorite. A composite spectrum of the 14 IDPs also resembled the spectra of the CM and CI meteorites, pointing to a possible link between IDPs and carbonaceous chondrites. This also illustrates that despite the inherent diversity in particles as small as 10-20  $\mu\text{m}$ , conclusions can be drawn about the possible origin and overall composition of such particles by looking not only at results from individual particles but also by including many particles in a study and basing conclusions on some kind of composite data.

## INTRODUCTION

Interplanetary dust particles (IDPs) are extraterrestrial materials consisting of primitive substances originating in small solar system bodies such as comets and asteroids (Mackinnon and Rietmeijer, 1987). IDPs are recovered from satellites and from collectors flown aboard specially designed aircraft flying in the stratosphere. A Cosmic Dust Collection Facility for obtaining additional IDPs has been proposed for Space Station Freedom.

In order to understand not only the composition but also the past histories of IDPs, it is particularly important to know the nature of the volatiles present. Gibson and Sommer (1986), Gibson *et al.* (1989), and Hartmetz *et al.* (1990, 1991b) have studied volatiles released from a number of IDPs. However, a large number of particles must be studied in order to establish trends, to classify types of IDPs, and to have comparison data for determining the origins of IDPs.

## EXPERIMENTAL

### Collection and Processing

The IDPs in this study were from the Large Area Collectors L2005 and L2006 flown aboard a NASA ER-2 aircraft during a series of flights that were made within west-central North America during the fall of 1989. The collectors were coated with a 20:1 mixture of silicone oil and freon. They were installed in a specially constructed wing pylon, exposed to the stratosphere at an altitude of 20 km by barometric controls, and then retracted into sealed storage containers prior to descent (Zolensky *et al.*, 1990, 1991).

The IDPs were processed in an ultraclean (Class-100) laboratory at Johnson Space Center. The particles were removed from the collection flag and rinsed with hexane to remove the silicone oil remaining on the surface from the collection procedure. They were then mounted on small pieces of gold which had been cleaned with ethanol in an ultrasonic cleaner followed by surface cleaning in an oxygen plasma. The particles in this study were all cluster particles, small pieces of larger, friable particles which fragmented during collection.

## Analysis

The 14 IDPs in this study were classified as cosmic dust by the examination team (Zolensky *et al.*, 1990, 1991). An SEM photomicrograph was taken of each of the particles, and an energy dispersive X-ray (EDX) analysis was done using a JEOL-35CF Scanning Electron Microscope. Results of the EDX analyses are shown in Table 1.

The piece of gold containing the IDP was placed in the sample chamber of the apparatus shown in Figure 1, and the system was evacuated to a pressure of  $2 \times 10^{-7}$  torr. The IDP was then hit with a focused laser beam from a Jarrell-Ash neodymium-glass, Q-switched laser. Volatiles released were analyzed by a Hewlett Packard 5970 Mass Selective Detector. The particles were so small that the laser beam hit not only the particle but also the surrounding gold. To account for the volatiles coming from the surface of the gold, an average "gold" spectrum was obtained from several laser hits on the clean gold away from the particle, and this spectrum was subtracted from the spectrum of the particle. This also had the advantage of subtracting out the majority of the peaks due to surface contaminants left from processing and cleaning the IDP.

The data were normalized (Hartmetz *et al.*, 1990) in order to compare them with analyses of other IDPs, and only those peaks that were greater than one standard deviation (calculated from the gold measurements) above the gold background were displayed.

To help in evaluating the spectra of the IDPs, spectra were obtained from three minerals (azurite, calcite, and troilite), from three meteorites (Murchison, Orgueil, and Allende), and from several small particles of Murchison and Orgueil of approximately the same size range as the IDPs.

## RESULTS AND DISCUSSION

The EDX spectra indicated that all IDPs studied except possibly L2006A6,7 were chondritic, based on the similarity of their elemental compositions and those of the chondritic meteorites, particularly the carbonaceous chondrites.

Individual IDPs can be classified according to the volatiles identified in the mass spectrum. Table 3 lists the major classes, and Figures 2 through 7 are examples of each class.

The mass spectra showed that the volatile inventories of the IDPs varied dramatically from almost no volatiles (Figure 2) to what is considered volatile-rich (Figure 3)

because of the presence of several hydrocarbon "families" in addition to species such as C, O, CO, CO<sub>2</sub>, and COS. Table 2 lists the indigenous volatile species found in all 14 IDPs studied. Because many IDPs are porous and may retain some silicone oil or freon from the collection device or some hexane used to remove the silicone oil from the surface, a species is considered to be indigenous only if it does not occur in the mass spectrum of silicone oil, freon, or hexane.

None of the IDPs studied has all the peaks expected from a sulfur-rich species such as a sulfide or sulfate. However, several particles appear to contain some sulfur. An example is L2005E38 (Figure 4). Even though this particle does not contain many volatiles, three peaks are due at least partially to sulfur-containing species (S, SO, and CS<sub>2</sub>). CS<sub>2</sub> is a major species released from both terrestrial sulfides and elemental sulfur.

Information about carbonaceous matter, particularly hydrocarbons, in IDPs is important not only for classification purposes but also in determining sources and origins of IDPs. High abundances of carbon-bearing compounds have been found in the dust released from Comet Halley (Kissel and Krueger, 1987). Carbonaceous chondrites also contain hydrocarbons (Hartmetz *et al.* 1991a). Blanford *et al.* (1988) found that some anhydrous chondritic IDPs contain as much as 49 wt. % carbon which has not been fully characterized. Carbonaceous material was found in six of the IDPs in this study.

In studying hydrated IDPs, Tomeoka and Buseck (1986) found a carbonate-rich, hydrated IDP. Infrared studies of IDPs revealed a band associated with carbonate (Sandford, 1986). Two IDPs in this study, L2006A6,7 and L2006A12, contained large peaks for both CO and CO<sub>2</sub>, indicating the likelihood of a carbonate phase. Both of these also contained carbon, a prominent peak in the spectra of known carbonate-containing minerals.

Nine of the 14 particles studied had a peak at either 17 or 18, indicating the presence of either hydroxide-bearing minerals or hydrated species.

To give some idea of how representative of the parent body a 10-20  $\mu$ m particle really is, spectra were obtained from several small particles each of Murchison and Orgueil, a CM and a CI chondrite, respectively. There was considerable diversity in the individual spectra (Figures 8-11). Some particles appeared to be mineral grains; some could not even have been identified as being meteoritic; and others were fairly representative of the typical meteorite matrix. All meteorite particles were not the same size. In most cases, the larger particles gave spectra most similar

to the parent meteorite. For both Orgueil and Murchison, a composite of all particles yielded a spectrum similar to that of the parent meteorite (Figures 12-15). Sulfur-bearing species, aliphatic hydrocarbon groups, aromatics, carbonates, and water were present in each of these. Based on the total ion chromatograms, the IDPs had the least amount of total volatiles; small Murchison particles had only slightly more volatiles (about 1.15 times); and small Orgueil particles had about 2.3 times as much volatile material as the IDPs. A large piece of Murchison was only 1.4 times as volatile-rich as the IDPs, but the large grains of Orgueil evolved 20 times as much volatile material as the IDPs. This is in keeping with previous studies which reported Orgueil to be more volatile-rich than Murchison (Wiik, 1956 and Hartmetz *et al.*, 1991).

In order to envision what a parent body containing all 14 of our IDPs might resemble, a composite spectrum was prepared (Figure 16), using a typical gold spectrum for the subtracted background. It is not necessary to use a large number of particles to give a representative composite spectrum. The composite from eight spectra looked almost identical to this 14-particle composite. The IDP composite spectrum is very much like the spectra from the carbonaceous chondrites. The most obvious difference is the decreased intensity of the sulfur-related peaks. Although clearly present, the SO and SO<sub>2</sub> peaks are much smaller than the same peaks in either meteorite spectrum, indicating that the IDPs in this study probably contained sulfate but not in large amounts. The intensity of the COS peak in the IDP spectrum is about the same as that of SO<sub>2</sub>, whereas in the meteorite spectra, the SO<sub>2</sub> peak is much larger than the COS peak; the CS<sub>2</sub> peak is small, and the H<sub>2</sub>S peak is barely noticeable. The H<sub>2</sub>S, COS and CS<sub>2</sub> peaks are significant peaks in the Murchison spectrum but are not as intense as they are in the spectrum of Orgueil. Because of this, the IDP spectrum resembles the Murchison spectrum a little more closely than that of Orgueil.

#### SUMMARY

Despite the inherent diversity in particles the size of IDPs, it is possible to identify specific mineral fragments and classes of compounds which occur in such particles. By comparing results from analyses of many particles, it is clear that IDPs may contain sulfur-bearing species, water or hydroxyl groups, and carbonaceous material, including carbonates. By looking at composite data and comparing with data from meteorites, a definite resemblance is seen between IDPs and carbonaceous chondrites.

TABLE 1. EDX MAJOR ELEMENT ANALYSIS<sup>i</sup>

Particle	Major Components
L2005B21	Si, Fe, Mg, O, (Al)
L2005C21	Si, S, Mg, O, Fe, Ca, Na, Al
L2005C24	Si, Mg, Fe, O, Ca, (Al)
L2005C26	Si, Mg, Fe, O, (Ca), (Al), (Ni)
L2005C28	S, Si, Fe, Mg, O, (Al), (Ni)
L2005C30	Si, Mg, Fe, O, (Ca), (Ti), (Al), (Na)
L2005D27	Si, Mg, O, S, Fe, (Na), (Al), (Ca)
L2005D34	Si, Mg, O, Na, Fe
L2005E38	Si, Mg, Fe, O, (Na)
L2005E39	Si, Mg, C, Fe, O, (Na)
L2006A6,7	C, Si, Na, (O)
L2006A12	Si, Mg, O, Fe, (Ca), (C), (Na), (Al)
L2006A26	Si, Ca, Mg, O, Fe, C
L2006B16	Si, Mg, O, Fe, C

<sup>i</sup>Elements are listed in order of abundances, and trace amounts are placed in parentheses. It was difficult to detect whether or not sulfur was present in some species because of the overlap with the intense gold peak from the sample mount.

TABLE 2. INDIGENOUS VOLATILE SPECIES

Particle	Volatile Components
L2005B21	OH
L2005C21	C, C <sub>2</sub> H <sub>5</sub> , O <sub>2</sub> or S, SO <sub>2</sub> , C <sub>5</sub> H <sub>6</sub> , C <sub>6</sub> H <sub>6</sub> , C <sub>6</sub> H <sub>7</sub> , C <sub>6</sub> H <sub>5</sub> CH <sub>3</sub>
L2005C24	OH, C <sub>2</sub> H <sub>5</sub> , C <sub>2</sub> H <sub>6</sub> , C <sub>4</sub> or SO, C <sub>4</sub> H, C <sub>5</sub> H <sub>8</sub> , C <sub>5</sub> H <sub>9</sub> , C <sub>6</sub> H <sub>6</sub> , C <sub>6</sub> H <sub>5</sub> CH <sub>3</sub>
L2005C26	C, CH, and some high m.w. hydrocarbons
L2005C28	CH, OH, SOH?, C <sub>5</sub> H <sub>7</sub> , CS <sub>2</sub> , C <sub>6</sub> H <sub>6</sub> , C <sub>6</sub> H <sub>7</sub> , C <sub>7</sub> H <sub>11</sub>
L2005C30	OH, C <sub>2</sub> H <sub>5</sub> , C <sub>2</sub> H <sub>6</sub> , CO <sub>2</sub> , C <sub>5</sub> H <sub>8</sub> , C <sub>5</sub> H <sub>9</sub>
L2005D27	C, C <sub>2</sub> H <sub>5</sub> , CO <sub>2</sub> , SOH?, SO <sub>2</sub> , CS <sub>2</sub> , C <sub>6</sub> H <sub>6</sub> , C <sub>6</sub> H <sub>7</sub> , C <sub>6</sub> H <sub>5</sub> CH <sub>3</sub> , C <sub>7</sub> H <sub>9</sub> , C <sub>7</sub> H <sub>11</sub> , C <sub>7</sub> H <sub>16</sub>
L2005D34	CH, OH, C <sub>6</sub> H <sub>6</sub>
L2005E38	OH, O <sub>2</sub> or S, SO
L2005E39	C, C <sub>2</sub> H <sub>5</sub> , C <sub>5</sub> H <sub>5</sub> , C <sub>5</sub> H <sub>6</sub> , C <sub>5</sub> H <sub>7</sub>
L2006A6,7	C, OH, C <sub>2</sub> H <sub>5</sub> , CO <sub>2</sub> , C <sub>5</sub> H <sub>5</sub> , C <sub>5</sub> H <sub>6</sub> , C <sub>6</sub> H <sub>6</sub>
L2006A12	C, CC <sub>2</sub> H <sub>5</sub> , CO <sub>2</sub> , C <sub>5</sub> H <sub>5</sub> , C <sub>5</sub> H <sub>7</sub> , C <sub>6</sub> H <sub>6</sub>
L2006A26	None
L2006B16	SO

TABLE 3. OVERVIEW OF VOLATILE SPECIES FOUND IN 28 IDPS ANALYZED BY LASER MICROPROBE/  
MASS SPECTROMETRY<sup>i</sup>

Little or No Indigenous Volatiles	Large Amount of Indigenous Volatiles	Sulfur Species	Carbonaceous Material	Carbonate	Water or Hydroxyl
L2001D3	L2002C4	(L2002C4) ii	L2002C4	L2003D2	L2005B21
L2004D3	L2003D2	(L2003D2)	L2003D2	L2006A6,7	L2005C24
L2005B21	L2003E3	(L2004C3)	L2004C3	L2006A12	L2005C28
L2005C21	L2004C3	(L2004D3)	L2003E3	U2034D7	L2005C30
L2005C24	L2006A12	L2005C21	L2005C21		L2005D34
L2005C26	U2017A4	L2005C24	L2005C24		L2005E38
L2005C28	U2017A5	L2005C26	L2005C26		L2006A6,7
L2005C30	U2022G13	L2005E38	L2005D34		L2006B16
L2005D27	U2034D7	L2006A12	L2005E39		U2022F5
L2005D34		(L2006B16)	L2006A6,7		U2022F20
L2005E38		U2017A4	U2034D7		U2034D7
L2006A26		U2017A5			
L2006B16		U2022G13			
U2015B20		(U2034D7)			
U2015F20					
U2022F5					
U2034D1					

<sup>i</sup>Samples in bold print are those analyzed in this investigation. Others are from Hartmetz et al., 1990, 1991b.

<sup>ii</sup>Parentheses indicate that the IDP contained only one type of sulfur species, often in very small amounts.

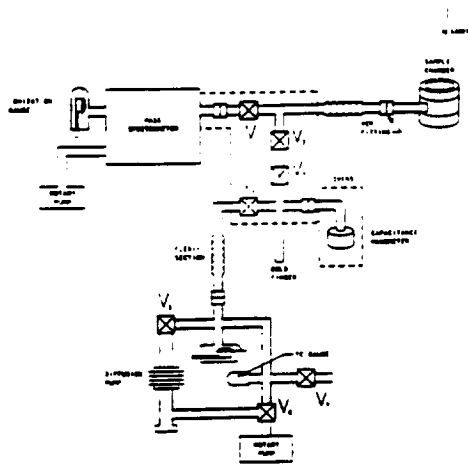


Figure 1. Schematic of the laser microprobe-mass spectrometer, from Gibson and Carr (1989)

**PARTICLE L2005B21**  
On Gold

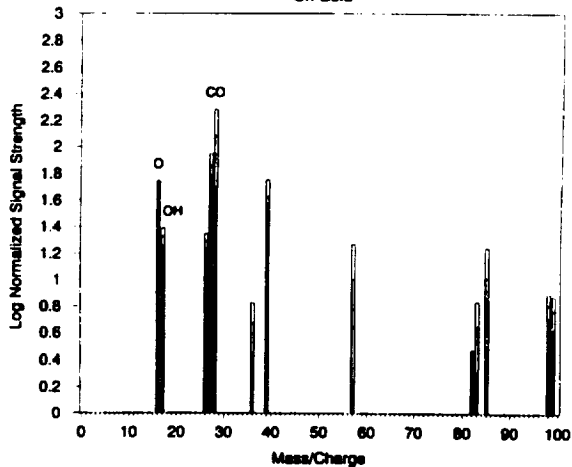


Figure 2. Mass spectrum of an IDP containing very few volatiles

**PARTICLE 2006A12**  
On Gold

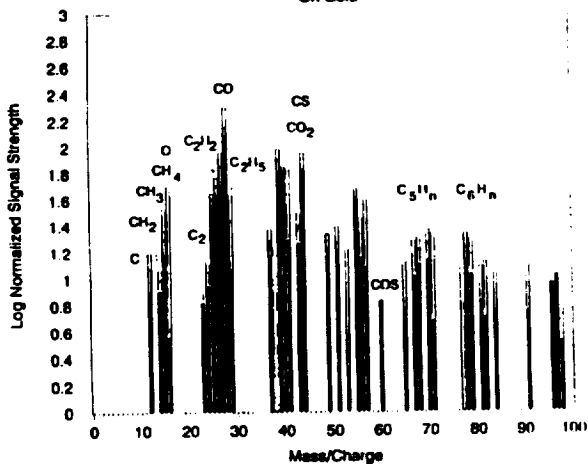


Figure 3. Mass spectrum of a volatile-rich IDP

**PARTICLE L2005E38**  
On Gold

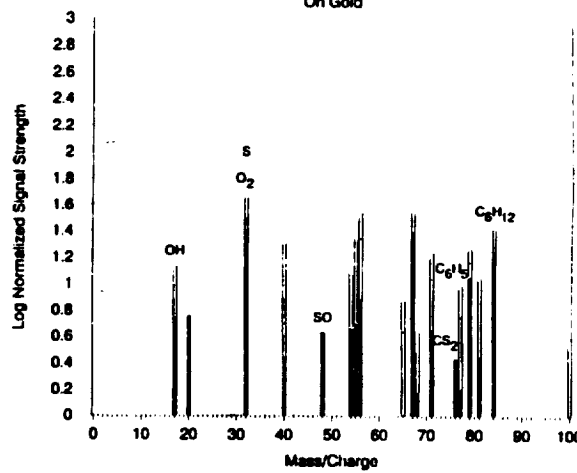


Figure 4. Mass spectrum of a sulfur-containing IDP

ORIGINAL PAGE IS  
OF POOR QUALITY

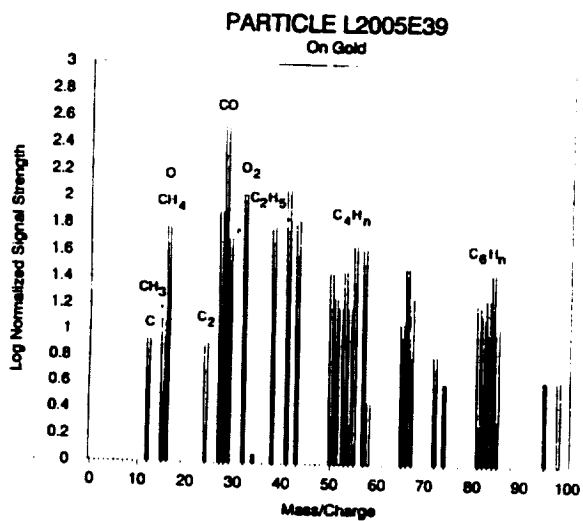


Figure 5. Mass spectrum of an IDP containing carbonaceous material

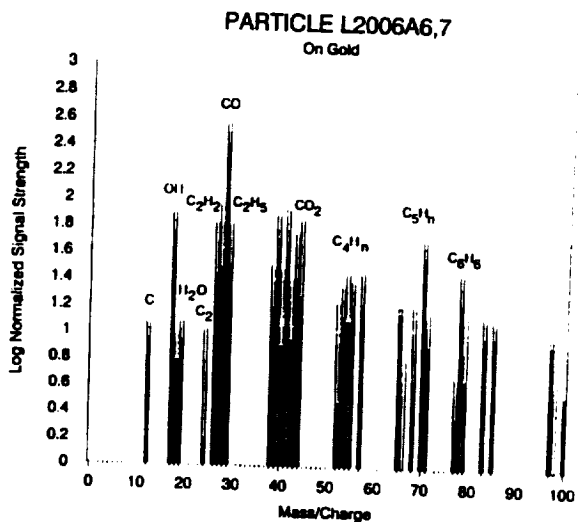


Figure 6. Mass spectrum of an IDP containing carbonate

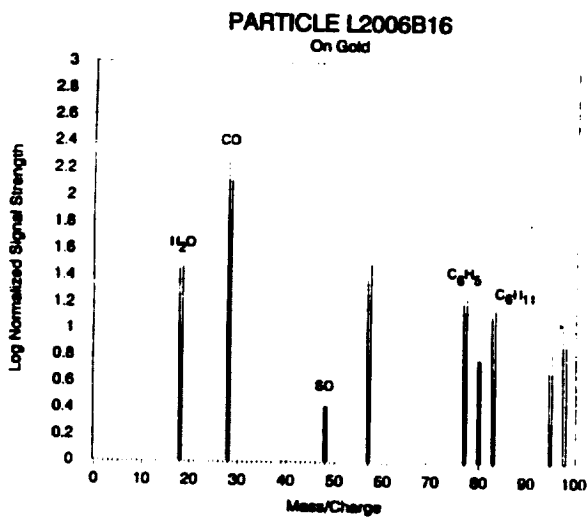


Figure 7. Mass spectrum of an IDP containing water

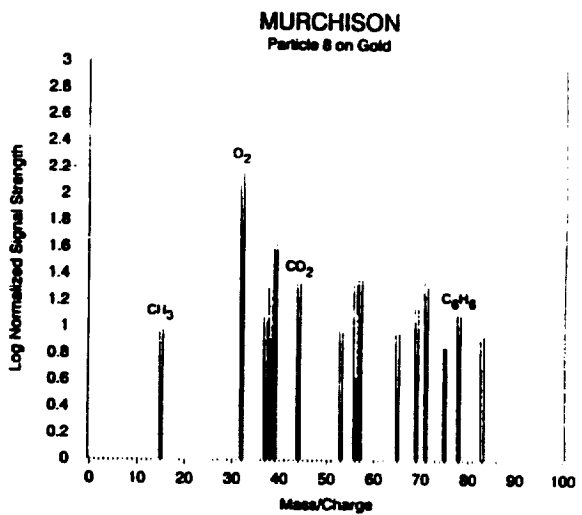


Figure 8. Mass spectrum of a Murchison particle with few volatiles

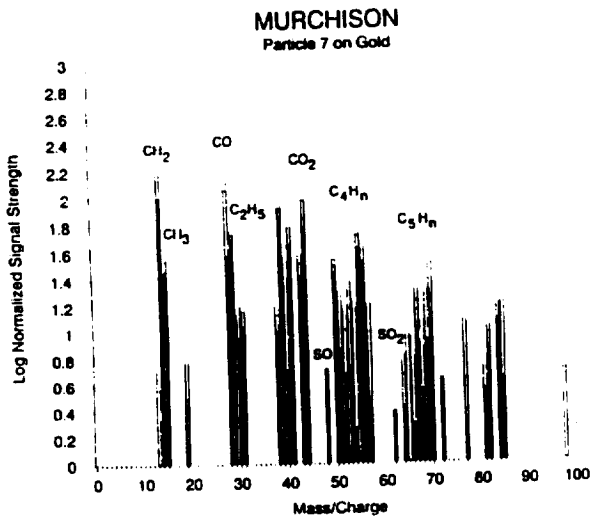


Figure 9. Mass spectrum of a volatile-rich Murchison particle

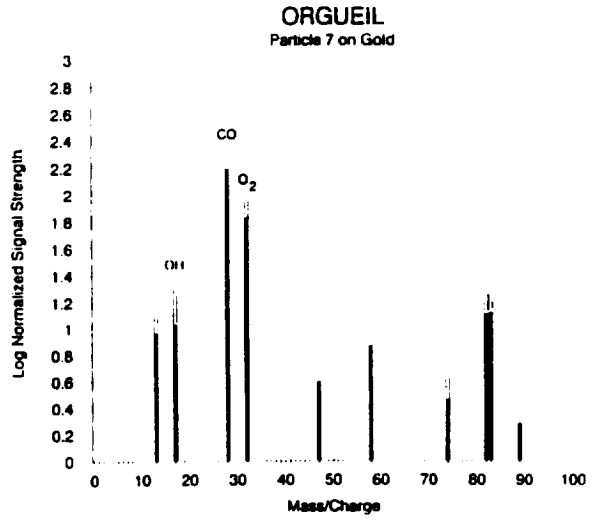


Figure 10. Mass spectrum of an Orgueil particle with few volatiles

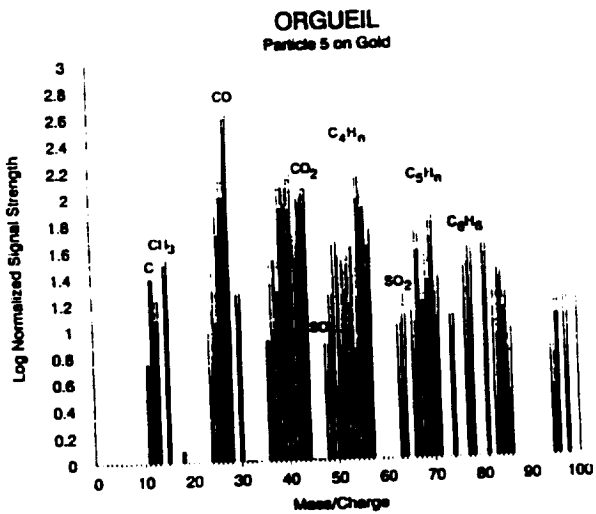


Figure 11. Mass spectrum of a volatile-rich Orgueil particle

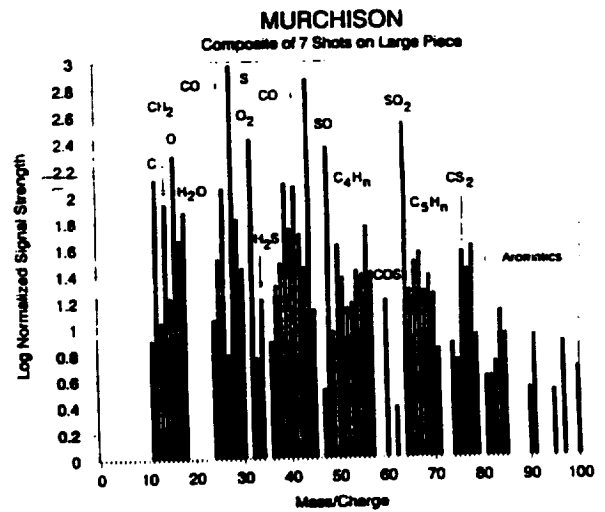


Figure 12. Composite of mass spectra of 7 different locations on a large piece of Murchison

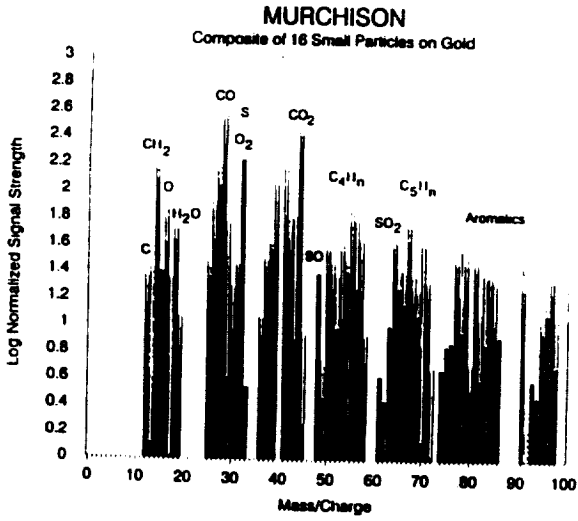


Figure 13. Composite of mass spectra of 16 small particles from Murchison

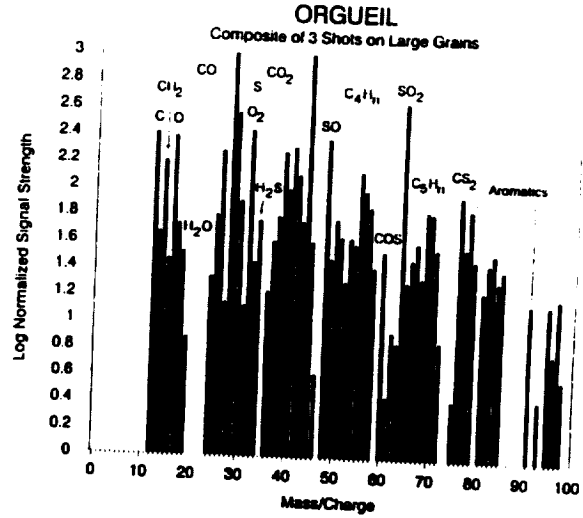


Figure 14. Composite of mass spectra of 3 different locations on large grains of Orgueil

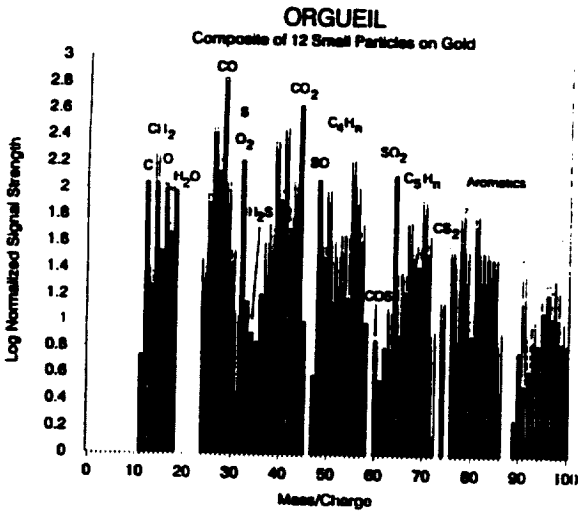


Figure 15. Composite of mass spectra of 12 small particles from Orgueil

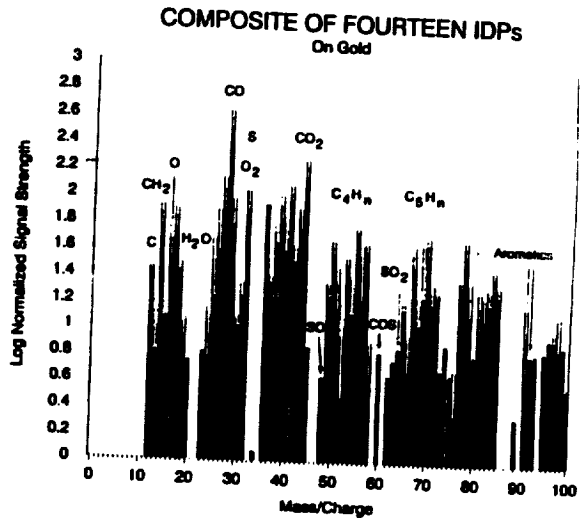


Figure 16. Composite of mass spectra of the 14 IDPs examined in this study

## REFERENCES

- Blanford, G. E., Thomas K. L., and McKay D. S., Microbeam analysis of four chondritic interplanetary dust particles for major elements, carbon, and oxygen, Meteoritics, 23, 113-121, 1988.
- Gibson E. K. Jr. and Carr R. H. (1989) Laser microprobe-quadrupole mass spectrometer system for the analysis of gases and volatiles from geologic materials. In New Frontiers in Stable Isotope Research: Laser Probes, Ion Probes, and Small Sample Analysis, pp. 35-49. U. S. Geol. Surv. Bull. 1890.
- Gibson E. K. Jr. and Sommer, M. A. (1986) Laser microprobe study of cosmic dust (IDPs) and potential source materials. Lunar and Planetary Science XVII, 260-261.
- Gibson E. K. Jr., Hartmetz, C. P. and Blanford, B. E. (1989) Analysis of interplanetary dust particles for volatiles and simple molecules. Lunar and Planetary Science XX, 339-340.
- Hartmetz C. P., Gibson E. K. Jr., and Blanford G. E. (1990) In situ extraction and analysis of volatiles and simple molecules in interplanetary dust particles, contaminants, and silica aerogel, Proc. Lunar Planet. Sci. 20, 343-355.
- Hartmetz C. P., Gibson E. K. Jr., and Blanford G. E. (1991) In situ extraction and Analysis of volatile elements and molecules from carbonaceous chondrites, Proc. Lunar Planet. Sci. 21, 527-539.
- Hartmetz C. P., Gibson E. K. Jr., and Blanford G. E. (1991) Analysis of volatiles present in interplanetary dust and stratospheric particles collected on Large Area Collectors. Proc. Lunar Planet. Sci. 21, 557-567.
- Kissel J. and Krueger F. R., The organic component in dust from Comet Halley as measured by the PUMA mass spectrometer on board Vega 1, Nature, 326, 755-761, 1987.
- MacKinnon I. D. R. and Rietmeijer F. J. M. (1987) Mineralogy of chondritic interplanetary dust particles, Rev. Geophys., 25, 1527-1553.
- Sandford S. A. (1986) The world's smallest acid residue: The source of the 6.8 micron band seen in some IDP spectra, Lunar Planet. Sci. XVII, 756-757.

- Tomeoka K. and Buseck P. R. (1986) A carbonate-rich, hydrated interplanetary dust particle: Possible residue form protostellar clouds, Science 231, 1544-1546.
- Wiik H. B. (1956) The chemical composition of some stony meteorites. Geochim. Cosmochim. Acta, 9, 279-289.
- Zolensky M. E., Barrett R. A., Dodson A. L., Thomas K. L., Warren J. L., and Watts L. A. (1990, 1991) Cosmic Dust Catalogs 11 and 12, NASA Johnson Space Center.

**N 9 3 - 2 6 0 6 3**

**Use of Taguchi Design of Experiments  
to Optimize and Increase Robustness of Preliminary Designs**

**Final Report**

**NASA/ASEE Summer Faculty Fellowship Program--1992**

**Johnson Space Center**

**Prepared By:** Hector R. Carrasco, Ph.D., P.E.  
**Academic Rank:** Assistant Professor  
**University & Department:** Florida International University  
Industrial & Systems Engineering  
Miami, Florida 33199

**NASA/JSC**

**Directorate:** Engineering  
**Division:** Systems Engineering  
**Branch:** Systems Definition  
**JSC Colleague:** Charles J. Mallini  
**Date Submitted:** August 28, 1992  
**Contract Number:** NGT-44-005-803

## **ABSTRACT**

The research performed this summer includes the completion of work begun last summer in support of the Air Launched Personnel Launch System parametric study, providing support on the development of the test matrices for the plume experiments in the Plume Model Investigation Team Project, and aiding in the conceptual design of a lunar habitat.

After the conclusion of last years Summer Program, the Systems Definition Branch continued with the Air Launched Personnel Launch System (ALPLS) study by running three experiments defined by L27 Orthogonal Arrays. Although the data was evaluated during the academic year, the analysis of variance and the final project review were completed this summer.

The Plume Model Investigation Team (PLUMMIT) was formed by the Engineering Directorate to develop a consensus position on plume impingement loads and to validate plume flowfield models. In order to obtain a large number of individual correlated data sets for model validation, a series of plume experiments was planned. A preliminary "full factorial" test matrix indicated that 73,024 jet firings would be necessary to obtain all of the information requested. As this was approximately 100 times more firings than the scheduled use of Vacuum Chamber A would permit, considerable effort was needed to reduce the test matrix and optimize it with respect to the specific objectives of the program.

Part of the First Lunar Outpost Project deals with Lunar Habitat. Requirements for the habitat include radiation protection, a safe haven for occasional solar flare storms, an airlock module as well as consumables to support 34 extra vehicular activities during a 45 day mission. The objective for the proposed work was to collaborate with the Habitat Team on the development and reusability of the Logistics Modules.

## OVERVIEW OF PARAMETER DESIGN AND TAGUCHI METHODS

During product development, engineers and scientists are typically faced with two opposing requirements; improve or optimize performance and reduce or minimize cost. The process of searching for factors or parameters affecting performance and/or cost is usually experimental in nature. After a set of relevant parameters are assembled, the experimenter is faced with the task of determining which combination of parameter values achieve the desired results. It is the quality of this decision that can be improved when proper tests strategies are used. The most commonly used test plan is the evaluation and optimization of one parameter at a time. If there happens to be an interaction of the factor being studied with any other factor, the interaction will not be observed as all other factors are being held constant. This loss of interaction information is accepted as unavoidable as the only other perceived alternative is to perform a full factorial experiment, testing every possible combination of factors. This is usually not feasible as most real problems involve many parameters with three or more possible levels requiring thousands of experiment runs. Taguchi is an advocate of more efficient test plans, which are referred to as fractional factorial experiments (FfEs). FfEs use only a portion of the total possible combinations to estimate the main factor effects and some, not all, of the interactions [1]. FfEs are balanced experiments developed using orthogonal arrays. They can be used to evaluate many parameters with a minimum number of tests.

As suggested above, the goal of parameter design is to determine the parameter values of a product or process so that the product is functional, exhibits a high level of performance and is minimally sensitive to noise. The strategy is to design a high quality product which can be produced from low grade, low cost components with broad tolerances. This improved quality and reduced variability is achieved by selecting the optimum parameter values so that the product is least sensitive to input and noise variations. Conventional quality improvement techniques reduce product variation by removing the cause which is usually expensive, while Taguchi methods reduce variation by becoming less sensitive to input variations without removing the cause of variation. Improved quality is, therefore, achieved without or with minimal increase in cost. Taguchi Methods take advantage of non-linear effects and the interaction between control factors and noise factors in order to obtain designs that are more "robust". Taguchi's approach to design of experiments utilizes techniques that are cost effective and directly applicable to the problems and requirements of modern industry.

A parameter design experiment typically involves two types of factors:

**Control Factors** whose levels can be set and maintained.

**Noise Factors** whose level either cannot or will not be set or maintained, yet which could affect the performance of the functional characteristics.

Parameter design examines interactions between control factors and noise factors in order to achieve robustness. It is a search for parameter levels at which a characteristic is stable, despite the use of inexpensive components and materials or external conditions.

The major steps in designing, conducting, and analyzing an experiment are as follows:

1. Selection of factors and/or interactions to be evaluated
2. Selection of number of levels for the factors
3. Selection of appropriate Orthogonal Array
4. Assignment of factors and/or interactions to columns
5. Performance of experiments
6. Analysis of results
7. Performance of confirmation experiment.

In the design of products or processes, Taguchi's design of experiments can be used to determine the optimal parameter settings to obtain the best and most robust design with the least number of experiments. Even for optimization using analytical approaches, Taguchi's methods can significantly reduce computer time. When testing or experimenting to gain new knowledge or better understand how something works, the need to obtain usable results with the least number of tests is important as time, equipment, and funding are always limited.

### **AIR LAUNCHED PERSONNEL LAUNCH SYSTEM (ALPLS) PROJECT**

The Systems Definition Branch, Systems Engineering Division, recently assessed the engineering feasibility, safety and reliability, and the infrastructure and operational requirements of an Air Launched Personnel Launch System for transportation of personnel to low earth orbit. One of the study requirements called for the determination of ascent delta-V sensitivities to release conditions (Altitude, Mach, Flight Path Angle, Delay Time) and vehicle parameters (Specific Impulse, Ignition Thrust to Weight Ratio, Lift to Weight Ratio).

This parametric study was accomplished by both the traditional one parameter at a time approach and with Taguchi's design of experiment methods. The goal was to evaluate the use of Taguchi methods for space vehicle design parametric

studies by performing an analysis of the ALPLS using both approaches to provide a mechanism for comparing the results and the effort necessary to complete the studies.

### **Selection of Parameters and Levels to be Evaluated**

The number of parameters given above was reduced to six with the conclusion that the aircraft would be flown at maximum velocity for the release of the PLS. The parameters and the levels selected for the Taguchi Study were as follows:

Variable	Levels		
Altitude:	25,000 ft.	35,000 ft.	45,000 ft.
Flight Path Angle:	0 degrees	10 degrees	20 degrees
Delay Time:	2 seconds	4 seconds	6 seconds
Specific Impulse (Isp):	LO <sub>x</sub> /LH <sub>2</sub>	A50/N <sub>2</sub> O <sub>4</sub>	HTBP
Ign Thrust to Weight (T/W):	1.5	1.7	1.9
Lift to Weight (L/W):	0.0	1.0	

The Flight Path Angle ( $\gamma$ ) was varied in 10 degree increments to conform with the increment size being used in the traditional approach. This limited the range to a total of 20 degrees in order to limit the number of levels in the Taguchi study to three. The remainder of the parameters conformed well with the parameter ranges used in the traditional approach.

### **Selection of Appropriate Orthogonal Array**

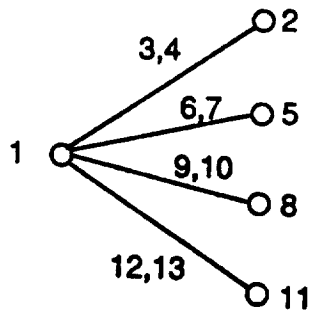
The selection of an orthogonal array depends on the number of factors and interactions to be modeled and the number of levels for the factors. Initially, little was known about the relevant interactions. It was assumed that the engine specific impulse and L/W parameters were the dominant factors; therefore, only the interaction between Isp and L/W was modeled. This resulted in a total of 13 degrees of freedom suggesting the use of an L<sub>18</sub> Orthogonal Array. The L<sub>18</sub> Array was also deemed appropriate as it can model one 2-level and seven 3-level parameters [2]. It is a specially designed array that models the interaction between the first two columns without sacrificing any other column and distributes interactions between the 3-level columns more or less uniformly among all of the 3-level columns [3]. After analyzing the data obtained from this initial set of computer runs, it became apparent that the selection of the L<sub>18</sub> orthogonal array was not appropriate. The gross lift-off mass ( $m_{glow}$ ) was very responsive to changes in L/W and Isp and there were significant interactions between altitude and the other parameters.

In order to eliminate the L/W - Isp and the L/W - Altitude interactions the ballistic and winged vehicles were studied separately. An L27 orthogonal array was selected with Isp occupying the first column. As Isp was the dominant parameter, two way interactions with the other parameters were modeled. Refer to Table I. The same 27 trials were repeated for three different levels of L/W (0.0, 0.5, & 1.0). This required a total of 81 computer setups and enough computer runs to minimize the vehicle mass at the specified parameter conditions.

### Performance of the Experiment

The computer analysis was performed by the Systems Definition Branch of the systems Engineering Division and their engineering support contractor, Lockheed Engineering and Science Company. The analysis required for the traditional parametric study consisted of approximately 90 computer program setups, each requiring approximately 30 computer runs for a total of approximately 2700 computer runs. The Taguchi approach required a total of 99 computer setups, including the initial L18 experiment, each requiring only a few computer runs to determine optimal delta-V splits and flight profile to minimize total vehicle mass at the specified parameter conditions. Although only about one-quarter as many computer runs were necessary, Lockheed personnel indicated that the Taguchi method required approximately one-half the effort of the traditional approach.

Table I. Assignment of Factors to Columns



Trial no.	Isp	T/W		Alt			Gamma			Delay			
	1	2	3	4	5	6	7	8	9	10	11	12	13
1	LOx/LH2	1.5	1	1	25K	1	1	0'	1	1	2	1	1
2	LOx/LH2	1.5	1	1	35K	2	2	10'	2	2	4	1	1
:	:	:	:	:	:	:	:	:	:	:	:	:	:
26	HTPB	1.9	2	1	35K	1	3	0'	3	2	6	2	1
27	HTPB	1.9	2	1	45K	2	1	20'	1	3	2	3	2

## Analysis of Results

The Response Graphs, shown in Figure 1, show the sensitivity of the Delta-V with respect to the five parameters modeled for a winged vehicle having a L/W ratio of 1.0. By observing the slope of the curves, it can be seen that the Delta-V is sensitive to Isp and Ignition T/W and relatively insensitive to variations in Release Altitude, Flight Path Angle, and Drop Time. This compares favorably with the data obtained by the traditional parametric study as demonstrated in Figure 2.

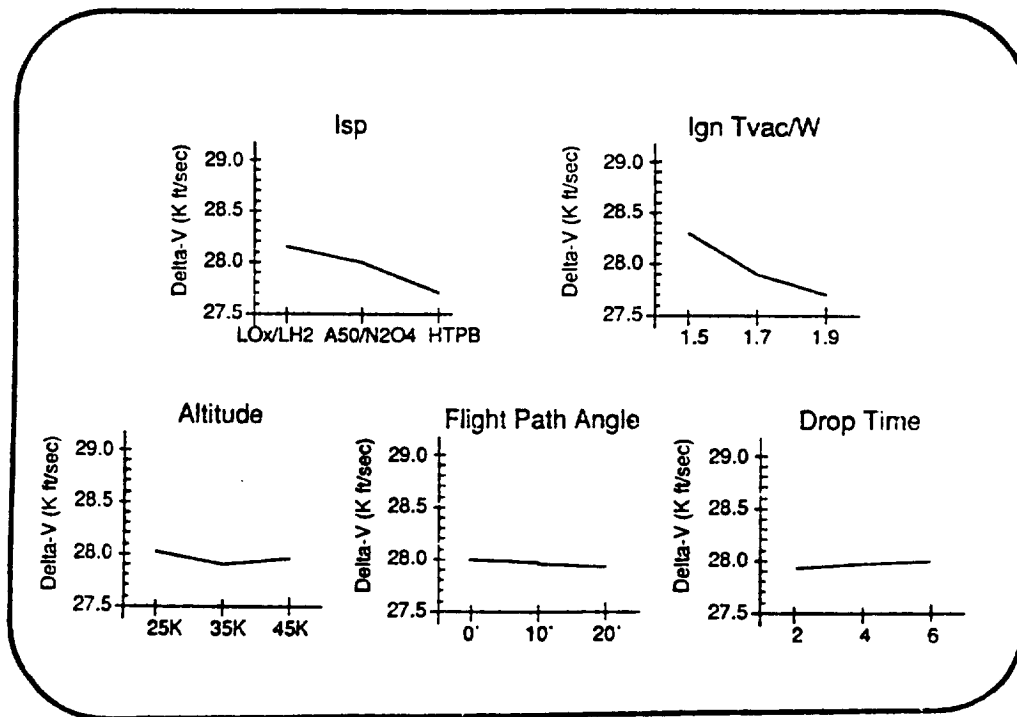


Figure 1. Delta-V Response with Winged Vehicle

This agreement with the traditional parametric results was obtained with less engineering time and significantly less computer time.

### Engineering Man/Hours Needed for Study

#### Traditional Parametric Study

$$(90 \text{ computer setups}) \times (0.5 \text{ hours/setup}) = 45 \text{ hours}$$

#### Taguchi Approach

$$(72 \text{ computer setups}) \times (0.5 \text{ hours/setup}) = 36 \text{ hours}$$

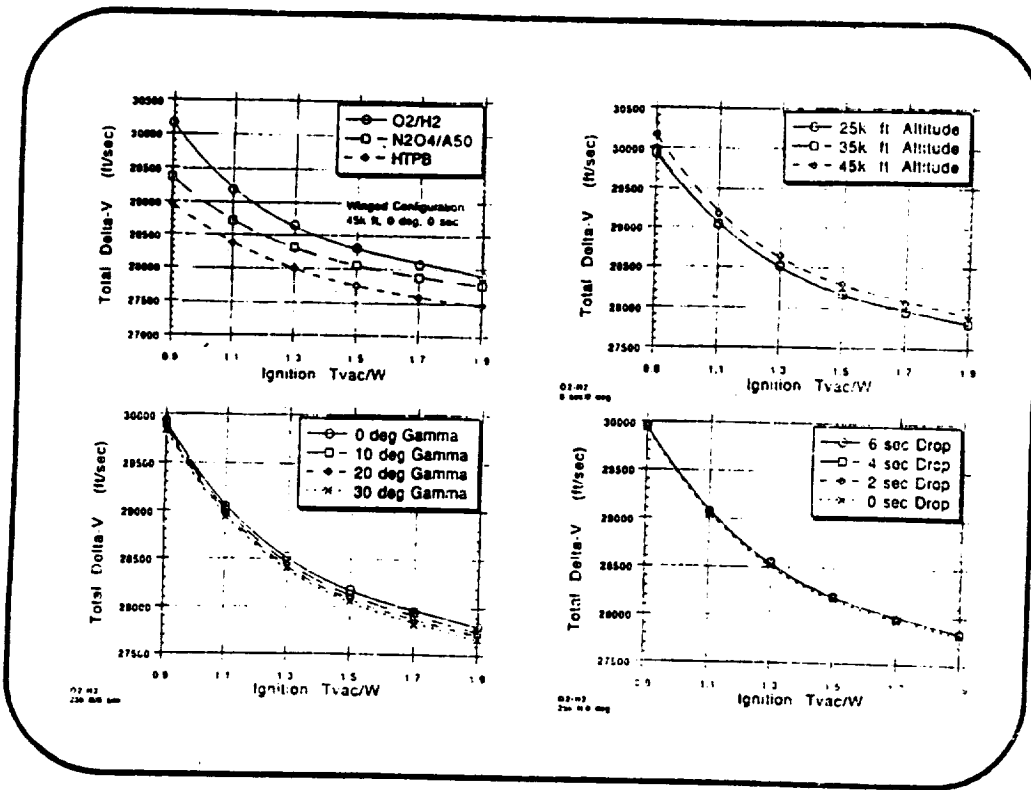


Figure 2. Results from Traditional Parametric Study

### Computer Run Time

#### Traditional Parametric Study

$$(90 \text{ setups}) \times (21 \text{ runs/setup}) \times (0.1 \text{ hrs/run}) = 189.0 \text{ hours}$$

#### Taguchi Approach

$$(72 \text{ setups}) \times (1 \text{ run/setup}) \times (0.1 \text{ hours/run}) = 7.2 \text{ hours}$$

It should be noted that the savings resulting from the application of Taguchi's design of experiment methods were achieved at the cost of reduced detail in the sensitivity analysis. In addition the validity of the Taguchi results would have been questionable without the availability of the traditional data as the L27 Orthogonal Array did not model all of the parameter interactions that were observed.

### Conclusions

Knowledge of the system being modeled is important to reduce the total number of experiments necessary to model the significant interactions. Significant experience has been gained through this project. The application of Design of Experiments must be evaluated with regard to the objectives of the study and the

available resources. If determining the optimal level for the parameters is the primary concern or if the analysis results are needed very quickly, DOE would be the preferred approach; however, if little is known of the system being studied or if a detailed sensitivity analysis is needed a traditional parametric study is recommended.

### **PLUME MODEL INVESTIGATION TEAM (PLUMMIT)**

The PLUMMIT goal is to "validate Space Station plume impingement load predictions in a timely and cost effective manner." The team recently completed a series of vacuum chamber tests to validate instrumentation utilizing Johnson Space Center's (JSC) Vacuum Chamber E. The next phase of the investigation includes instrumentation checkout and chamber effects characterization in JSC's Vacuum Chamber A, followed by the plume flowfield mapping.

The PLUMMIT test program is designed to validate plume impingement calculation methodologies for application to space station load predictions. This series of experiments will provide baseline data for the validation of source flow plume models, gas surface interaction data for validation of impingement models, and data for the validation of high fidelity plume models. In addition, sufficient data will be obtained to characterize the uncertainty of current baseline plume impingement tools and construct models for nozzle scarfing, multiple jet interactions, and temporal plume variations which are neglected at this time.

#### **Experiment Plan**

The current test plan in progress is comprised of:

1. Instrument Validation Testing
  - Utilizes JSC Vacuum Chamber E
  - 1.25# cold gas jet with conical nozzle
  - Characterize instrument response, sensitivity, and accuracy
  - Test dates of June 6-10, July 27-31, and August 24-28
2. Plume Characterization Testing
  - Utilizes JSC Vacuum Chamber A
  - 2.5# and 10# cold gas jets, 25# O<sub>2</sub>H<sub>2</sub> thruster
  - Characterize plume flowfield parameters
  - Test dates of November 16-20 and December 7-11
3. Numerical Code Development
4. Material Accommodation Testing (proposed for FY'93)
5. SPIFEX flight experiment (currently in design, with flight in FY'94)

The experimental layout, shown in Figure 3, requires the mounting of the cold gas jets and the  $O_2H_2$  thruster near the chamber floor with the main instrument cluster mounted on a boom with the capability of sweeping  $\pm 45^\circ$  and having a vertical movement from 0 to 40 feet above the engine platform.

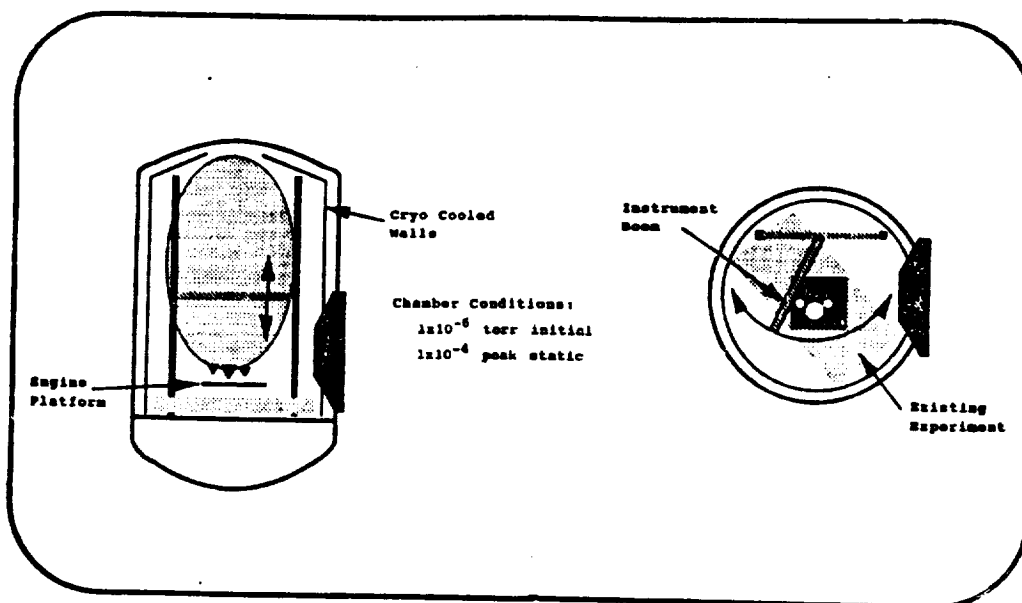


Figure 3. Vacuum Chamber A Test Schematic

### Experiment Optimization

As the testing must meet the project objectives at minimum cost, a significant effort has been made to optimize the plume characterization testing utilizing Vacuum Chamber A. The initial test matrix, given on Table II, was modeled using an inner array having six parameters, two with two levels, two with three levels, and the remaining two parameters with four levels. The sweeping of the sensing instrumentation was modeled as an outer or noise array with sweep angles of  $-45^\circ$  to  $+45^\circ$  (stepped every  $15^\circ$ ) and a total of 28 vertical positions. This resulted in an initial full factorial experiment that would require 73,024 rocket firings. Careful review of the relevant parameters and their levels has resulted in a reduction of the number of rocket firings to 679. The most recent inner and outer test matrices are given in Tables III and IV. As a better understanding of the instrumentation and the plume flowfield is obtained after each chamber test, the Vacuum Chamber A test matrices will continue to be revised to permit the optimization of each subsequent experiment.

Table II. Initial Test Matrix

### Engine Parameters

	<b>-Hot-</b>	<b>-Cold-</b>
<b>Types of Propellants</b>	<b>O<sub>2</sub>/H<sub>2</sub></b>	<b>N<sub>2</sub>,Ar,CO<sub>2</sub></b>
<b>0's of Scarfing</b>	<b>0<sup>0</sup></b>	<b>0<sup>0</sup>,15<sup>0</sup>,30<sup>0</sup></b>
<b>0's of Gimbal</b>	<b>0<sup>0</sup></b>	<b>0.0<sup>0</sup>,2.5<sup>0</sup>,5.0<sup>0</sup></b>
<b># of Engines</b>	<b>1</b>	<b>1,2</b>
<b>Firing Duration</b>	<b>80,160, 240,480 m.s.</b>	
<b>Thrust Levels</b>	<b>1</b>	<b>1,2</b>

### Boom Position Parameters

<b>Sweep Angles</b>	<b>-45<sup>0</sup> to +45<sup>0</sup> by 15 steps (Scarfed)</b> <b>0<sup>0</sup> to +45<sup>0</sup> by 15<sup>0</sup> steps (Unscarfed)</b>
<b>Vertical Position</b>	<b>1 point at less than 100R</b> <b>1 point at 100R</b> <b>1 point at slightly more than 100R</b> <b>25 points at 120R to 40 feet.</b>

### Total Number of Test Runs

$$4 \cdot 112 + 3 \cdot (48 \cdot 112 + 96 \cdot 196) = 73,024$$

### Continuing Effort

Prior to the November test week, the final inner and outer matrices will be combined forming a single matrix with each of the 679 experiments defined by a row of the matrix. This matrix will then be sorted in such a manner that the time necessary to set-up for each following run will be minimized. It is hoped that the selection of an optimal test sequence will permit the completion of all 679 runs during the first week. This would permit the use of the second week of testing to repeat questionable data points and perform multiple runs under the most important configurations to reduce the uncertainty of the results.

Table III. Final Inner Experimental Array

Experimental Array (Rows 8-11 & 12-15 utilize a Full Factorial L4 OAs)  
 (Rows 16-24 utilize a Full Factorial L9 OA)

	Propellents	Scarfig	Gimbal	No. Engines	Thrust	Duration	Outer Array	Comments
1	O <sub>2</sub> /H <sub>2</sub>	0°	0.0°	1	1	80 ms	A 25	<i>Reacting Chem/High Enthalpy Flows</i> Outer Array has four sweeps with a fuller sweep at the third level.
2	O <sub>2</sub> /H <sub>2</sub>	0°	0.0°	1	1	240 ms	A 25	
3	O <sub>2</sub> /H <sub>2</sub>	0°	0.0°	1	1	480 ms	A 25	
4	N <sub>2</sub>	0°	0.0°	1	1	80 ms	B 18	<i>Instrument &amp; Flow Characterization</i> Outer array has three sweeps with a fuller sweep at second level. Last row has reduced Outer Array.
5	N <sub>2</sub>	0°	0.0°	1	1	240 ms	B 18	
6	N <sub>2</sub>	0°	0.0°	1	1	480 ms	B 18	
7	N <sub>2</sub>	0°	0.0°	1	1	720 ms	C 6	
8	N <sub>2</sub>	0°	0.0°	1	1	240 ms	D 28	<i>Multi-jet Effects</i> Outer array has three sweeps with fuller sweeps at the lower levels. Need better defined levels & angles.
9	N <sub>2</sub>	0°	0.0°	1	2	240 ms	D 28	
10	N <sub>2</sub>	0°	0.0°	2	1	240 ms	D 28	
11	N <sub>2</sub>	0°	0.0°	2	2	240 ms	D 28	
12	N <sub>2</sub>	0°	0.0°	1	1	240 ms	D 28	<i>Multi-jet Effects with Electron Gun</i> Same outer arrays as above.
13	N <sub>2</sub>	0°	0.0°	1	2	240 ms	D 28	
14	N <sub>2</sub>	0°	0.0°	2	1	240 ms	D 28	
15	N <sub>2</sub>	0°	0.0°	2	2	240 ms	D 28	
▶ 16	N <sub>2</sub>	0°	-15°	1	1	240 ms	E 38	<i>Scarfig Characterization</i> Gimbal used to increase plume area being mapped
▶ 17	N <sub>2</sub>	0°	0°	1	1	240 ms	E 38	
▶ 18	N <sub>2</sub>	0°	15°	1	1	240 ms	E 38	
▶ 19	N <sub>2</sub>	15°	-15°	1	1	240 ms	F 28	The E outer array has five sweeps each from -45 to 45 as the plume is not symmetric. The F outer array has been reduced to only three sweeps. Marked rows may be omitted for a reduced minimal matrix.
▶ 20	N <sub>2</sub>	15°	0°	1	1	240 ms	F 28	
▶ 21	N <sub>2</sub>	15°	15°	1	1	240 ms	F 28	
▶ 22	N <sub>2</sub>	40°	-15°	1	1	240 ms	F 28	
▶ 23	N <sub>2</sub>	40°	0°	1	1	240 ms	F 28	
▶ 24	N <sub>2</sub>	40°	15°	1	1	240 ms	F 28	
25	Ar	0°	0.0°	1	1	240 ms	G 19	<i>Gamma Effect</i> Three sweeps, first fuller
26	CO <sub>2</sub>	0°	0.0°	1	1	240 ms	G 19	<i>Gamma Effect</i> Three sweeps, first fuller

▶ These experiments can be omitted for the reduced set of experiments.

Number of Reduced Experiments 491

Number of Primary (Baseline) Experiments 679

Number of Secondary Experiments



## FIRST LUNAR OUTPOST PROJECT

The development and evaluation of the reusability of Logistics Modules to increase the lunar habitat usable volume was performed independently by Carolina Vargas, a student participant in the Faculty Fellowship Program. The results of her study have been reported separately in Section 25 of the Annual Summer Faculty Fellowship Program Report.

### REFERENCES

- [1] Ross, P.J.: *Taguchi Techniques for Quality Engineering*. McGraw-Hill, 1988.
- [2] Phadke, M.S., *Quality Engineering Using Robust Design*. Prentice Hall, 1989.
- [3] Taguchi, G.; Konishi, S.: *Orthogonal Arrays and Linear Graphs: Tools for Quality Engineering*. American Supplier Institute, Inc. (Dearborne), 1987.

**STUDY OF PLATE-FIN HEAT EXCHANGER AND COLD PLATE FOR THE  
ACTIVE THERMAL CONTROL SYSTEM OF SPACE STATION**

**Final Report**

**NASA/ASEE Summer Faculty Fellowship Program -1992**

**Johnson Space Center**

**Prepared by:** Ming-C. Chyu, Ph.D.  
**Academic Rank:** Associate Professor  
**University & Department:** Texas Tech University  
Department of Mechanical Engineering  
Lubbock, Texas 79409-1021

**NASA/JSC**

**Directorate:** Engineering  
**Division:** Crew and Thermal Systems  
**Branch:** Systems Engineering Analysis Office  
**JSC Colleague:** Eugene K. Ungar, Ph.D.  
**Date Submitted:** July 31, 1992  
**Contract Number:** NGT-44-005-803

## ABSTRACT

Plate-fin heat exchangers will be employed in the Active Thermal Control System of Space Station Freedom. During ground testing of prototypic heat exchangers, certain anomalous behaviors have been observed. Diagnosis has been conducted to determine the cause of the observed behaviors, including a scrutiny of temperature, pressure, and flow rate test data, and verification calculations based on such data and more data collected during the ambient and thermal/vacuum tests participated by the author. The test data of a plate-fin cold plate have been also analyzed. Recommendation was made with regard to further tests providing more useful information of the cold plate performance.

## INTRODUCTION

The compactness and high efficiency of plate-fin heat exchangers have led to their application in the Active Thermal Control System of the Space Station Freedom. In such application, ammonia is evaporated by means of warm water flowing through the heat exchanger composed of a number of finned flow passages. In a similar device, cold plate, the heat applied to a plate is removed by the evaporating ammonia flowing in a finned passage on the other side of the plate. Both plate-fin heat exchanger and plate-fin cold plate have been tested in the Space Station Ground Test Article (GTA) at NASA Johnson Space Center.

## PLATE-FIN HEAT EXCHANGER

### Introduction

The prototypic plate-fin heat exchanger (PPFHX) tested in GTA was manufactured by Allied Signal Aerospace Company, with a core of 10.50 in  $\times$  2.75 in  $\times$  1.65 in, which is composed of 10 water passages interlaminated with 9 ammonia passages with all passages featuring offset fin structure. The results of the February 1992 GTA test indicated a performance inferior to the design expectation. The objectives of the present work are (a) to diagnose the PPFHX based on the existing test data, (b) to design and conduct further tests, and (c) to characterize the heat exchanger based on all test data available.

### Diagnostic Analysis

During the GTA test conducted in February 1992, very large pressure drop has been observed on the water side (about 4.7 psid compared with 1.1 psid design specification at 1800 lbm/hr). Such high pressure drop is considered due to blockage of flow passages. The flow passages can be blocked if the heat exchanger was not properly brazed during manufacturing. According to the manufacturer, the plates and fins were brazed together by interposed braze sheets, which melted and being sucked into the interstices during a controlled oven-heating process. If the heating process is not well controlled in terms of temperature levels, timing, and uniformity of heat, stray molten braze may partially or even entirely block the finned passages. The current heat exchanger is a custom-built unit which required a special heating process to braze. However, according to the manufacturer, the unit was heated along with other units following a regular heating procedure because of constraint of time and cost.

An ensuing problem of blockage of water flow passages is uneven heating of ammonia flow passages. In a blocked water passage, the flow rate is low, and the heat transfer rates to the adjacent ammonia passages are low. On the other hand, the water flow rate in an unblocked (or less blocked) passage is high, and the heat transfer rates to the adjacent ammonia passages are high. The heat transfer rate can be so high that the ammonia becomes superheated vapor at the outlet. The superheated vapor then mixes at the ammonia outlet with the saturated vapor and saturated liquid from passages with low heat rates. The saturated liquid temperature ought to be detected if a thermocouple is installed at the bottom of the ammonia outlet manifold. The saturated liquid can be vaporized by the superheated vapor. However, the vaporization rate is low because of the low heat transfer coefficient between the superheated vapor and the saturated liquid.

Therefore, it takes a long time for such two-phase flow to reach a thermal equilibrium. The temperature measurement taken at the ammonia outlet 10 in away from the body of the heat exchanger indicated significant superheating within the heat exchanger.

Superheating of ammonia results in a low heat exchanger performance due to the low heat transfer coefficient between the ammonia vapor and the fin structure which is supposed to be wetted by ammonia liquid. This is considered the reason why the present heat exchanger did not measure up the design expectation.

The core of the heat exchanger was examined using a borescope in order to detect any visible blockage. There was no sign of blockage in the fin structure as viewed from the water inlet and outlet manifolds. The size of the borescope prohibited viewing of the internal core structure.

Another concern regarding the inferior heat exchanger performance is the material compatibility. The braze alloy used in binding the plates and fins, AMS 4778, contains 91% of Ni, 4.5% of Si, 3.5% of B, 0.8% of Fe, and 0.05% of C, of which iron has "severe effect" when in contact with ammonia (Grainger Catalog No. 380). The supplier of the heat exchanger indicated that no compatibility test had ever been conducted with such braze alloy and ammonia, even though a report on the ammonia compatibility tests of a number of other braze alloys was provided.

The heat exchanger has been returned to the manufacturer after the GTA test in June, 1992, to go through regular testing which should have been conducted before shipping.

### Experimental Results and Discussion

After reviewing the February 1992 test data, the author participated in the GTA test in June. The results of the June test, both ambient and thermal/vacuum, are presented and compared with February 1992 test data (Sifuentes et al., 1992) below. All the data were taken at the water flow rates between 1781 and 1837 lbm/hr, and the ammonia flow rates ranging from 75 to 113 lbm/hr. The heat load or the heat exchange rate between two streams,  $Q$ , the quality at the ammonia outlet,  $x$ , the heat exchanger effectiveness,  $\epsilon$ , and overall heat transfer coefficient,  $UA$ , are calculated using the following equations:

$$Q = \dot{m}_{H_2O} \times C_{p,H_2O} \times (T_{H_2O,in} - T_{H_2O,out})$$

$$x = \frac{Q}{\dot{m}_{NH_3} h_{fg,NH_3}}$$

$$\epsilon = \frac{T_{H_2O,in} - T_{H_2O,out}}{T_{H_2O,in} - T_{NH_3,in}}$$

$$UA = \frac{Q}{\Delta T_{lm}}$$

where  $\Delta T_{lm}$  is the log-mean temperature difference. Figure 1 shows the expected trend of heat load increasing with approach temperature, the temperature difference at the inlet. There is a reasonable agreement among the data of three different tests, viz., February ambient test, June ambient test, and June thermal/vacuum test. However, the design

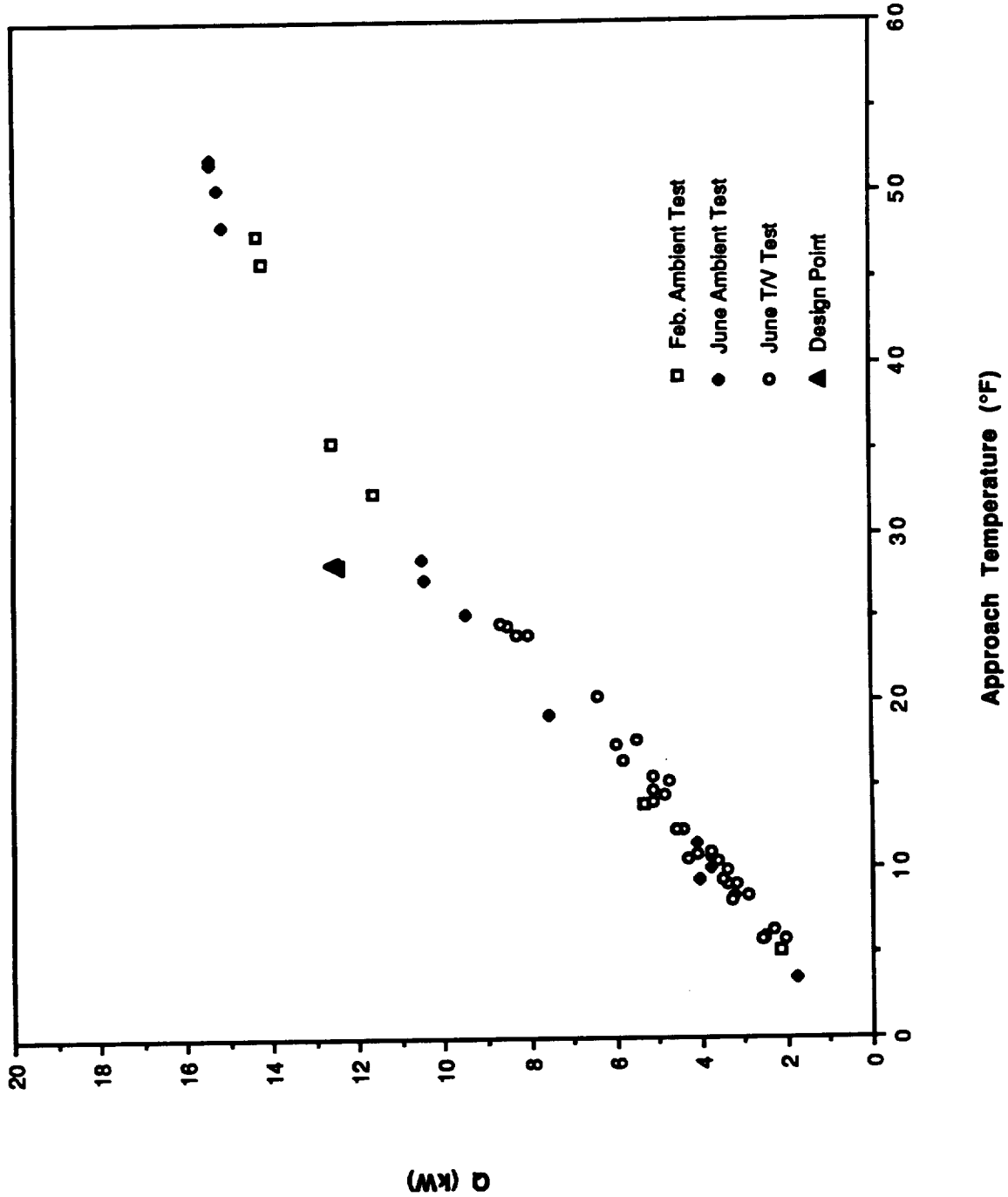


Figure 1. - Heat Load vs Approach Temperature

points are above the data curve, indicating that at the design approach temperature (28°F), the heat exchanger falls short of achieving the desired heat transfer rate (12.5 kW) by about 16%. The pinch temperature (difference between the water outlet and the ammonia inlet temperatures) versus approach temperature data exhibited in Fig. 2 show that all test data demonstrate pinch temperature increasing with approach temperature. It is also indicated that at the design approach temperature, the pinch temperature is about three times as large as the design specification (3°F). The pinch temperature vs. heat load plot (Fig. 3) shows that at the design heat load (12.5 kW), the pinch temperature is approximately four times as large as the design specification. Since quality is directly proportional to heat load, Fig. 4 is simply a different presentation of Fig. 1.

Both the effectiveness and the overall heat transfer coefficient data presented in Figs. 5 and 6, respectively, demonstrate decreasing trends with heat load. This trend is due to a large dryout area in the ammonia passages at a high heat rate, resulting in a low heat transfer coefficient as well as heat exchanger effectiveness. Figure 7 in fact is a different presentation of Fig. 6; however, it clearly exhibits a trend contrary to all the published results that heat transfer coefficient increases with quality. Heat transfer coefficient increases with quality because at a high quality, the fin surfaces are covered with liquid films, and the heat transfer coefficient of thin film evaporation increases with smaller film thickness as quality increases. The reverse trend of the present data is due to the large dryout area in the heat exchanger as quality increases with heat load.

### **Conclusion of Experimental Study**

All the data obtained under different times and test conditions demonstrated reasonable agreement and consistent trends, and strongly suggesting a heat exchanger performance inferior to the design specification. The effectiveness and overall heat transfer coefficient data support the proposed diagnostic mechanism for the inferior heat exchanger performance of premature ammonia side dryout due to uneven water side heating.

### **Evaluation of Proposed Heat Exchangers for Prototypic Test Article (PTA)**

Ten heat exchangers have been ordered from Hughes-Treitler Mfg. Corp. for the forthcoming Prototypic Test Article (PTA). These are also offset plate-fin heat exchangers with slightly different design specifications than the Allied Signal GTA heat exchanger. The proposed design was evaluated. The major difference compared with the GTA heat exchanger seems to be in the flow configuration. The GTA heat exchanger operates in parallel flow, while the PTA heat exchanger will operate in counterflow arrangement. The possible advantage of a parallel-flow evaporator is the large temperature difference at the inlet which facilitates inception of nucleate boiling on the cold (ammonia) side. However, such advantage does not exclude the possibility that a well-designed counterflow unit can do equally well. In fact, it has been observed that nucleate boiling does not occur in the evaporating flow in an offset-finned passage (Carey and Mandrusiak, 1986, Mandrusiak et al., 1988). Therefore, the large inlet temperature difference in a parallel-flow evaporator perhaps does not substantiate any advantage over a counterflow evaporator.

### **PLATE-FIN COLD PLATE**

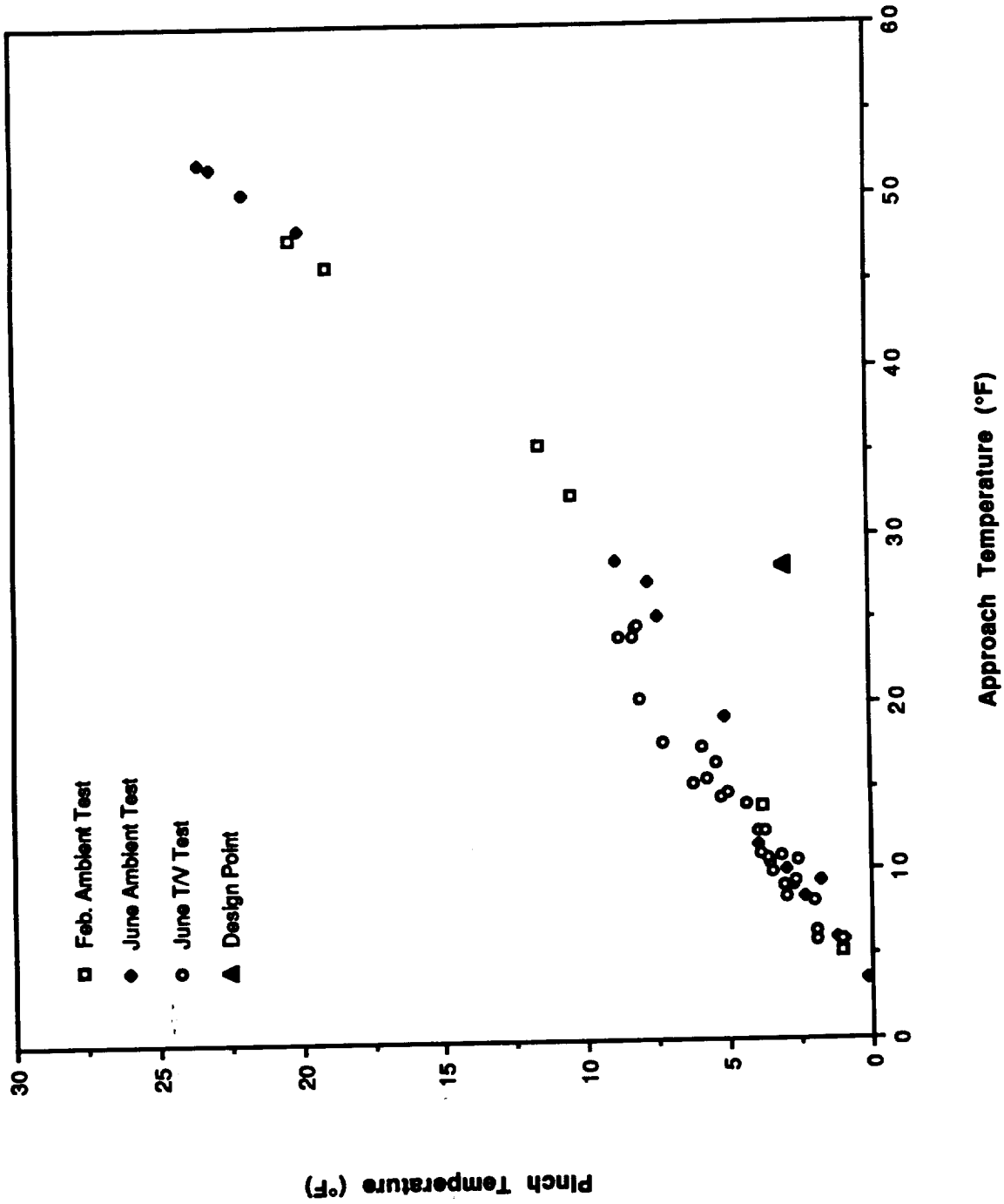


Figure 2. - Pinch Temperature vs Approach Temperature

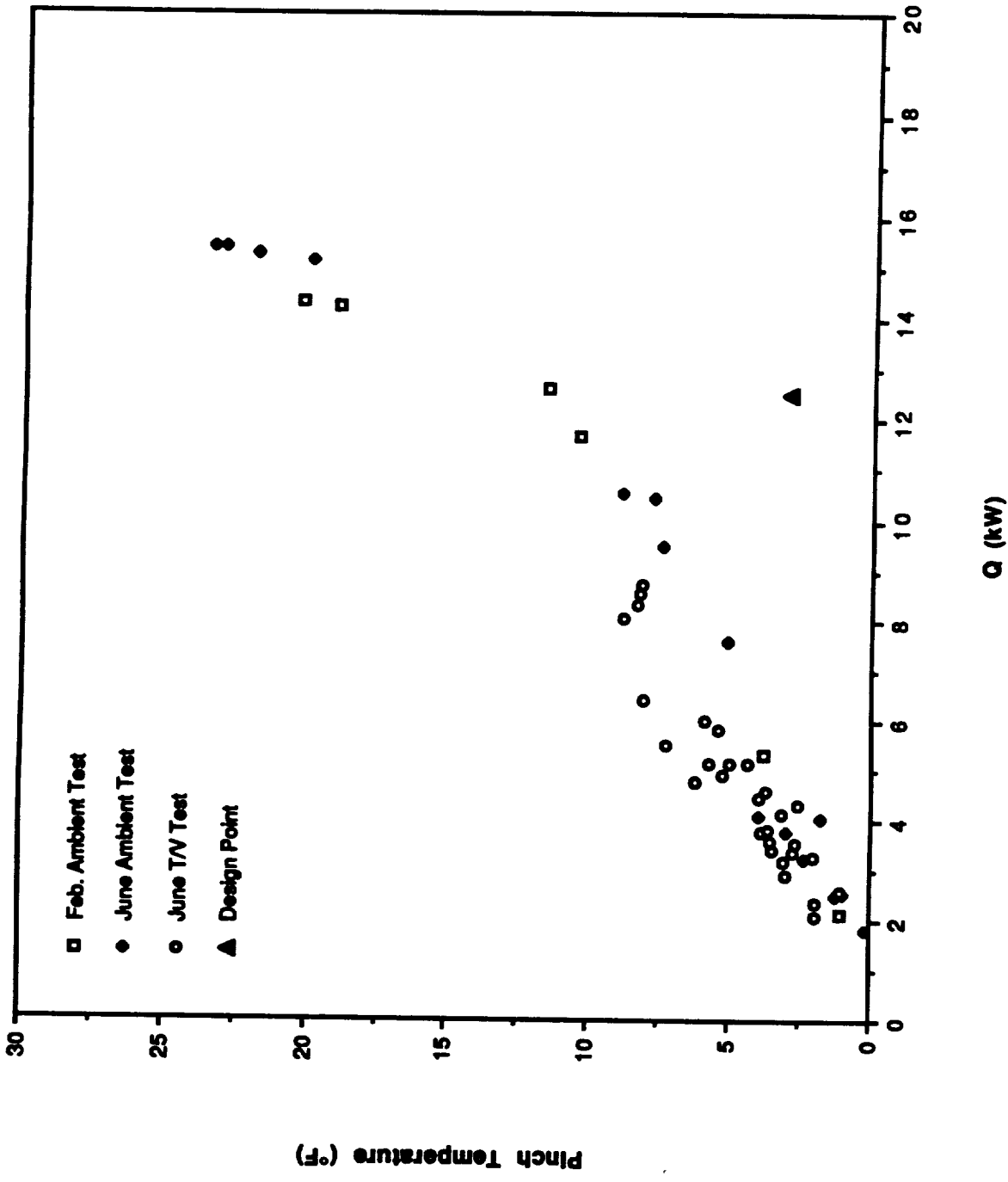


Figure 3. - Pinch Temperature vs Heat Load

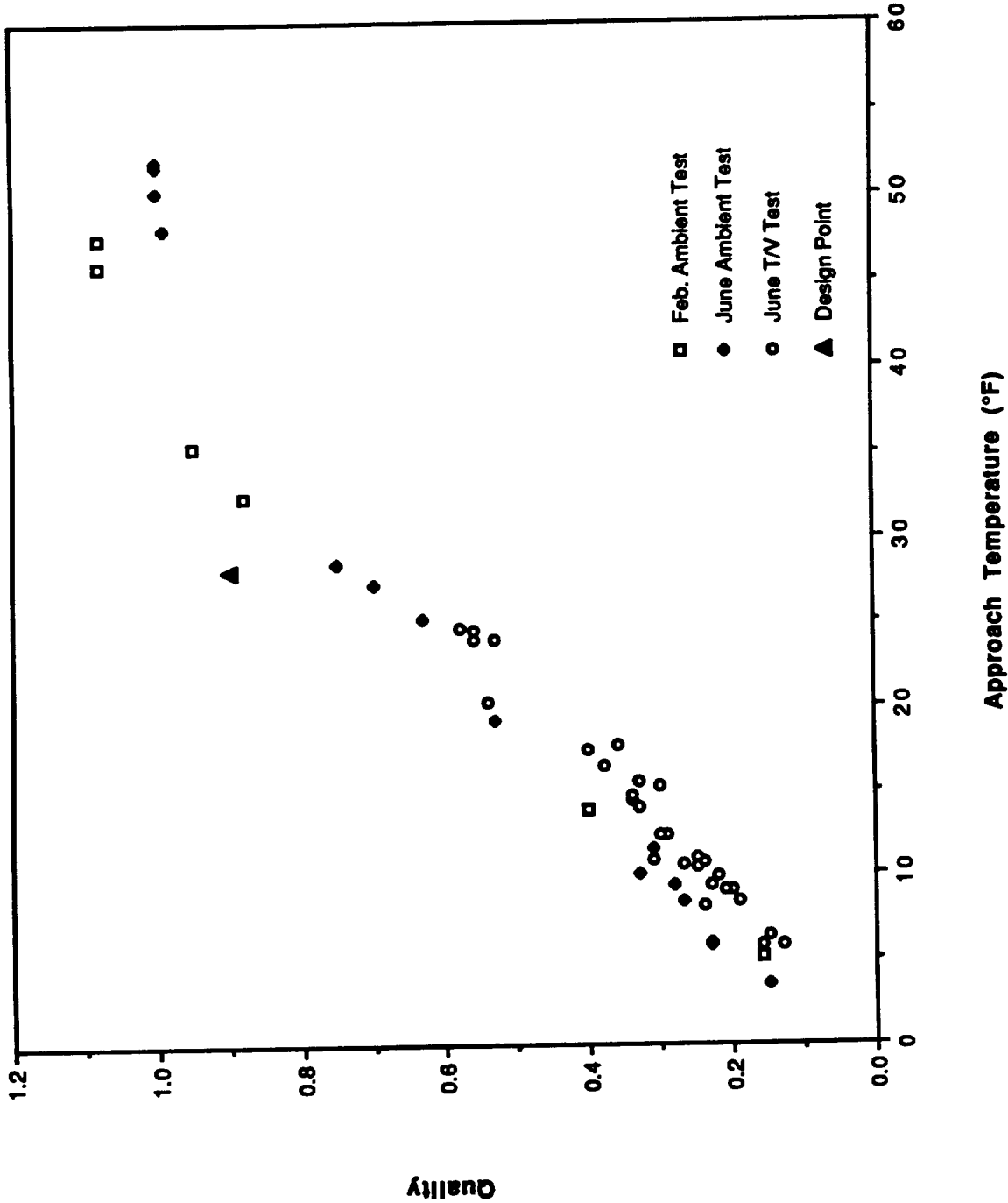


Figure 4. - Quality vs Approach Temperature



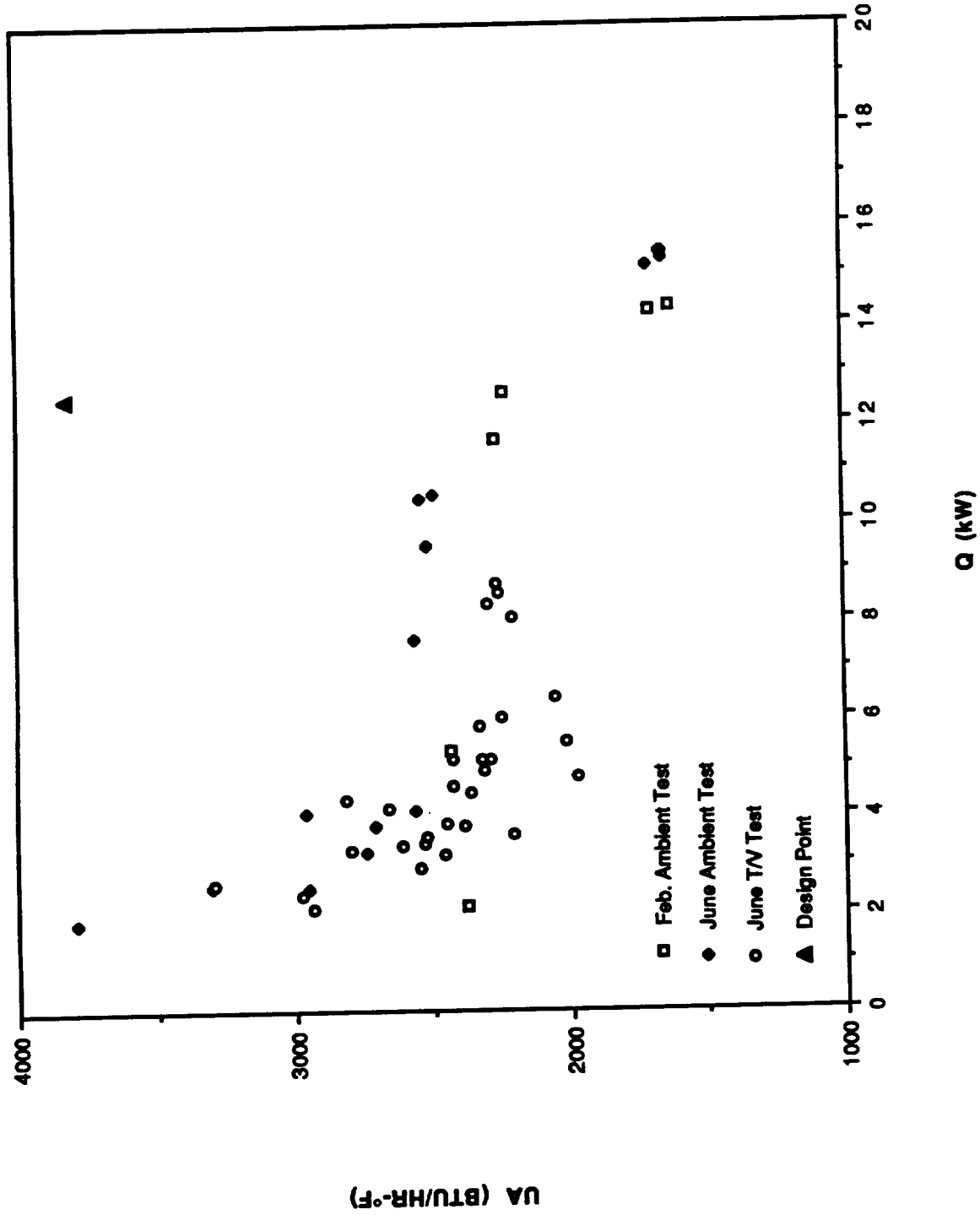


Figure 6. - Overall Heat Transfer Coefficient vs Heat Load

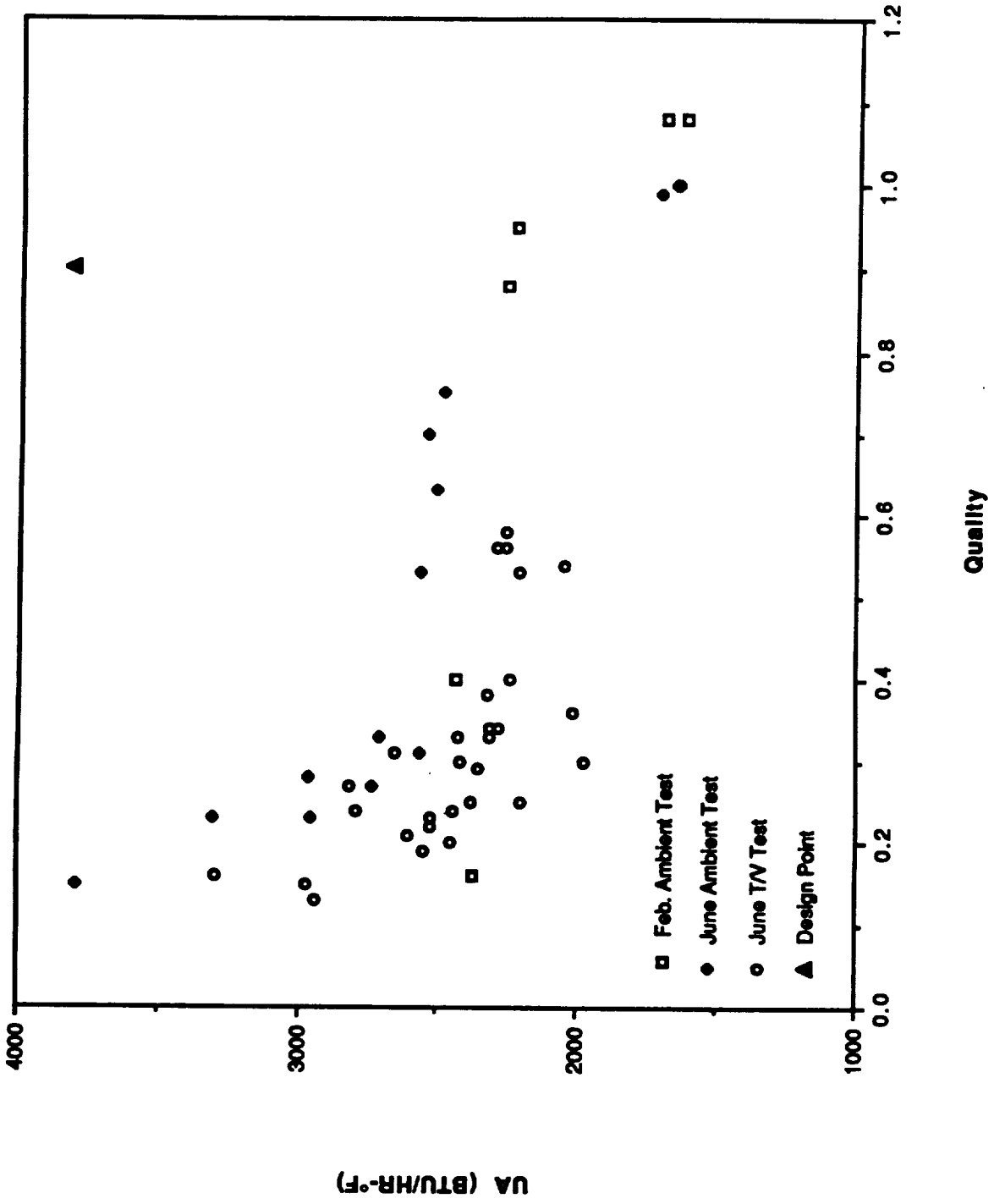


Figure 7. - Overall Heat Transfer Coefficient vs Quality

## Introduction

An offset fin cold plate was tested in the GTA for its appropriateness as a means of temperature control of thermally active units such as electronic components. The Allied Signal plate-fin cold plate (26.90 in  $\times$  26.65 in  $\times$  0.85 in) has one serpentine offset-finned flow passage sandwiched between two plates, as shown in Fig. 8. Both the fins and the plates are of commercial 6061 aluminum. Commercial electric heaters (Minco etched-foil heaters) are installed on the top plate outside surface to simulate the heat sources. Tape thermocouples are installed on the bottom plate outside surface. The objective of this part of study is (a) to quantitatively characterize the performance of the cold plate by calculating the heat transfer coefficient, (b) to compare the performance data with published results, and (c) to develop improved performance prediction method for cold plates of this type.

## Analysis

Considering one dimensional heat transfer across the cold plate, the temperature profile is qualitatively shown in Fig. 8. The broken curve across the finned flow passage indicates the unknown temperature profile along the fin, depending on the convective heat transfer coefficient on the fin surface. Owing to the insulation at the bottom plate surface, the temperature distribution across the bottom plate should be very uniform. Therefore, the temperature at the bottom plate surface, as measured by the thermocouples, is very close to the bottom wall temperature of the finned flow passage. The cold plate data collected in February 1992 test generally demonstrated higher wall temperatures at the inlet and lower wall temperatures at the outlet, a trend consistent with the published results that heat transfer coefficient increases with quality.

However, the present temperature data at the bottom plate surface are not appropriate for the calculation of the heat transfer coefficient of the cold plate. Since only the top plate was heated and the bottom plate was insulated, the heat transfer coefficient should be based on the top wall temperature which, however, was not measured in the test. Even if heat transfer coefficient is determined based on the bottom plate surface temperature, there is no published experimental data or correlation available for comparison. The published works on offset fin heat transfer data are mainly for heat exchangers with the finned flow passage subject to heating on both walls forming the passage (e.g., Chen et al., 1981, Robertson and Lovegrove, 1983, Panchal, 1989, Panchal and Arman, 1991). The only data available for the condition of one wall heated and the other wall insulated, as in the case of the present cold plate, are for water and methanol (Mandrusiak, et al., 1988) and *n*-butanol (Carey and Mandrusiak, 1986). No study has been conducted for the heat transfer of an evaporative ammonia flow in a passage with offset fins and with only one wall heated. A proposal has been submitted to NASA/JSC, which includes such experiment to be performed at Texas Tech University.

## Conclusion

In summary, the results of the present study on plate-fin cold plate suggest the following: (a) The data collected for the present cold plate are not appropriate for the development of a prediction correlation. (b) A reliable prediction correlation for the cold

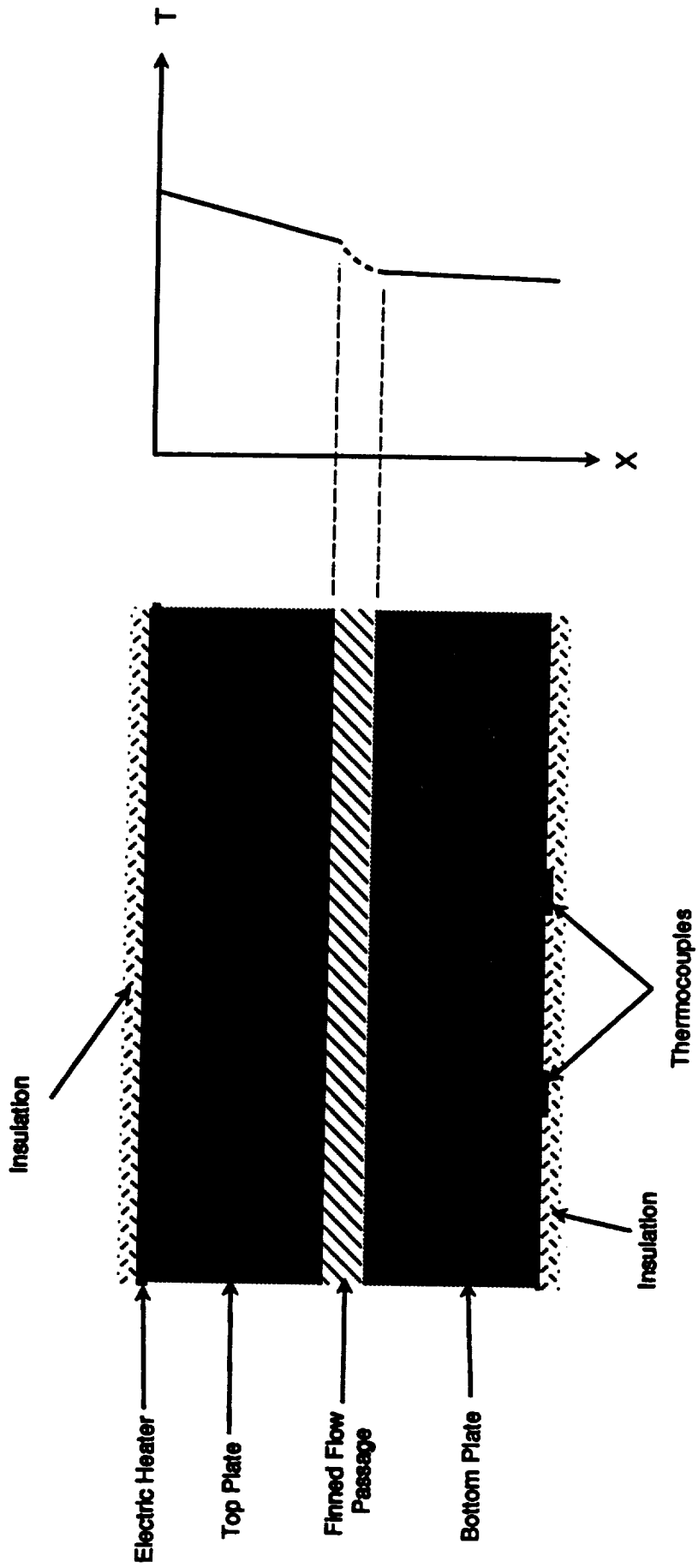


Figure 8. - Plate-Fin Cold Plate

plate should be based on the temperature of the heated wall and should be independent of the plate thickness. A design practitioner can predict the operating temperature of the heat source mounted on the heated plate based on such correlation and a conduction analysis across the plate. (c) There is a need of research for the evaporation of ammonia in a plate-fin cold plate with only one wall heated to provide heat transfer data for the development of reliable correlations. It is recommended that the heated wall temperature of the finned flow passage be determined by extrapolation of the temperature profile based on the readings of three or more thermocouples installed at different locations across the thickness of the heated plate.

## REFERENCES

- Carey, V. P., and Mandrusiak, G. D., 1986. "Annular Film-Flow Boiling of Liquids in a Partially Heated, Vertical Channel With Offset Strip Fins," *Int. J. Heat Mass Transfer*, Vol. 29, No. 6, pp. 927-939.
- Chen, C. C., Loh, J. V., and Westwater, J. W., 1981. "Prediction of Boiling Heat Transfer Duty in a Compact Plate-Fin Heat Exchanger Using the Improved Local Assumption," *Int. J. Heat Mass Transfer*, Vol. 24, No. 12, pp. 1907-1912.
- Grainger Catalog No. 380, W. W. Grainger, Inc., pp. 2251.
- Mandrusiak, G. D., Carey, V. P., Xu, X., 1988. "An Experimental Study of Convective Boiling in a Partially Heated Horizontal Channel With Offset Strip Fins," *J. Heat Transfer*, Vol. 110, pp. 229-236.
- Panchal, C. B., and Arman, B., 1991. "Analysis of Condensation and Evaporation of Ammonia/Water Mixtures in Matrix Heat Exchangers," paper presented at 1991 ASME/AIChE National Heat Transfer Conference, Minneapolis.
- Panchal, C. B., 1989. "Analysis of Flow Boiling of Ammonia and R-114 in a Matrix Heat Exchanger," Proc. 1989 ASME/AIChE National Heat Transfer Conference, Philadelphia.
- Robertson, J. M., and Lovegrove, P. C., 1983. "Boiling Heat Transfer With Freon 11 (R 11) in Brazed Aluminum, Plate-Fin Heat Exchangers," *J. of Heat Transfer*, Vol. 105, pp. 605-610.
- Sifuentes, R., Bryant, M., Teunisse, B., Lee, L., 1992. "GTA Phase II Ambient Test Quick-Look Summary," March 18, 1992.



N93-26065

A PROTOTYPE FOR SIMULATION OF THE SPACE-TO-GROUND  
ASSEMBLY/CONTINGENCY SYSTEM OF SPACE STATION FREEDOM

Final Report

NASA/ASEE Summer Faculty Fellowship Program 1992

Johnson Space Center

Prepared by: Louis A. DeAcetis, Ph.D.

Academic Rank: Professor of Physics

University & Department: Bronx Community College of the  
City University of New York  
Physics Department  
Bronx, NY 10453

NASA/JSC

Directorate: Engineering

Division: Tracking and Communications

Branch: Systems Engineering

JSC Colleague: Oron Schmidt

Date Submitted: August 14, 1992

Contract Number: NGT-44-0005-803

## ABSTRACT

This project was a continuation of work started during the Summer of 1991 when techniques and methods were investigated for simulating equipment components of the Communications and Tracking System on Space Station Freedom (SSF). The current work involved developing a design for simulation of the entire Assembly/Contingency Subsystem (ACS), which includes the Baseband Signal Processor, standard TDRSS Transponder and the RF Group antenna assembly. A design prototype of the ACS was developed.

Methods to achieving "high fidelity" real-time simulations of the ACS components on IBM-PC compatible computers were considered. The intention is to have separate component simulations running on separate personal computers (PC's), with the capability of substituting actual equipment units for those being simulated when such equipment becomes available for testing. To this end, a scheme for communication between the various simulated ACS components was developed using the serial ports of the PC's hosting the simulations. In addition, control and monitoring of ACS equipment on SSF will be via a MIL-STD 1553B bus. The proposed simulation includes actual 1553B hardware as part of the testbed.

## INTRODUCTION

The design of Space Station Freedom is constantly undergoing revision and change. The Communications and Tracking (C&T) Systems in particular have undergone extensive revisions. These will impact on testing and verification schedules if current timetables are to be maintained. Since simulations of the hardware can permit testing of various aspects of a system without having all of the hardware in hand, they can permit certain levels of system testing that might not otherwise be possible. Any simulator development and implimentation methods must be flexible to readily permit modifications as further changes are (inevitably) introduced. Last summer [1], techniques and methods for simulating C&T components were investigated, and a prototype for the standard TDRSS Transponder was developed that ran on a separate IBM compatible personal computer which contained a MIL-STD 1553B bus interface card. All simulations were written in Ada, and include interfaces to the 1553B card driver software which is written in the "C" programming language. This summer, the investigation was continued by considering methods of integrating and linking together the separate equipment simulations in such a way that if an actual item of equipment were available, it could be incorporated into the testbed by removing the PC running its simulation and using the actual equipment. Such a substitution should in principle be transparent to the rest of the system.

## METHOD

Paradigms for simulating operating equipment has been developed [1,2] which can be used for elements of the Assembly/ Contingency Subsystem (ACS) of Space Station Freedom (SSF). Figure 1 [3] is a diagram of the current configuration of equipment for the ACS. As a result of the work of both summers, a prototype of the Baseband Signal Processor (BSP) simulation has been added to the Standard TDRSS Transponder simulation of last summer.

*ASSEMBLY/CONTINGENCY  
TDRSS S-BAND SUBSYSTEM*

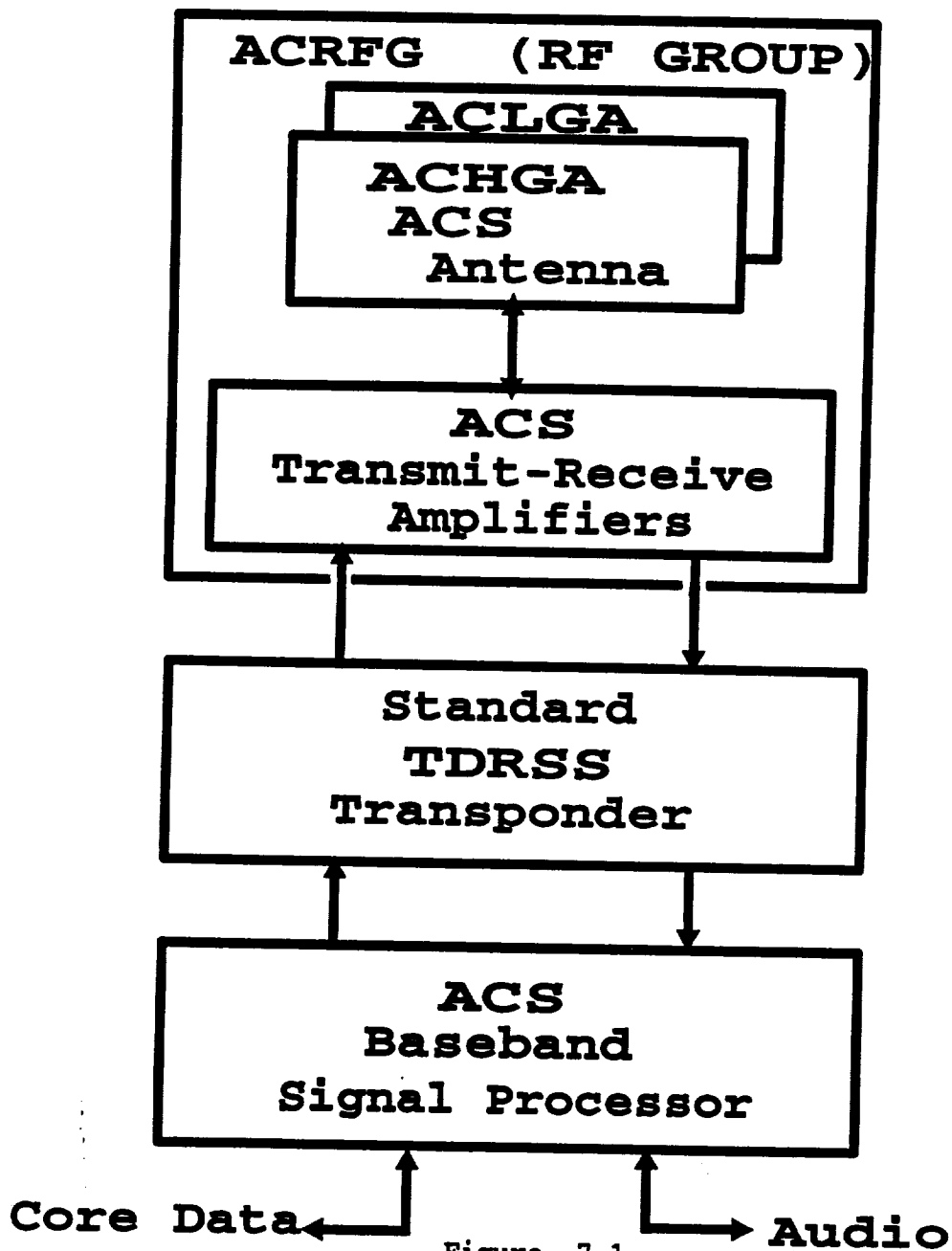


Figure 7-1

Each simulator is written in Ada and resides on a PC/AT level (or higher) personal computer with a MIL-STD 1553B [4] interface card installed. Driver software, in C, for the cards was supplied by the manufacturer [5,6], and the Ada programs interface with these drivers. Commands are sent to the simulated equipment via the 1553B bus that connects the various PC's together in a bus "network" of the type that will exist on the space station. The form of the commands, taken from current documents [7], is the same as is anticipated to actually be used. The simulation software responds to the commands in a manner similar to that which the actual equipment would, based upon the (limited) information available at this time. The software is capable of being readily modified as more information about the actual equipment characteristics becomes available, so that the fidelity of the responses, and therefore the entire simulation, can be fine-tuned. Once an actual unit of equipment is available, it should be possible to disconnect the PC simulating that unit from the 1553B bus, and connect the unit in its place. Such a replacement should ideally be transparent to the rest of the elements on the bus.

One of the issues that had to be addressed was the need to "transmit" signals between the various pieces of equipment. In particular, if the Baseband Signal Processor is passing data to the Standard TDRSS Transponder and the BSP fails, then this would cause the data flow to cease. The interconnection between the Transponder and the BSP must therefore also be simulated. Each of the PC's hosting a simulation was equipped with two serial ports, and it was decided to use each of these two-way ports as the means of passing "signals" between connected pieces of equipment. This means that if an actual piece of equipment is substituted for its simulation, then the 1553B bus connection will be made to the equipment, but the PC (with appropriate substitute software), will still be connected to the serial ports of the other PC's to maintain the semblance the communication string being simulated. The simultaneous use of the serial ports and the 1553B bus interface thus appears to be a viable means of achieving the signal flow emulation.

## DISCUSSION and CONCLUSIONS

The major goals of this project were:

- a) To establish whether a PC programmed using Ada could be used to simulate a piece of ACS equipment with sufficient fidelity, and
- b) To demonstrate the capability of testing actual equipment on a testbed by substituting it for its simulation.

Although firm conclusions cannot be drawn on the basis of work done thus far, there is as yet no indication that either of the above goals cannot be met. That is, the work thus far indicates that both goals are viable using the methods described above. The main unanswered question is one of "sufficient fidelity." This will only be resolved when more information is obtained about the specifications of the various equipment. It is expected that this project will be ongoing, and that firmer answers can be made in the near future as the operational characteristics of the simulations are further developed and tested.

References:

1. "Investigation of Techniques for Simulating Communications and Tracking Subsystems on Space Station Freedom", Final Report, NASA/ASEE Summer Faculty Fellowship Program, Contract #NGT44-001-800, NASA Contractor Report 185670 (1991).
2. "Using Ada Tasks to Simulate Operating Equipment", L. A. DeAcetis, O. Schmidt, and K. Krishen, *Comp.Phys.*4, 521-525 (1990).
3. Adapted from "B1 Prime Item Development Specification Assembly/Contingency Subsystem (ACS)", Specification No. 10033098, Revision 4, GE Aerospace, Camden NJ 08102, May 9, 1991, P. 16.
4. "MIL-STD-1553 Designer's Guide, Third Edition", ILC Data Device Corporation, Bohemia NY 11716, 1990.
5. "BUS-69008 Microsoft C MIL-STD 1553B Driver, Rel. 1.52", ILC Data Device Corporation, Bohemia NY 11716, July 1989.
6. "BUS-69052 C Software for BUS-65515, Version 1.21", ILC Data Device Corporation, Bohemia NY 11716, August 1989.
7. "Software Interface Requirements Document (Communications and Tracking System Firmware-- Orbital Replacement Units and 1553 Local Bus", IRD No. GE 10033288, McDonnell Douglas Space Systems Co., Space Station Division, March 1992.



**METABOLIC RESPONSE OF ENVIRONMENTALLY ISOLATED  
MICROORGANISMS TO INDUSTRIAL EFFLUENTS: USE OF A NEWLY  
DESCRIBED CELL CULTURE ASSAY**

**Final Report  
NASA/ASEE Summer Faculty Fellowship Program -1992  
Johnson Space Center**

**Prepared By:** Robert N. Ferebee, Ph.D.  
**Academic Rank:** Associate Professor  
**University and Department:** University of Houston - Clear  
Lake  
Department of Biological  
And Environmental Sciences  
Houston, Texas 77058

**NASA/JSC**  
**Directorate:** Space and Life Sciences  
**Division:** Medical Sciences  
**Branch:** Biomedical Operations and  
Research

**JSC Colleague:** Duane L. Pierson, Ph.D.  
**Date Submitted:** September 15, 1992  
**Contact Number:**

**Metabolic Response of Environmentally Isolated Microorganisms To  
Industrial Effluents; Use of a Newly Described Cell Culture Assay.**

**Robert N. Ferebee, Ph.D.  
University of Houston-Clear Lake  
June 16, 1992**

**Duane L. Pierson, ph.D.  
Biomedical Research and Operations Division**

**Abstract of Proposed Work Plan**

**An environmental application using a microtiter culture assay to measure the metabolic sensitivity of microorganisms to petrochemical effluents will be tested.**

**The Biomedical Operations and Research Branch at NASA JSC has recently developed a rapid and nondestructive method to measure cell growth and metabolism. Using a colorimetric procedure the uniquely modified assay allows the metabolic kinetics of prokaryotic and eukaryotic cells to be measured. Use of such an assay if adapted for the routine monitoring of waste products, process effluents, and environmentally hazardous substances may prove to be invaluable to the industrial community.**

**The microtiter method as described will be tested using microorganisms isolated from the Galveston Bay aquatic habitat. The microbial isolates will be identified prior to testing using the automated systems available at JSC. Sodium dodecyl sulfate (SDS), cadmium, and lead will provide control toxic chemicals. The toxicity of industrial effluent from two industrial sites will be tested.**

**An effort will be made to test the efficacy of this assay for measuring toxicity in a mixed culture community.**

# Metabolic Response of Environmentally Isolated Microorganisms to Industrial Effluents: Use of a Newly Described Cell Culture Assay.

## Introduction:

Bioassays performed upon industrial process effluents continue to present problems related to time, difficulty in maintaining the animal species used, and the expense of such procedures. While this study does in no way suggest that bioassays using higher life forms be discontinued it does suggest there is a need to develop a rapid screening procedure that allows a daily monitoring of potentially toxic effluents.

Use of a recent modification of the tetrazolium reduction assay that allows simultaneous solubilization of the end product formazan indicated that the method could be used as a rapid screening assay for industrial wastes. This procedure not only allows one to detect changes in the physicochemical nature of effluents, but also provides a method to quickly screen for microorganisms that would be sensitive to toxic substances.

This research was designed to measure the effects that industrial effluents taken from three separate industrial process plants had on actively growing bacteria. The treated effluents from each of these industries are ultimately released into the Galveston Bay estuary system. Each of the industries were eager to cooperate in supplying samples for these studies.

## Materials and Methods:

**Test Organisms ;** Nine separate bacterial genera were collected in grab samples taken from selected sites on Galveston Bay - Texas. The bacteria were identified to species using both " Vitek" ( Vitek Systems Inc., Hazelwood, Mo.) and " Biolog" ( Biolog Inc., Hayward, Ca.), computer assisted, automated systems. These environmental isolates were tested in the presence of control chemicals of known toxicity as well as both treated and untreated (raw) industrial effluents. Of the bacteria tested Staphylococcus hominis and Pseudomonas putida showed greatest promise as indicator species and were used in subsequent tests. These same organisms were obtained from stock culture collections (Chrisope Technologies Lake Charles, LA) ; the sensitivity of these bacteria were compared to that of the environmental isolates.

**Chemicals;** Chemicals for toxic controls were obtained from Mallinckrodt Chemical Works St. Louis ,Mo.. Cadmium Chloride, Mercuric Sulfate , Lead Acetate, and Sodium Dodecyl Sulfate were all tested . Cadmium chloride gave the most consistent results with all the bacteria tested and was used for subsequent testing. Chemical for the tetrazolium assay were obtained from Sigma Chemical Co., St. Louis, Mo. Tetrazolium 1-(4,5- dimethylthiazol-2-yl)- 3,5 - diphenylformazan (MTT formazan), 2-phenazine methosulfate (PMS), and t-octylphenoxypolythoxyethanol (Triton X-100) were used in the assay for bacterial growth.

Culture media were obtained from BBL Microbiological Systems (Cockeysville, Md.). Bacteria were maintained on standard methods agar while the media used for microtiter culture was R2A broth.

**Tetrazolium Assays:** Testing for the bacterial activity was measured by reduction of MTT spectrophotometrically at 390nm minus 650nm. Test bacteria were removed from 18 hour cultures by sterile cotton swabs and suspended in filter sterilized deionized water. Cell suspensions were adjusted to OD 590 nm = 0.6 cell numbers. This density gave  $2 \times 10^9$  cells/ml. From this suspension 25 ul were added to 50 ul of double strength R2A broth in 96 well flat bottomed microtiter culture plates. All wells except cell controls received 50 ul known toxicants or 50 ul treated or raw effluent. Indicator chemicals were finally added as follows: 15 ul of 1.2 mM MTT, 10 ul of 0.06 mM PMS, and 25 ul of 160 mM Triton X-100. All controls and tests were set as replicates of four wells. Cultures were maintained at 30C and continually monitored at 590nm - 650nm for a maximum of two hours. The microtiter cultures were read using a microtiter plate reader (Molecular Device Co. Menlo Park, CA).

#### Results:

Each of the environmental bacteria as well as those obtained from stock collections exhibited an expected response when toxic chemicals were added to the cultures. There was a progressive inhibition of growth as the concentrations of the chemicals were increased, (Fig 1 & 2). The cadmium chloride gave the most consistent response and was used as the toxicant control (Fig 1&2). None of the chemicals tested caused any reduction of MTT; these represented chemical controls. When the bacteria selected for indicators were tested with industrial effluents only a single sample gave a significant change in bacterial growth and MTT reduction (figure 1 & 2). The sample identified as effluent (2R) did indicate toxicity; further testing of this effluent showed a pH of 2.8 could account for the reduction in growth. When this sample was buffered to pH  $7.0 \pm 0.5$  the toxicity was reversed. Staphylococcus hominis cultures were not effected by any of the effluent samples; while the Pseudomonas putida indicated changes that were minimum.

#### Discussion:

This new procedure for rapid reduction of tetrazolium allows for a rapid assay with good sensitivity and processing of large numbers of samples. The procedure offers a simple procedure that can easily be adapted for industrial operations. As testing continues there will probably be other microbial indicators identified that may be as good for screening as the ones used in this study. It is deemed somewhat important to choose environmental isolates that are part of the resident population. Many of these resident organisms represent members of the natural

bioremediation/biodegradation community that ecosystems have become dependent upon for recycling, etc;. As is suggested by this study it may be beneficial to name more than a single indicator genera or even different species. Some of the preliminary results suggested that some of the chemicals will enhance the growth of certain bacteria. This was true in the case of sodium dodecyl sulfate (SDS) as a control toxicant. This type of activity indicates the eutrophic activity of many chemicals and only supports the value of this procedure in the testing of effluents.

**TABLE 1: BACTERIAL ISOLATES COLLECTED FROM GALVESTON BAY - TEXAS**

Acinetobacter calcaeticus

Aeromonas veronii

Alcaligenes faecalis

Bacillus coagulans

Enterobacter cloacae

Pseudomonas putida

Serratia marcesens

Staphylococcus hominis

Vibrio metschnikovii

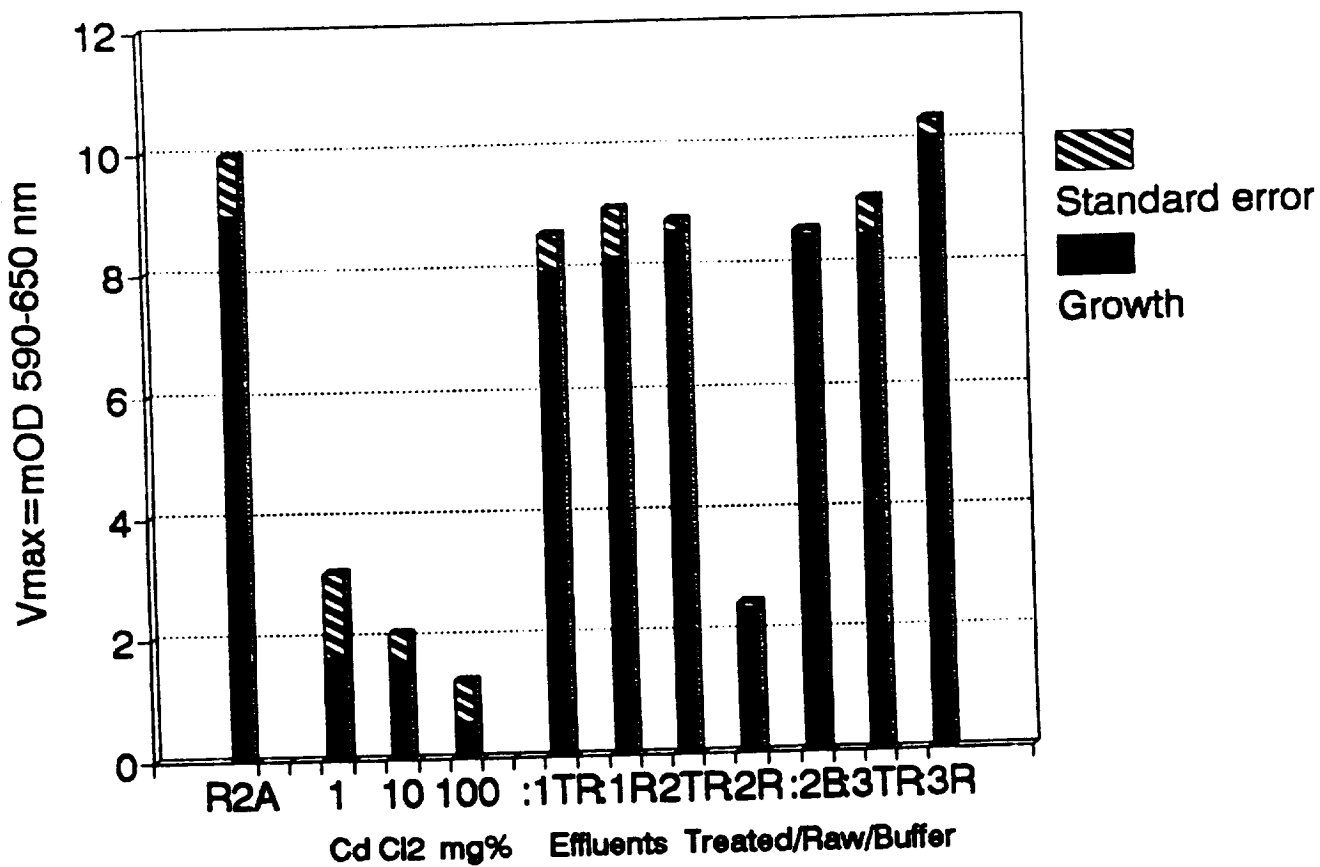


**Figure 1: *Staphylococcus hominis* Growth in Industrial Effluent**

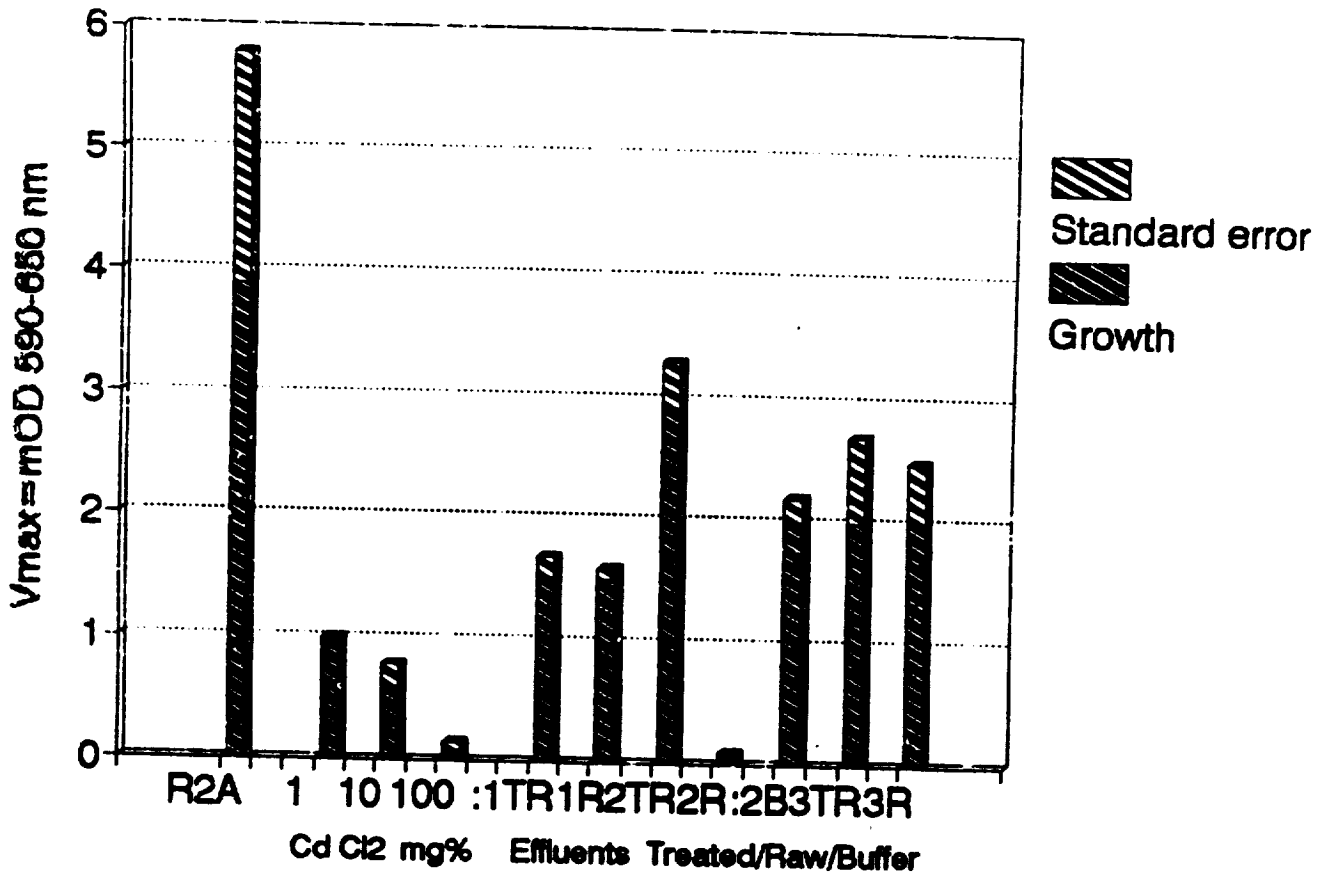


**Figure 2: *Pseudomonas putida*  
Growth in Industrial Effluent**

## LITERATURE REVIEWED

1. Bartlett, R. C., M. Mazens, and B. Greenfield. 1976. Acceleration of tetrazolium reduction by bacteria. *J. Clin. Microbiol.* 3(3): 327-329.
2. Bochner, B.A., and M.A. Savageau. 1977. Generalized Indicator Plate for Genetic, Metabolic, and Taxonomic Studies with Microorganisms. *Applied and Environmental Microbiology*. Vol.33 No.2, p. 434-444.
3. Denizot, F. and R. Lange. 1986. Rapid colorimetric assay for cell growth and survival: Modifications to the tetrazolium dye procedure giving improved sensitivity and reliability. *J. Immunological Methods* (89): 271-277.
4. Findlay, R. H. , M. B. Trexler, J. B. Guckert, and D. C. White. 1990. Laboratory study of disturbance in marine sediments: response of a microbial community. *Marine Ecology Prog. Ser.* Vol. 62: 121-133.
5. Garland, J. L., and A. L. Mills. 1991. Classification and Characterization of Heterotrophic Microbial Communities on the Basis of Patterns of Community- Level Sole-Carbon-Source Utilization. *Applied and Environmental Microbiology*. Vol. 57, No.8. 2351-2359.
6. Gillan, F. T. and R.W. Hogg. 1984. A Method for the estimation of Bacterial biomass and Community Structure in Mangrove-Associated sediments. *Journal of Microbiological Methods*. 2:275-293.
7. Jeffrey, W. H., and J.H. Paul. 1986. Activity of an attached and free-living *Vibrio* sp. as measured by thymidine incorporation, p-iodonitrotetrazolium reduction, and ATP/DNA ratios. *Appl. Environ. Microbiol.* 51(1):150-156.
8. Kasugai, S. N. Hasegawa, and H. Ogura. 1990. A simple in vitro cytotoxicity test using the MTT (3-(4,5)-dimethylthiazol-2-yl)-2,5-diphenyl tetrazolium bromide) colorimetric assay: Analysis of eugenol toxicity on dental pulp cells (RPC-C2A). *Japan J. Pharmacol.* 52:59-100.
9. Karner, V. C., D. M. Calabrese, and K. W. Nickerson. 1980. Growth of *Enterobacter cloacae* in the presence of 25 % sodium dodecyl sulfate. *Appl. Environ. Microbiol.* 40: 711-713.
10. Mosmann, T. 1983. Rapid colorimetric assay for cellular growth and survival: application to proliferation and cytotoxicity assays. *J. Immunol. Methods*. 65: 55-63.

11. Page' M., N. Bejaoui, B. Cinq-Mars and P. Lemieux. 1988. Optimization of the Tetrazolium - Based Colorimetric Assay for the Measurement of Cell Number and Cytotoxicity. Vol. 10. No. 7 p.785-793.
12. Roszak, D. B. and R. R. Colwell. 1987. Survival Strategies of Bacteria in the Natural Environment. Microbiological Reviews.Vol. 51. No. 3. p.365-379.
13. Schnaitman, C. A. 1971. Effect of Ethylenediaminetetracetic acid, triton X-100, and lysozyme on the morphology and chemical composition of isolated cell walls of Escherichia coli. J. Bacteriology 108: 553-563.
14. Stowe, R. A.,D. W. Koenig,S.K. Mishra, and D. L. Pierson.1992. In preparation. A Nondestructive Tetrazolium Microtiter Assay for Measurement of Cell Metabolism and Growth. Biomedical Operations and Research Branch National Aeronautics and Space Administration, Lyndon B. Johnson Space Center, Mail Code SD4 Houston, Tx. 77058.
15. Weber, C. A. et.al. 1988. Short-Term Methods for Estimating the Chronic Toxicity of Effluents and Eceiving Waters to Marine and Estuarine Organisms. Biological Methods Branch Environmental Monitoring and Support Laboratory - Cincinnati , U. S. Environmental Protection Agency Cincinnati, Ohio 45268.

GEOCHEMISTRY AND PETROLOGY OF PRIMITIVE ACHONDRITE  
METEORITES LEW 88280, MAC 88177, ALHA 81187, EET 84302, AND  
LEW 88663

Final Report  
NASA/ASEE Summer Fellowship Program--1992  
Johnson Space Center

Prepared by	Stephen W. Field, Ph.D.
Academic Rank	Assistant Professor
University and Department	Stockton State College Department of Geology Pomona, New Jersey 08240
NASA/JSC	
Directorate:	Space and Life Sciences
Division	Solar Systems Exploration
Branch	SN2 Office of the Curator
Date Submitted	August 14, 1992
Contract Number	NGT-44-005-803

## ABSTRACT

Primitive achondrites are meteorites that have mineral and bulk chemical compositions similar to the most primitive meteorites (chondrites) but have textures similar to more evolved meteorites (achondrites). The unique geochemistry and texture of the primitive achondrites suggest these meteorites may be genetic intermediates between chondrites and achondrites and may preserve evidence of processes occurring in the early solar system. Five primitive achondrites LEW 88280, MAC 88177, ALHA 81187, EET 84302, and LEW 88663 were examined in this study in order to classify the meteorites and to determine processes that have affected them. Bulk chemical analyses of  $\text{Na}_2\text{O}$ ,  $\text{K}_2\text{O}$ ,  $\text{CaO}$ ,  $\text{FeO}$ ,  $\text{Cr}$ ,  $\text{Co}$ ,  $\text{Ni}$ ,  $\text{Sc}$ ,  $\text{Ir}$ ,  $\text{Au}$ ,  $\text{As}$ ,  $\text{Sb}$ ,  $\text{Se}$ ,  $\text{Br}$ ,  $\text{Cs}$ ,  $\text{Ba}$ ,  $\text{La}$ ,  $\text{Ce}$ ,  $\text{Nd}$ ,  $\text{Sm}$ ,  $\text{Eu}$ ,  $\text{Tb}$ ,  $\text{Yb}$ , and  $\text{Lu}$  were determined for each meteorite by Instrumental Neutron Activation Analysis (INAA). Concentrations of  $\text{Hf}$ ,  $\text{U}$ , and  $\text{Th}$  were determined for some meteorites. Polished thin sections of the five meteorites were examined in transmitted and reflected light microscopy to identify minerals and examine petrographic relationships. Minerals found in the meteorites include olivine, orthopyroxene, clinopyroxene, plagioclase, Cr-spinel, phosphates, troilite, kamacite, and taenite along with other minor phases. Mineral compositions were determined with an electron microprobe. The initial study suggests that the meteorites have been altered by metamorphic processes although igneous processes may also have played a role in the evolution of these rocks. Further studies of isotope and bulk chemistry are planned for these meteorites.

## INTRODUCTION

Meteorites are fragments of planetary bodies that impact into Earth. Some meteorites are thought to be fragments of the Moon, blasted into space by impacts that created the large craters on the lunar surface (Lindstrom et al., 1991; Yanai, 1991; Delaney, 1989) and a few meteorites are thought to possibly be fragments of Mars (Bogard et al., 1984). Most meteorites however, are thought to originate in the asteroid belt (McSween, 1987).

The most common meteorites to impact the Earth are called chondrites. Chondritic meteorites are composed of mineral grains, fragments of mineral grains, and features called chondrules, set in a fine-grained matrix of minerals and glass. Chondrules come in a wide variety of shapes and sizes but a typical chondrule is a round or rounded feature composed of a variety of minerals and glass. Olivine and enstatite are minerals commonly found in chondrules. In addition to their unique textures, chondrites have a distinctive chemical composition. Chondrites may be samples of the most primitive and least altered material left over from early planetary formation

Not all meteorites have chondritic textures. Meteorites without chondritic textures are called achondrites. Although texturally distinct from chondrites, some achondrites have chemical signatures which are similar to chondritic chemistries. These primitive achondrites may be chondrites whose textures were altered or obliterated by deformational processes such as metamorphism or igneous processes such as partial melting or crystallization.

Igneous and metamorphic processes have undoubtedly altered the early nebular material which was incorporated into planetary bodies like Earth and Mars. Examining and understanding processes which have affected primitive achondrites may help in understanding the processes which have shaped Earth and other planets.

## PROCEDURES

Five achondrites were examined in this study in order to classify the meteorites and to ascertain their origin and evolution. The five meteorites, collected in Antarctica, are labeled ALHA 81187, LEW 88280, LEW 88663, MAC 88177, and EET 84302. A small amount of each meteorite was crushed

into a powder and irradiated in a nuclear research reactor at the University of Missouri. A small group of major elements and a large group of trace elements were then determined using the INAA facilities at the Johnson Space Center in Houston.

Five polished thin-sections of the meteorites were examined optically by reflected and transmitted light microscopy. Minerals and petrographic relationships were examined and targets were selected for chemical analysis. Mineral chemistries were determined on the Cameca Camebax electron microprobe at the Johnson Space Center. Backscatter photographs of minerals and textures were also obtained from the Cameca microprobe.

#### METEORITE LEW 88280.23

#### Petrography

Meteorite LEW 88280.23 is a medium-grained rock composed of approximately 80 volume % silicate minerals and 20 volume % opaque metals, sulfides and oxides. Silicate minerals include olivine, clinopyroxene, and orthopyroxene. Olivine is the dominant silicate and comprises approximately 90 volume % of the silicates. The opaque suite of minerals is dominated by the Fe-Ni metal kamecite but smaller amounts of the Fe-Ni metal taenite and the Fe-sulfide troilite are present.

The rock has an overall granular texture defined by subhedral, roughly equant olivines. These mineral grains are commonly fractured and may contain small rounded inclusions of metals, sulfides, and pyroxenes. Larger subhedral elongate clinopyroxenes and smaller amounts of orthopyroxene are locally found in the meteorite. Clinopyroxenes contain abundant exsolution lamellae of orthopyroxene and minor rounded inclusions of olivine and elongate ovoid inclusions of metals and sulfides. Discrete orthopyroxene may contain small amounts of clinopyroxene exsolution lamellae.

Metal and sulfide phases are located in anhedral interstitial intergrowths between silicate minerals. The most abundant metal is kamecite which is crystallographically intergrown with more Ni-rich taenite. Distinct patches of troilite are common around the exterior of the kamecite/taenite intergrowths.

Veins of metals, sulfides, and Fe-oxide/hydroxide minerals cut across and fill in between silicates. Sulfides and metal intergrowths are generally surrounded by a rim or partial rim of Fe-oxide/hydroxides. These minerals are probably secondary alteration products.

#### Mineral Chemistry

Representative mineral analyses for LEW 88280 are given in Table 1. Olivines are magnesium rich (Fog7) and contain small amounts of Mn and Cr. Orthopyroxene is also Mg-rich and has an average composition of  $En_{85}Wo_3Fs_{12}$ . The mineral contains minor amounts of Cr, Al, and Ca. Clinopyroxene is a Ca-Mg silicate containing small amounts of Al and Cr. Its average composition is  $En_{50}Wo_{45}Fs_5$ .

Kamesite varies in composition but has a general bimodal compositional distribution. One group of metals has an average composition of 93 wt % Fe and 7 wt % Ni and the other metal group has an average composition of 86 wt % Fe and 14 wt % Ni. Taenite in this sample contains approximately 64 wt % Fe and 36 wt % Ni.

#### Bulk Chemistry

The bulk chemistries of the five meteorites will be described relative to the C1 chondrite abundances of Anders and Ebihara (1982). This is a standard reference for examining abundances of major and trace elements in meteorites and terrestrial igneous rocks.

Meteorite 88280 is approximately chondritic in CaO content and slightly chondrite depleted in FeO. Potassium and sodium contents are very depleted with respect to C1 chondritic abundances. The rock is enriched in the metals Au, Cr, Ni, and Co and Depleted in rare earth elements (REE) when compared to the chondritic standard.

### METEORITE MAC 88177.37

#### Petrography

Meteorite MAC 88177.37 is a medium-grained (0.1-0.7mm) granular rock which resembles a depleted terrestrial harzburgite in texture. The rock is composed of approximately 90 volume % silicates and 10 volume % metals, sulfides, and oxides. The major silicate phases present are orthopyroxene and olivine but minor amounts of clinopyroxene

TABLE 1.- MINERAL COMPOSITIONS FROM METEORITE LEW 88280.23

Oxide	Olivine	Opx	Cpx .
SiO2	40.43	57.46	55.06
TiO2	0	.09	.31
Al2O3	.01	.19	.94
Cr2O3	0	.15	1.17
FeO	12.69	8.30	3.39
MgO	46.90	32.66	19.40
MnO	.48	.51	.35
CaO	.04	.68	18.96
NiO	.06	.08	0 .
Na2O	.01	.01	.58
K2O	.01	0	.02
-----			
Total	100.63	.100.13	100.18

Oxide weight %

Element	Kam	Tae	Troi	Ni-Troi
Al	.02	.03	0	.01
Cr	.01	0	.83	.04
Mg	0	0	0	.05
Fe	91.91	64.14	61.26	57.76
Ni	7.19	35.61	1.04	13.05
S	0	.01	37.73	29.47
-----				
Total	99.13	99.79	100.86	100.38

Elemental weight %

are also present. Orthopyroxenes are euhedral to subhedral and colorless in plane light. They show zoned extinction and contain small localized regions of concentrated clinopyroxene and metal lamellae. Large round olivine inclusions are present in some grains. Discrete olivines are euhedral to subhedral and are slightly elongate. Some grains appear to be interstitial to orthopyroxenes. Olivines can be fractured but otherwise appear optically homogeneous. Clinopyroxene is found as rounded subhedral to angular interstitial grains or as lamellae in orthopyroxenes. Orthopyroxene exsolution lamellae permeate most clinopyroxenes and sulfide and metal inclusions are common.

Opaque phases are dominantly discrete anhedral kamecites and troilites or intergrowths of kamecite + troilite or kamecite + troilite + chrome-spinel. The intergrowths are generally composed of coarse homogeneous regions of kamecite, troilite, and lesser amounts of chrome-spinel and patches of fine-grained intergrown kamecite and troilite. Some discrete grains of taenite and chrome-spinel occur in the sample. A small phosphate mineral was found associated with a kamecite + troilite + chrome-spinel intergrowth.

#### Mineral Chemistry

Orthopyroxenes in MAC 88177 have average compositions of  $En_{84}Wo_4Fs_{12}$  (Table 2). Aluminum oxide contents average approximately 0.65 wt % and  $Cr_2O_3$  and MnO contents average about 0.50 wt %. There are analyses that indicate rims of orthopyroxenes are slightly enriched in Ca and Fe and slightly depleted in Cr and Mn with respect to core compositions. Olivines are Mg-rich with an average

composition of  $Fo_{86}$ . The minerals contain approximately 0.5 wt % MnO but few other trace elements. Clinopyroxenes have an average composition of  $En_{53}Wo_{40}Fs_7$  and contain approximately 1.2 wt %  $Al_2O_3$  and 1.4 wt %  $Cr_2O_3$ . Minor amounts of  $TiO_2$  and  $Na_2O$  are also present. The one analyzed phosphate grain is composed mostly of calcium and phosphorus. It does, however, contain small amounts of Fe, Na, and Cr. This mineral is tentatively identified as apatite.

Spinel in the opaque intergrowths is FeO (24 wt%) and  $Cr_2O_3$  (59 wt%) rich and magnesium and aluminum poor. The oxide contains slightly less than 1 wt% of MnO and  $TiO_2$ . Approximately 0.5 wt% vanadium oxide is present in the spinel. Kamecite contains an average of 6 wt% Ni and Ni contents of taenite average about 25-26 wt%. Troilites contain little except Fe and S.

TABLE 2.- MINERAL COMPOSITIONS FROM METEORITE MAC 88177.37

Oxide	Olivine	Opx	Cpx	Apa	Cr-Sp
SiO2	40.74	57.24	54.22	.02	.03
TiO2	.03	.14	.32	.01	.85
Al2O3	0	.62	1.19	.01	9.01
Cr2O3	0	.54	1.34	.26	58.76
FeO	13.04	8.51	3.50	.44	23.38
MgO	46.20	31.33	17.04	.03	5.56
MnO	.52	.51	.32	.04	.98
CaO	.01	1.87	21.27	57.01	0 .
NiO	0	0	0	0	0 .
Na2O	.02	.05	.60	.25	0 .
K2O	0	.01	.01	0	0 .
P2O5	.01	0	.03	41.61	0 .
V2O3	.02	.08	.07	.02	.66
-----					
Total	100.59	100.90	99.91	99.70	99.23

Oxide weight %

Element	Tae	Kam	Troi
Cr	0	.03	.08
Mg	.02	.01	.01
Fe	73.82	93.29	62.47
Ni	25.49	5.73	37.67
S	0	.02	0 .
P	.02	.03	0 .
V	.02	0	0 .
-----			
Total	99.37	99.11	100.23

Elemental weight %

## Bulk Chemistry

Meteorite MAC 88177 contains approximately chondritic amounts of CaO but is extremely depleted in Na<sub>2</sub>O and K<sub>2</sub>O and moderately depleted in FeO relative to C1 chondritic abundances. Ir, Au, Ni, and Co concentrations are lower than chondritic values but Cr content is higher. The rock contains negligible amounts of As, Sb, and Se.

## METEORITE ALHA 81187.17

### Petrography

Meteorite 81187.17 is a medium-grained (0.2-0.7mm) granular rock composed of the minerals olivine, orthopyroxene, clinopyroxene, chrome-spinel, kamecite, and taenite. The silicate portion of the rock is dominated by subhedral grains of orthopyroxene which constitutes approximately 80 volume % of the meteorite. Olivine accounts for most of the rest of the silicate fraction. A few clinopyroxenes are scattered through the sample. Kamecite dominates the opaque fraction of the meteorite. Small amounts of taenite locally rim the kamecite and small chrome-spinels are found at the edges of some metals.

### Mineral Chemistry

Representative mineral analyses for meteorite ALHA 81187.17 are given in Table 3. Olivines are low in Fe content and have an average composition of Fo<sub>95</sub>. These minerals also have minor concentrations of Mn and traces of Ni. Orthopyroxenes are also Mg-rich and have approximate average compositions of En<sub>7</sub>Wo<sub>3</sub>Fs<sub>7</sub>. The pyroxenes contain up to 1.0 wt% Cr<sub>2</sub>O<sub>3</sub>, 0.6 wt% MnO and 0.5 wt% Al<sub>2</sub>O<sub>3</sub>. Clinopyroxenes are Ca-rich with an average composition of roughly En<sub>50</sub>Wo<sub>49</sub>Fs<sub>1</sub>. These minerals also have minor amounts of aluminum, chromium, and manganese. Kamecite is approximately 94 wt% Fe and 6 wt% Ni and taenite contains roughly equal amounts of Fe and Ni. Spinel is chromium and iron rich but contains on average 9 wt% MgO and 8 wt% Al<sub>2</sub>O<sub>3</sub>.

### Bulk Chemistry

Meteorite ALHA 81187.17 is enriched in Ir, Au, and Cr with respect to C1 chondrites but is depleted in Ni, Co, and As. Sodium, potassium, and iron concentrations are similar

TABLE 3.- MINERAL COMPOSITIONS FROM METEORITE ALHA 81187.17

Oxide	Olivine	Opx	Cpx	Cr-Sp
SiO <sub>2</sub>	42.12	58.27	55.03	0 .
TiO <sub>2</sub>	0	.20	.55	.31
Al <sub>2</sub> O <sub>3</sub>	0	.43	1.03	7.56
Cr <sub>2</sub> O <sub>3</sub>	.04	.96	1.81	63.22
FeO	4.13	4.45	1.94	15.29
MgO	52.34	33.40	18.20	9.21
MnO	.50	.60	.35	3.32
CaO	.13	1.75	20.33	.04
NiO	.03	.04	0	.07
Na <sub>2</sub> O	0	.09	.71	0 .
K <sub>2</sub> O	0	0	.01	.02
-----				
Total	99.29	100.19	99.96	99.04

Oxide weight %

Element	Kam	Tae
Al	0	.01
Cr	0	.01
Mg	0	.01
Fe	92.48	42.88
Ni	6.24	43.65
S	0	.04
-----		
Total	98.73	86.59

Elemental weight %

to those of the C1 chondrite standard and CaO totals are slightly higher. This rock is depleted in light REEs and has approximately chondritic heavy REEs.

#### METEORITE EET 84302.20

#### Petrography

Meteorite EET 84302.20 is a medium-grained (0.05-4.0mm) granular rock composed of approximately 55 volume % silicates and 45 volume % opaques. Orthopyroxene, kamecite, and chrome-spinel dominate the rock with olivine, clinopyroxene, and plagioclase occurring in significantly smaller amounts. The silicates are large subhedral discrete grains and the metal and oxide phases appear to have formed or filled in around the silicates. Orthopyroxenes generally contain tens to hundreds of rounded to elongate inclusions of metals. These metal inclusions are localized in linear patches within the pyroxene, dominantly but not always in the centers of the host grains. The rims of the orthopyroxenes are generally free of inclusions. Some orthopyroxenes also contain round inclusions of olivine. Clinopyroxenes are modally less important than orthopyroxenes but are larger than the average orthopyroxene. Orthopyroxene exsolution lamellae are abundant in clinopyroxenes and some euhedral inclusions of Na-plagioclase exist in some clinopyroxenes. Na-plagioclase is also present as partial rims around or as subhedral rounded grains adjacent to clinopyroxene containing Na-plagioclase inclusions. Rounded metal and olivines are also included in some clinopyroxenes.

Chrome-spinels are concentrated in one region of the rock and comprise about 30 volume % of the opaques. The grains are optically homogeneous. Kamecite dominates the opaque mineralogy but is generally absent in the region of spinel concentration. Some kamecites have thin rims of troilite and/or thin rims of alteration around them. No apparent chondrules are present.

#### Mineral Chemistry

Orthopyroxenes (Table 4) in this rock have an average composition of  $En_{90}Wo_{2}Fs_{8}$ . They contain approximately 0.5 wt%  $Al_2O_3$ ,  $Cr_2O_3$ , and MnO and smaller amounts of Na and Ti. There is some suggestion of a slight iron enrichment in the orthopyroxene cores. Clinopyroxene has an average composition of  $En_{52}Wo_{4}Fs_{44}$ . The pyroxene contains around

TABLE 4.- MINERAL COMPOSITIONS FROM METEORITE EET 84302.20

Oxide	Olivine	Opx	Cpx	Plag	Cr-Sp
SiO <sub>2</sub>	41.33	58.04	54.96	66.20	.02
TiO <sub>2</sub>	.01	.20	.55	.05	1.09
Al <sub>2</sub> O <sub>3</sub>	0	.51	1.23	25.05	8.10
Cr <sub>2</sub> O <sub>3</sub>	.04	.49	1.59	.02	62.28
FeO	8.24	5.57	2.16	.08	15.66
MgO	49.04	33.34	17.52	.01	10.50
MnO	.43	.53	.28	0	1.08
CaO	.05	1.28	21.36	4.32	0 .
NiO	0	0	0	0	.03
Na <sub>2</sub> O	0	.03	.70	4.28	.02
K <sub>2</sub> O	.01	.01	.01	.57	.03
-----					
Total	99.15	100.00	100.36	100.58	98.81

Oxide weight ‡

Element	Kam	Troi
Al	0	.01
Cr	.06	.57
Mg	.02	0 .
Mn	.02	.02
Fe	94.19	61.36
Ni	5.09	.14
S	0	38.01
-----		
Total	99.38	100.11

Elemental weight ‡

0.7 wt% Na<sub>2</sub>O, 1.2 wt% Al<sub>2</sub>O<sub>3</sub>, and 1.6 wt% Cr<sub>2</sub>O<sub>3</sub>. MnO concentrations average about 0.5 wt%. Plagioclase compositions in EET 84302.20 are approximately Ab<sub>75</sub>An<sub>22</sub>Or<sub>3</sub>. Olivine compositional averages are about Fo<sub>87</sub>. The mineral composition includes about 0.5 wt% MnO but few other trace elements are present.

Spinel is Cr- and Fe-rich and Al- and Mg-poor. MnO constitutes a substantial 1.0 wt% total in most of the spinels. Kamecite consists of roughly 95 wt% Fe and 5 wt% Ni. Troilite is composed dominantly of Fe and S but some grains have small amounts (<0.5 wt%) of Cr<sub>2</sub>O<sub>3</sub>.

#### Bulk Chemistry

The most distinctive feature of the bulk chemistry of EET 84302 is its elevated content of Fe, Ir, Au, Cr, Ni, Co, and As with respect to C1 chondrites. Gold contents range up to 8X chondritic abundances and FeO may be up to 2.5X chondritic values. These high contents reflect the high concentration of metal in the rock. Na and Ca totals are approximately chondritic in abundance. EET 84302 appears to have chondritic light REE abundances but slightly enriched heavy REE abundances.

### METEORITE LEW 88663.17

#### Petrography

Meteorite 88663.17 is a granular achondrite composed dominantly of silicates. Metals make up only about 5 modal % of the sample. The major silicate phase is olivine (50 volume %) which is found as equant subhedral to anhedral rounded crystals poikilolitically surrounded by networks of orthopyroxenes (35 volume %) and plagioclase (10 volume %). Plagioclase and orthopyroxenes within individual networks are intimately intergrown. Small patches of clinopyroxene are associated spatially with orthopyroxene. Small grains of a phosphate mineral are intergrown with some orthopyroxene-plagioclase networks.

Large anhedral troilite grains are scattered through the meteorite. Smaller rounded troilites and Ni-rich troilites are present and occur throughout the meteorite but are concentrated preferentially with the orthopyroxene and plagioclase in the poikilitic networks. Troilites, especially large grains, are badly altered by secondary Fe-

oxides or hydroxides. Thin veins of troilite or Fe-oxide/hydroxide surround many of the silicates.

### Mineral Chemistry

Olivine in meteorite 88663 is iron rich with an average composition of Fo<sub>76</sub>. The mineral contains less than 0.5 wt% of MnO and Cr<sub>2</sub>O<sub>3</sub>. Orthopyroxene is also Mg-rich and has an average composition of En<sub>76</sub>Wo<sub>4</sub>Fs<sub>20</sub>. Orthopyroxene generally contains approximately 0.5 wt% Al<sub>2</sub>O<sub>3</sub>, 0.4 wt% Cr<sub>2</sub>O<sub>3</sub>, and 0.4 wt% TiO<sub>2</sub>. Iron appears to be enriched at the edges of the grains and depleted in the cores of the orthopyroxenes. Clinopyroxene is Ca-rich and has an average composition of En<sub>48</sub>Wo<sub>42</sub>Fs<sub>10</sub>. The mineral contains an average of 0.9 wt% Al<sub>2</sub>O<sub>3</sub>, 0.6 wt% Na<sub>2</sub>O, and 0.5 wt% MnO. Plagioclase in 88663 is Na-rich and has an average composition of Ab<sub>75</sub>An<sub>22</sub>Or<sub>3</sub>. A few crystals of a phosphate mineral, tentatively identified as merrillite, exist in the rock. This mineral is composed of roughly equal parts calcium and phosphorus with minor amounts of Na, Mg, and Fe.

Opaque phases in the meteorite are mostly troilites, which contain Fe and S but little else. Some Ni-rich troilite (Ni = 8.5 wt%) is locally associated with olivine. Chrome-spinels are found with some troilites. These spinels contain an average of 56.9 wt% Cr<sub>2</sub>O<sub>3</sub> and 30.5 wt% FeO. MgO contents are approximately 2.0 wt% and Al<sub>2</sub>O<sub>3</sub> contents average 5.8 wt%. Poor analyses of a Ni-Fe metal intergrowth were obtained. The metal contains at least 34 wt% Fe and 43 wt% Ni.

### Bulk Chemistry

Meteorite LEW 88663.17 contains approximately C1 chondritic abundances of Ca, Fe, and Na but has roughly 2X chondritic values of potassium. The rock is also relatively enriched in Au and Cr but is slightly depleted in Ir, Ni, Co, and As. Antimony is almost absent but Sc contents are slightly enriched relative to C1 chondrite standard abundances.

### CONCLUSIONS

This study is in its preliminary stages and much work still needs to be done to reach definite conclusions. The bulk major element composition needs to be analyzed from fused beads and radioactive and stable isotopes composition must be determined in order to suggest with some certainty

TABLE 5.- MINERAL COMPOSITIONS FROM METEORITE LEW 88663.17

Oxide	Olivine	Opx	Cpx	Plag	Merr	Cr-Sp
SiO <sub>2</sub>	38.87	55.53	54.59	63.89	.01	.01
TiO <sub>2</sub>	0	.38	.43	.14	0	2.99
Al <sub>2</sub> O <sub>3</sub>	0	.48	.88	22.93	.01	5.71
Cr <sub>2</sub> O <sub>3</sub>	.02	.41	1.21	0	.02	56.83
FeO	22.05	13.23	5.75	.46	2.23	30.48
MgO	38.74	27.66	16.13	.02	3.27	2.07
MnO	.40	.40	.42	0	.90	.68
CaO	.01	1.70	19.99	4.41	45.74	.03
Na <sub>2</sub> O	.04	.06	.63	8.45	2.36	.03
K <sub>2</sub> O	0	.01	.01	.58	.10	.01
P <sub>2</sub> O <sub>5</sub>	.19	0	.03	.09	43.80	.01
V <sub>2</sub> O <sub>3</sub>	0	0	.06	0	.01	.70
-----						
Total	100.32	99.86	100.13	100.97	98.54	99.60

Oxide weight %

Element	Ni-Troi	Troi
Mg	.01	0 .
Mn	.03	.01
Fe	54.88	62.81
Ni	8.34	.01
S	36.87	37.55
V	0	.02
-----		
Total	100.13	100.40

Elemental weight %

an origin and evolutionary history of the five achondrites. Some preliminary conclusions have, however, been reached.

1. There are no apparent chondrules in the five achondrites studied.
2. All of the achondrites have textures which seem to be metamorphic or igneous in origin.
3. Meteorites MAC 88177 and LEW 88280 have mineral compositions and textures similar to a group of meteorites known as lodranites. This confirms the findings of other workers (Keil, et al., 1992).
4. Meteorite ALHA 81187 has mineral compositions and textures which resemble the textures and compositions of a group of meteorites known as winoaites.
5. Meteorite EET 84302 has mineral compositions that are intermediate between mineral compositions in lodranites and mineral compositions in winoaites. Texturally the meteorite has features similar to features in metal rich meteorites, lodranites, and winoaites.
6. Meteorite LEW 88663 is unusual in its mineral chemistry and textures. The mineral chemistries resemble the chemistries of L or LL chondrites but no chondrules are apparent. The poikilitic orthopyroxene-plagioclase texture is similar to textures in some mesosiderites.

## REFERENCES

- Anders, E., and Ebihara, M. (1982) Solar system abundances of the elements. *Geochim. Cosmochim. Acta* 37, 2363-2380
- Bogard D.D., Nyquist L.E., and Johnson P. (1984) Noble gas contents of shergotites and implications for the Martian origin of the SNC Meteorites. *Geochim. Cosmochim. Acta* 48, 1723-1739.
- Lindstrom M.M., Mittlefehldt D.W., Martinez R.R., Lipschutz M.E., Wang M. (1991) Geochemistry of Yamato-82192, -86032 and -793274 Lunar Meteorites. *Proceedings of the NIPR Symposium on Antarctic Meteorites, No 4, National Institute of Polar Research, Tokyo, 12-32.*
- Delaney J.S. (1989) Lunar basalt breccia identified among Antarctic meteorites. *Nature* 342,889-890.
- Keil K., Mayeda T.K., Clayton R.N. (1992) Petrogenesis of the Lodranite-Acapulcoite parent body. *Meteoritics* 27, 258-259.
- Yanai K. (1991) Gabbroic Meteorite Asuka-31: Preliminary Examination of a New Type of Lunar Meteorite in the Japanese Collection of Antarctic Meteorites. *Proceedings of Lunar and Planetary Science* 21, 317-324.



N93-26068

THE ROLE OF PYRIDOXINE AS A COUNTERMEASURE FOR  
IN-FLIGHT LOSS OF LEAN BODY MASS

Final Report

NASA/ASEE Summer Faculty Fellowship Program 1992

Johnson Space Center

Prepared By:	Joyce A. Gilbert, Ph.D., RD, LD
Academic Rank:	Assistant Professor
University & Department:	Pennsylvania State University Department of Nutrition University Park, Pennsylvania 16802
NASA/JSC	
Directorate:	Space and Life Sciences
Division:	Medical Sciences
Branch:	Biomedical Operations & Research
JSC Colleague:	Helen W. Lane, Ph.D
Date Submitted:	August 18, 1992
Contract Number:	NGT-44-005-803

## ABSTRACT

Ground based and inflight research has shown that humans, under conditions of microgravity, sustain a loss of lean body tissue (protein) and changes in several biological processes including, reductions in red blood cell mass, and neurotransmitters. The maintenance of muscle mass, the major component of lean body mass, is required to meet the needs of space station EVAs. Central to the biosynthesis of amino acids, the building blocks of protein, is pyridoxine (vitamin B-6). Muscle mass integrity requires the availability of vitamin B-6 for protein metabolism and neurotransmitter synthesis. Furthermore, the formation of red blood cells require pyridoxine as a cofactor in the biosynthesis of hemoglobin, a protein that carries oxygen to tissues. In its active form, pyridoxal-5'-phosphate (PLP), vitamin B-6 serves as a link between amino acid and carbohydrate metabolism through intermediates of glycolysis and the tricarboxylic acid cycle. In addition to its role in energy metabolism, PLP is involved in the biosynthesis of hemoglobin and neurotransmitter which are necessary for neurological functions. Alterations in pyridoxine metabolism may affect countermeasures designed to overcome some of these biochemical changes.

The focus of this research is to determine the effects of microgravity on the metabolic utilization of vitamin B-6, integrating nutrition as an integral component of the countermeasure (exercise) to maintain lean body mass and muscle strength. The objectives are: 1) to determine whether microgravity effects the metabolic utilization of pyridoxine and 2) to quantitate changes in B-6 vitamer distribution in tissue and excreta relative to loss of lean body tissue. The rationale for this study encompasses the unique challenge to control biochemical mechanisms effected during space travel and the significance of pyridoxine to maintain and counter muscle integrity for EVA activities. This experiment will begin to elucidate the importance of biochemical interactions between micronutrients and the homeostasis condition of biological processes in the space environment.

To address this research topic a simulated microgravity model has been developed. The experiment uses radioisotopically labelled pyridoxine administered as an oral dose to rats which are maintained by tail suspension to simulate a microgravity environment. At the termination of the study, liver, muscle, blood and urine are collected and analyzed by reverse phase high pressure liquid chromatography to determine the quantity and distribution of the B-6 vitamers in tissue and excreta relative to lean body tissue loss. Earlier studies, published by this investigator, have shown that differences in vitamer distribution among samples from experimental verses control subjects indicate changes in metabolic utilization and storage of vitamin B-6.

## INTRODUCTION

Ground based and inflight research has shown that humans, under conditions of microgravity, sustain a loss of lean body tissue (protein) and changes in several biological processes including, reductions in red blood cell mass, and neurotransmitters. The maintenance of muscle mass, the major component of lean body mass, is required to meet the needs of space station EVAs. Central to the biosynthesis of amino acids, the building blocks of protein, is pyridoxine (vitamin B-6). Muscle mass integrity requires the availability of vitamin B-6 for protein metabolism and neurotransmitter synthesis. Furthermore, the formation of red blood cells require pyridoxine as a cofactor in the biosynthesis of hemoglobin, a protein that carries oxygen to tissues. In its active form, pyridoxal-5'-phosphate (PLP), vitamin B-6 serves as a link between amino acid and carbohydrate metabolism through intermediates of glycolysis and the tricarboxylic acid cycle. In addition to its role in energy metabolism, PLP is involved in the biosynthesis of hemoglobin and neurotransmitter which are necessary for neurological functions. Alterations in pyridoxine metabolism may affect countermeasures designed to overcome some of these biochemical changes.

The focus of this research is to determine the effects of microgravity on the metabolic utilization of vitamin B-6, integrating nutrition as an integral component of the countermeasure (exercise) to maintain lean body mass and muscle strength. The objectives are: 1) to determine whether microgravity effects the metabolic utilization of pyridoxine and 2) to quantitate changes in B-6 vitamers distribution in tissue and excreta relative to loss of lean body tissue. The rationale for this study encompasses the unique challenge to control biochemical mechanisms effected during space travel and the significance of pyridoxine to maintain and counter muscle integrity for EVA activities. This experiment will begin to elucidate the importance of biochemical interactions between micronutrients and the homeostasis condition of biological processes in the space environment.

## MATERIALS AND METHODS

To address this research topic a simulated microgravity model has been developed. The experiment uses radioisotopically labelled pyridoxine administered as an oral dose to rats which are maintained by tail suspension to simulate a microgravity environment. At the termination of the study, liver, muscle, blood and urine are collected and analyzed by reverse phase high pressure liquid chromatography to determine the quantity and distribution of the B-6 vitamers in tissue and excreta relative to lean body tissue loss. Earlier studies, published by this investigator, have shown that differences in vitamers distribution among samples from

experimental verses control subjects indicate changes in metabolic utilization and storage of vitamin B-6. The chromatographic methodologies are being adapted to the HPLC equipment at NASA. All of the above analytical methodologies are being performed on a Hewlett-Packard HPLC with a loop injection valve, a fluorometric detector, and an electronic integrator. Excitation and emission wavelength are 295 nm and 405 nm respectively. Two mobile phases are being employed in a gradient elution procedure using a Bondapak IP column. Mobile phase A contains 0.033 mol/l phosphoric acid, and 8 mmol/l 1-octanesulfonic acid, adjusted to pH 2.2. Mobile phase B contains 0.033 mol/l phosphoric acid and 3.4 mol/l acetonitrile, adjusted to pH 2.2 and no ion pairing reagent.

#### RESULTS

The results of this study will determine the effects of microgravity on the metabolic utilization of pyridoxine and establish the requirement for vitamin B-6 during space travel. Alterations in pyridoxine metabolism may effect vitamin B-6 nutriture and the maintenance of lean body mass and muscle strength, which are necessary components for EVA activities. Statistical analysis on the distribution of vitamin B-6 vitamers between groups will be compared by the method of least squares ANOVA using general linear model procedures SAS, following a logarithmic transformation of the data to normalize the variance if necessary. Data will be reported as least squares mean +/- the pooled standard error of the least squares mean (SEM). Orthogonal contrasts will be made to examine the linear and quadratic effects of different independent variables on dependent variables.

#### DISCUSSION

The bioavailability of vitamin B-6 vitamers is a function of their extent of absorption and metabolic conversion to active coenzymatic forms. Pyridoxine that is absorbed from the intestinal tract is concentrated initially in the liver and is the sole source of plasma PLP. Thus, liver plays a central role in the overall metabolism of vitamin B-6. The major transformations in hepatic vitamin B-6 metabolism involve phosphorylation catalyzed by pyridoxal kinase, oxidation of PNP and PMP by pyridoxine (pyridoxamine) 5'-phosphate oxidase, along with interconversion of PLP and PMP through transamination reactions. The principal forms of vitamin B-6 in liver are PLP and PMP. Pyridoxine 5'-phosphate is usually present in only trace quantities because of its rapid oxidation to PLP. The non-phosphorylated B-6 vitamers constitute <10% of the total vitamin B-6 content in the liver. The metabolic pathway for the degradation of PLP involves enzymatic hydrolysis of the phosphate ester bond, and the oxidation of pyridoxal to 4PA. As a terminal product of vitamin B-6 metabolism, urinary 4PA reflects the in vivo metabolic utilization of the vitamin.

**ANALYSIS OF THE LETTUCE DATA FROM THE VARIABLE PRESSURE GROWTH  
CHAMBER AT NASA-JOHNSON SPACE CENTER:  
A THREE-STAGE NESTED DESIGN MODEL**

**Final Report**

**NASA/ASEE Summer Faculty Fellowship Program-- 1992**

**Johnson Space Center**

<b>Prepared By:</b>	<b>Tze-San Lee, Ph.D.</b>
<b>Academic Rank:</b>	<b>Associate Professor</b>
<b>University &amp; Department:</b>	<b>Western Illinois University Dept. of Mathematics Macomb, Illinois 61455</b>
 <b>NASA/JSC</b>	
<b>Directorate:</b>	<b>Engineering</b>
<b>Division:</b>	<b>Crew and Thermal Systems</b>
<b>Branch:</b>	<b>Life Support Systems</b>
<b>JSC Colleague:</b>	<b>Donald L. Henninger, Ph.D.</b>
<b>Date Submitted:</b>	<b>August 12, 1992</b>
<b>Contract Number:</b>	<b>NGT-44-005-803</b>

## ABSTRACT

A model of three-stage nested experimental design was applied to analyze the lettuce data obtained from the variable pressure growth chamber test bed at NASA-Johnson Space Center. From the results of an application of the analysis of variance and covariance on the data set, it was noted that all of the (uncontrollable) factors, Side, Zone, Height and (controllable) PAR (photosynthetically active radiation), had nonhomogeneous effects on the dry weight of the edible biomass of lettuce per pot. Incidentally, the variations accountable to the (uncontrollable) factorial heterogeneities are merely 9% and 17% of the total variation for both the first and second crop test, respectively. After adjusting for the PAR as a covariate in the no-intercept model, the accountable variations to all the four factors are 94% and 92% for the first and the second crop test, respectively. With the use of a no-intercept simple linear regression model, the accountable variations to the factor PAR are 92% and 90% for the first and the second crop test, respectively. Evidently, the (controllable) factor PAR is the dominating one.

## 1. INTRODUCTION

The aim of this report is to apply a three-stage nested experimental design in modeling the lettuce data generated from the variable pressure growth chamber (VPGC) test bed at NASA's Johnson Space Center (Tri, et al 1991). The purpose of the research is that for long duration space missions such as a Lunar or Martian outpost technologies will be needed to revitalize atmospheric constituents, to process wastes, to regenerate water, and to produce food for human consumption under the premises of minimizing dependency on resupply from earth and attaining self-sufficiency. NASA's Controlled Ecological Life Support Systems Program (CELSS) was studying the use of biological processes for integration into regenerative life support systems. Higher plants could be used as an integral part of these life support systems, because they remove carbon dioxide and produce oxygen through photosynthesis, purify water through transpiration, and produce food (Schwartzkopf 1992).

The data set used in this report was the same as that of Barta, et al (1992). As a result of the specific engineering design of the growth chamber test bed, it was noted that the factor Zone (representing four independent nutrient solution irrigation systems) was nested within the factor Side (representing two atmospheric conditioning systems), while the factor Height (representing the upper and lower growing area) was nested within the factor Zone. The tests were conducted under ambient atmospheric pressures in the VPGC, a vacuum chamber outfitted for plant growth. The VPGC encloses a total of 10.6 m<sup>2</sup> of area for crop growth, split into eight individual growing areas (Figure 1.1). Two atmospheric conditioning systems are present, one on each chamber side supporting four individual growing areas. Four independent nutrient solution irrigation systems are present. Each irrigation system, or zone, supports a pair of growing areas (one upper and one lower growing areas). A complete description of the chamber and its plant support systems is given in Tri, et al (1991). Two crop tests were replicated. The environmental conditions and cultural practices used during both crop tests are presented in Table 1.1. For both tests, each growing area was outfitted with 60 pots, for a total of 480 pots within the chamber. Each pot was filled with approximately 250 ml of calcined clay.

**Table 1.1.** Environmental Conditions and Cultural Practices Used During the First and Second Crop Test.

Parameter	Units	Crop Test	
		First	Second
Average Air Temperature	°C	22.8	23.1
Average Relative Humidity	%	73	72
Carbon Dioxide Level	$\mu\text{L L}^{-1}$	1000	1000
Average Photosynthetic Photon Flux (PPF)	$\mu\text{mol m}^{-2} \text{s}^{-1}$	365	346
Irrigation Frequency	Events day <sup>-1</sup>		
Week 1		1	1
Week 2		2	1
Weeks 3 & 4		3	3
Irrigation Amount	ml pot <sup>-1</sup> event <sup>-1</sup>	37	30

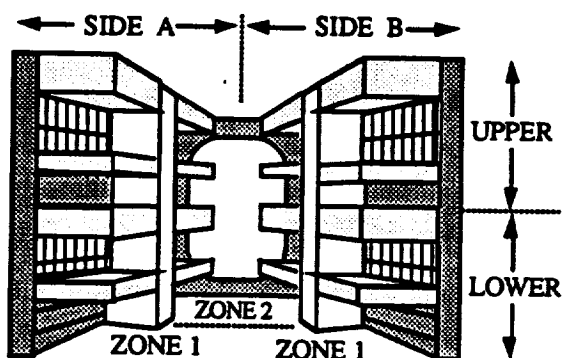


**Figure 1.1.** Interior Layout of the Variable Pressure Growth Chamber (VPGC).

Two seeds of lettuce were planted within each pot. The pots were irrigated with a modified half-strength Hoagland's nutrient solution. The plants were harvested 30 days after seeding. Here the conditions for each crop were nominally set to be the same for all growing areas.

## 2. STATISTICAL MODELING

A three-stage nested design model without/with the photosynthetically active radiation (PAR) as a covariate and/or with no-intercept term were employed in fitting the collected lettuce data as follows:

$$y_{ijkl} = \mu + \alpha_i + \beta_{(i)j} + \gamma_{(ij)k} + \varepsilon_{(ijk)l}, i = A, B, j = 1, 2, k = H, L, l = 1, \dots, 60; \quad (2.1)$$

$$y_{ijkl} = \mu + \alpha_i + \beta_{(i)j} + \gamma_{(ij)k} + \theta x_{ijkl} + \varepsilon_{(ijk)l}, i = A, B, j = 1, 2, k = H, L, l = 1, \dots, 60; \quad (2.2)$$

and

$$y_{ijkl} = \alpha_i + \beta_{(i)j} + \gamma_{(ij)k} + \theta x_{ijkl} + \varepsilon_{(ijk)l}, i = A, B, j = 1, 2, k = H, L, l = 1, \dots, 60; \quad (2.3)$$

where :

$x_{ijkl}$  - intensity of photosynthetically active radiation (PAR) received at the  $l$ -th plant in the  $k$ -th height within the  $j$ -th zone and the  $i$ -th side,

$y_{ijkl}$  - dry weight (DW) of edible biomass of the  $l$ -th lettuce in the  $k$ -th height within the  $j$ -th zone and the  $i$ -th side,

$\mu$  - mean biomass of all plants in the crop,

$\alpha_i$  - differential effect attributed to the  $i$ -th side ,

$\beta_{(i)j}$  - differential effect attributed to the  $j$ -th zone within the  $i$ -th side,

$\gamma_{(ij)k}$  - differential effect attributed to the  $k$ -th height within the  $i$ -th side and the  $j$ -th zone,

$\theta$  - regression coefficient of  $x_{ijkl}$ ,

$\varepsilon_{(ijk)l}$  - error term assuming to have a normal probability distribution with a mean zero and unknown constant variance  $\sigma^2 > 0$  representing the variation of biomass from plant to plant within each growing area.

Since the effect of the factors are fixed, we assume that the following constraints hold for Eqs. (2.1-2):

$$\sum_i \alpha_i = 0, \quad (2.4a)$$

$$\sum_j \beta_{(i)j} = 0, \quad (2.4b)$$

$$\sum_k \gamma_{(ij)k} = 0. \quad (2.4c)$$

Note that there are no interaction terms among the three factors in Eq. (2.1-3), because it can be shown (Montgomery 1992) that there is no need to include the interaction term in the model of multi-stage nested experimental design.

Table 2.1. Expected Mean Squares for the Three-Stage Nested Design Model of Eq. (2.1).

E(MS)	Side, Zone, Height: fixed
E(MS <sub>side</sub> )	$\sigma^2 + 240 \sum_i \alpha_i^2$
E(MS <sub>(side)zone</sub> )	$\sigma^2 + 120 \sum_i \sum_j \beta_{(i)j}^2$
E(MS <sub>(side,zone)height</sub> )	$\sigma^2 + 60 \sum_i \sum_j \sum_k \gamma_{(ij)k}^2$
E(MS <sub>error</sub> )	$\sigma^2$

Table 2.2. Analysis of Variance Table for the Three-Stage Nested Design Model of Eq. (2.1).

Source of Variation	Sum of Squares	Degrees of Freedom	Mean Square
Side	$\sum_i y_{i..}^2 / 240 - y_{...}^2 / 480$	1	MS <sub>s</sub>
Zone within side	$\sum_i \sum_j y_{ij.}^2 / 120 - \sum_i y_{i..}^2 / 240$	2	MS <sub>(s)z</sub>
Height within zone, side	$\sum_i \sum_j \sum_k y_{ijk}^2 / 60 - \sum_i \sum_j y_{ij.}^2 / 120$	4	MS <sub>(s,z)h</sub>
Error	$\sum_i \sum_j \sum_k \sum_l y_{ijkl}^2 - \sum_i \sum_j \sum_k y_{ijk}^2 / 60$	472	MS <sub>e</sub>
Total	$\sum_i \sum_j \sum_k \sum_l y_{ijkl}^2 - y_{...}^2 / 480$	479	

where  $y_{....}$ ,  $y_{i...}$ ,  $y_{ij..}$ , and  $y_{ijk.}$  are defined, respectively, as follows:

$$y_{....} = \sum_i \sum_j \sum_k \sum_l y_{ijkl},$$

$$y_{i...} = \sum_j \sum_k \sum_l y_{ijkl},$$

$$y_{ij..} = \sum_k \sum_l y_{ijkl},$$

$$y_{ijk.} = \sum_l y_{ijkl}.$$

The expected mean squares for Eq. (2.1) is given in Table 2.1. Since the effect of the factors Side, Zone and Height are regarded as fixed, it is noted from Table 2.1 that the null hypotheses  $H_0: \alpha_i = 0$ ,  $H_0: \beta_{(ij)k} = 0$ , and  $H_0: \gamma_{(ij)k} = 0$  can be tested by  $MS_{side}/MS_{error}$ ,  $MS_{(side)zone}/MS_{error}$ , and  $MS_{(side,zone)height}/MS_{error}$ , respectively. The test procedure is summarized in an analysis of variance table as shown in Table 2.2.

### 3. RESULTS AND ANALYSIS

All computations were performed on the Macintosh personal computer through the use of the MGLH procedure in SYSTAT (Wilkinson 1987). The analysis of variance and covariance with/without the intercept term for the first and the second crop test are summarized, respectively, in Tables 3.1-3 and 3.4-6. Numerical results summarized in Tables 3.1-6 were obtained by fitting Eqs. (2.1-3) to new data sets after a deletion of those data points which were identified as outliers and having zero dry weight in the first fitting of Eq. (2.1) to the original data set. From Table 3.1, all of the three factors, Side, Zone, and Height, had differential effects on the dry weight of the edible biomass of lettuce at the significance level of less than 1%. From Tables 3.2-3, it was noticed that after adjusting for the influence of the covariate PAR, the effects of Side, Zone, and Height are still significant. Yet the factor PAR is clearly the dominating one. Table 3.7 indicates that the lettuce plants growing, respectively, in Side B, Zone 1, and 'low' growing area had greater dry weights, on the average, than in Side A, Zone 2, and 'high' growing area.

**Table 3.1.** The Analysis of Variance of Eq. (2.1) for the First Crop Test.

Model	Source	Sum of Squares	d.f.	Mean-Square	F-ratio	Pr. > F
3-Stage Nested Design without covariate	Side	16.55	1	16.55	16.55	0.000
	Zone/Side	12.18	2	6.09	5.16	0.004
	Ht/Zone/Side	19.65	4	4.91	4.16	0.002
	Error	504.10	429	$\hat{\sigma}^2 =$ 1.18		
$R^2 = 0.09$						

**Table 3.2.** The Analysis of Covariance of Eq. (2.2) for the First Crop Test.

Model	Source	Sum of Squares	d.f.	Mean-Square	F-ratio	Pr. > F
3-Stage Nested Design with covariate	Side	33.66	1	33.66	34.44	0.000
	Zone/Side	9.53	2	4.77	4.88	0.008
	Ht/Zone/Side	16.68	4	4.17	4.27	0.005
	PAR	85.79	1	85.79	87.54	0.000
	Error	418.31	428	$\hat{\sigma}^2 =$ 0.98		
$R^2 = 0.24$						

Similar results hold for the second crop test as shown in Tables 3.4-6 and 3.8. The dry weight of edible biomass of lettuce in the upper growing area was lighter, on the average, than that of the lower growing area. This may have resulted from a less delivery of nutrient solution to the upper growing area as compared to the lower growing area. The average air temperature and relative humidity for Side A and B over the 30 day crop test were 22.1°C and 23.5°C and 80% and 66.5%, respectively. The warmer conditions present on Side B

**Table 3.3.** The Analysis of Covariance of Eq. (2.3) for the First Crop Test.

Model	Source	Sum of Squares	d.f.	Mean-Square	F-ratio	Pr. > F
3-Stage Nested Design with covariate  and no- intercept	Side	40.59	1	40.59	41.08	0.000
	Zone/Side	9.78	2	4.89	4.95	0.005
	Ht/Zone/Side	20.48	4	5.12	5.18	0.000
	PAR	6032.50	1	6032.50	6105.77	0.000
	Error	423.92	429	$\hat{\sigma}^2 =$ 0.99		
$R^2 = 0.94$						

**Table 3.4.** The Analysis of Variance of Eq. (2.1) for the Second Crop Test.

Model	Source	Sum of Squares	d.f.	Mean-Square	F-ratio	Pr. > F
3-Stage Nested Design without covariate	Side	20.07	1	20.07	24.18	0.000
	Zone/Side	31.74	2	15.87	19.12	0.000
	Ht/Zone/Side	24.26	4	6.06	7.30	0.000
	Error	382.43	463	$\hat{\sigma}^2 =$ 0.83		
	$R^2 = 0.17$					

may have increased the dry weight of edible biomass of lettuce. From Tables 3.3 and 3.6, it was noted that the variation accountable to all of the four factors for Eq. (2.3) were 94% and 92% (the value of  $R^2$ ), which were much higher than the corresponding one for Eq. (2.2), in the total variation of the dry weight of edible biomass of lettuce for the first and

**Table 3.5.** The Analysis of Covariance of Eq. (2.2) for the Second Crop Test.

Model	Source	Sum of Squares	d.f.	Mean-Square	F-ratio	Pr. > F
3-Stage Nested Design with covariate	Side	25.14	1	25.14	39.28	0.000
	Zone/Side	21.48	2	10.74	16.78	0.000
	Ht/Zone/Side	23.07	4	5.77	9.02	0.000
	PAR	86.66	1	86.66	135.41	0.000
	Error	295.77	462	$\hat{\sigma}^2 =$ 0.64		
$R^2 = 0.37$						

**Table 3.6.** The Analysis of Covariance of Eq. (2.3) for the Second Crop Test.

Model	Source	Sum of Squares	d.f.	Mean-Square	F-ratio	Pr. > F
3-Stage Nested Design with covariate and no- intercept	Side	25.00	1	25.00	39.12	0.000
	Zone/Side	22.13	2	11.07	17.32	0.000
	Ht/Zone/Side	23.09	4	5.77	9.03	0.000
	PAR	3222.96	1	3222.96	5042.77	0.000
	Error	295.92	463	$\hat{\sigma}^2 =$ 0.64		
$R^2 = 0.92$						

second crop test, respectively. It indicates that a no-intercept model of Eq. (2.3) fits the lettuce data much better than the model of Eq. (2.2) as far as the explainable variation due to the inclusion of covariate PAR in the model is concerned. Also, we note that although the error sum of squares for the second crop test is smaller than that of the first crop test, the dry weight of the edible biomass of lettuce for the first crop test is heavier than that for

**Table 3.7. The Summary Statistics for the First Crop Test.**

Factor	Level	No. of cases	Minimum	Maximum	Mean	s.d.
Side	A	222	0.508	6.3	3.495	1.011
	B	215	0.0	7.5	3.895	1.204
Zone	1	219	1.10	7.5	3.854	1.140
	2	218	0.0	7.4	3.529	1.173
Height	H	217	0.0	7.4	3.477	0.988
	L	220	0.508	7.5	3.904	1.213

**Table 3.8. The Summary Statistics for the Second Crop Test.**

Factor	Level	No. of cases	Minimum	Maximum	Mean	s.d.
Side	A	239	0.0	5.4	2.372	0.917
	B	232	0.10	5.4	2.783	1.016
Zone	1	235	0.7	5.4	2.830	0.927
	2	236	0.0	5.2	2.321	0.982
Height	H	238	0.1	4.2	2.355	0.824
	L	233	0.0	5.4	2.799	1.087

the second crop test. This is probably attributed to the less irrigation frequency in Week 2 for the second crop test and less delivered nutrient solution per irrigation event (Table 1.1). Incidentally, a checking for the validity of normality and independence assumption were carried out for all the model fitting exercises by plotting the residuals versus the predicted value of the dry weight of edible biomass of lettuce and a normal probability plot of residuals, respectively. The model assumptions of independence and normality were judged to be satisfactory for all the fitted models by visualization of the plots. The Pearson's correlation coefficient between DW and PAR for the first and the second crop test are 0.37 and 0.45 which were shown to be significantly different from zero. In fact,

after examining the plots of residuals for the validation of independence and normality assumptions, a simple no-intercept linear regression model given by

$$\hat{DW} = 0.01*PAR \text{ (or } = 0.008*PAR) \quad (3.1)$$

was determined to be adequate with  $R^2 = 0.92$  (or 0.90) and  $\hat{\sigma}^2 = 1.13$  (or 0.78) in describing a strong linear relationship between the response variable DW and the predictor variable PAR for the first (or second) crop test. As compared with a partially nested design model used in Barta (1992), the fully nested design models of Eqs. (2.1-3) are preferred since the interaction between the factors Side and Height was shown to be not significant as a result of hypothesis testing.

#### 4. CONCLUSION

Based upon the present analysis of the lettuce data, it is noted that the effects of two atmospheric conditioning systems, four independent nutrient solution irrigation systems, and two growing (high or low) areas on the plant biomass production are not homogeneous. This implies that the growth chamber environment is not spatially uniform. This phenomenon of nonuniformity even in controlled growth chambers was also observed in Lee-Rawlings (1982). Fortunately, the variation accountable to the three (uncontrollable) factors, Side, Zone, and Height, in the total variation of the dry edible biomass of lettuce are no more than 2% for either the first or the second crop test after adjusting for the (controllable) factor PAR (photosynthetically active radiation) as a covariate in the no-intercept model, the accountable variation for all the (uncontrollable and controllable) factors is more than 92% for both the first and the second crop test. With the use of a no-intercept simple linear regression model, the accountable variation for the factor PAR is more than 90% for both the first and the second crop test. Evidently, the (controllable) factor PAR is the dominating one. Further studies seem warranted to find the best combination of factor levels for the controllable factors which might provide the maximum yield of the dry edible biomass of lettuce.

## ACKNOWLEDGEMENTS

This study was supported by an appointment of the author in the summer of 1992 as a Summer Faculty Research Fellow at NASA-Johnson Space Center, Houston, Texas. The author is grateful for fruitful discussions on the topic with Drs. Dan Barta, Don Henninger, Bradley Eckhardt and other staff members in the Life Support Systems Branch of the Crew and Thermal Systems Division who contributed to the database upon which this analysis was based. All computations were facilitated with the use of SYSTAT on the Macintosh personal computer.

## REFERENCES

- Barta, D.J., Edeen, M.A., and Eckhardt, B.D. (1992), Regenerative life support systems test bed performance: Lettuce crop characterization, A pre-print of a paper to be presented at the 22nd International Conference on Environmental Systems, July 13-16, 1992, Seattle, WA, sponsored by the Society of Automotive Engineers.
- Montgomery, D.C. (1992), Design and Analysis of Experiments (Third Edition), John Wiley & Sons, New York.
- Lee, C.-S. and Rawlings, J.O. (1982), Design of experiments in growth chambers - uniformity trials in the North Carolina State University Phytotron, Crop Science, 22, 551-558.
- Schwartzkopf, S.H. (1992), Design of a controlled ecological life support system, Bioscience, 42, 526-535.
- Tri, T.O., Brown, M.F., Ewert, M.K., Foerg, S.L., and McKinley, M.K. (1991), Regenerative life support systems (RLSS) test bed development at NASA-Johnson Space Center, In: Regenerative Life Support Systems and Processes, SP-873, Soc. of Automotive Engineers, Warrendale, PA.
- Wilkinson, L. (1987), SYSTAT: The System for Statistics, SYSTAT, Inc., Evanston, IL.



# REPORT DOCUMENTATION PAGE

Form Approved  
OMB No. 0704-0188

Public reporting burden for this collection of information is estimated to average 1 hour per response, including the time for reviewing instructions, searching existing data sources, gathering and maintaining the data needed, and completing and reviewing the collection of information. Send comments regarding this burden estimate or any other aspect of this collection of information, including suggestions for reducing this burden, to Washington Headquarters Services, Directorate for Information Operations and Reports, 1215 Jefferson Davis Highway, Suite 1204, Arlington, VA 22202-4302, and to the Office of Management and Budget, Paperwork Reduction Project (0704-0188), Washington, DC 20503.

1. AGENCY USE ONLY (Leave blank)		2. REPORT DATE December 1992	3. REPORT TYPE AND DATES COVERED Contractor Report	
4. TITLE AND SUBTITLE National Aeronautics and Space Administration (NASA)/American Society for Engineering Education (ASEE) Summer Faculty Fellowship Program-1992 Volume 1			5. FUNDING NUMBERS NGT 44-005-803	
6. AUTHOR(S) Richard B. Bannerot and Stanley H. Goldstein, Editors				
7. PERFORMING ORGANIZATION NAME(S) AND ADDRESS(ES) University of Houston Houston, Texas			8. PERFORMING ORGANIZATION REPORT NUMBER	
9. SPONSORING / MONITORING AGENCY NAME(S) AND ADDRESS(ES) University Programs Office Lyndon B. Johnson Space Center Houston, Texas			10. SPONSORING / MONITORING AGENCY REPORT NUMBER NASA CR 188242	
11. SUPPLEMENTARY NOTES				
12a. DISTRIBUTION / AVAILABILITY STATEMENT Unclassified/Unlimited Star Category 99			12b. DISTRIBUTION CODE	
13. ABSTRACT (Maximum 200 words) The 1992 Johnson Space Center (JSC) National Aeronautics and Space Administration (NASA)/American Society for Engineering Education (ASEE) Summer Faculty Fellowship Program was conducted by the University of Houston and JSC. The program at JSC, as well as the programs at other NASA Centers, was funded by the Office of University Affairs, NASA Headquarters Washington, D.C. The objectives of the program, which began nationally in 1964 and at JSC in 1965, are (1) to further the professional knowledge of qualified engineering and science faculty members; (2) to stimulate an exchange of ideas between participants and NASA; (3) to enrich and refresh the research and teaching activities of participants' institutions; and (4) to contribute to the research objective of the NASA Centers.  Each faculty fellow spent at least 10 weeks at JSC engaged in a research project in collaboration with a NASA JSC colleague. This document is a compilation of the final reports on the research projects performed by the faculty fellows during the summer of 1992. Volume 1 contains reports 1 through 12, and Volume 2 contains reports 13 through 24.				
14. SUBJECT TERMS			15. NUMBER OF PAGES	
			16. PRICE CODE	
17. SECURITY CLASSIFICATION OF REPORT Unclassified	18. SECURITY CLASSIFICATION OF THIS PAGE Unclassified	19. SECURITY CLASSIFICATION OF ABSTRACT Unclassified	20. LIMITATION OF ABSTRACT Unlimited	



